GEOTHERMAL ENERGY POTENTIAL OF THE LOWER SAN FRANCISCO RIVER REGION, ARIZONA

by

James C. Witcher

Arizona Geological Survey
Open-File Report 81-7

January, 1981

Arizona Geological Survey
416 W. Congress, Suite #100, Tucson, Arizona 85701

Funded By The U.S. Department of Energy
Contract Number DE-FC07-79ID12009

This report is preliminary and has not been edited
or reviewed for conformity with Arizona Geological Survey standards

NOTICE

This report was prepared to document work sponsored by the United States Government. Neither the United States nor its agents, the United States Department of Energy, nor any federal employees, nor any of their contractors, subcontractors or their employees, makes any warranty, express or implied, or assumes any legal liability or responsibility for the accuracy, completeness, or usefulness of any information, apparatus, products or process disclosed, or represents that its use would not infringe privately owned rights.

Reference to a company or product name does not imply approval or recommendation of the product by the Bureau of Geology and Mineral Technology or the U.S. Department of Energy to the exclusion of others that may be suitable.

TABLE OF CONTENTS

	Page
List of Figures	i
List of Tables	ii
Summary	1
Geologic Settings	1
Hot Springs	3
Thermal Regime	5
Introduction	7
Land Ownership	11
Regional Setting	11
Stratigraphy	21
Structure	35
Hot Springs	46
Clifton Hot Springs	48
Gillard Hot Springs	64
Eagle Creek Hot Springs	69
Hanna Creek Hot Springs	70
Lower Frisco Hot Springs	70
Warm Spring	74
Geophysics	75
Gravity Surveys	76
Seismic Surveys	77
Electrical Surveys	81
Heat Flow	83
Conclusions and Recommendations	103
Tables	108
Bibliography	126

FIGURES

		Page
Figure 1	Lower San Francisco River Study Area	8
Figure 2	Land Status of the Lower San Francisco River Area	10
Figure 3	Location Map of the Lower San Francisco River Area and Physiographic-Tectonic Provinces	12
Figure 4	Map Showing "Texas Zone" Discontinuities and Lineaments	16
Figure 5	Generalized Stratigraphic Sections and Correlations of Mid-Tertiary Volcanic Rocks and Sediment in the Lower San Francisco River Area, Arizona & New Mexico	(pocket)
Figure 6	Generalized Map of Tertiary Basement, Southeastern Arizona	37
Figure 7	Lithium vs Boron, Clifton Hot Springs	50
Figure 8	Lithium vs Chloride, Clifton Hot Springs	51
Figure 9	Boron vs Chloride, Clifton Hot Springs	52
Figure 10	Temperature vs Chloride, Clifton Hot Springs	53
Figure 11	Silica vs Chloride, Clifton Hot Springs	54
Figure 12	Na-K-Ca (1/3) Geothermometer vs Chloride, Clifton Hot Springs	57
Figure 13	Enthalpy/Chloride Diagram, Clifton Hot Springs	58
Figure 14	Boron vs Chloride, San Francisco River below Clifton Hot Springs	60
Figure 15	Chloride vs Flow of San Francisco River below Clifton Hot Springs	62
Figure 16	Silica vs Temperature, Gillard Hot Springs	65
Figure 17	Chloride content vs Flow Rate of the Gila River 3 Miles above Gillard Hot Springs	66
Figure 18	Lithium vs Chloride, Lower Frisco Hot Springs (New Mexico)	71
Figure 19	Geothermometers vs Chloride, Lower Frisco Hot Springs (New Mexico)	72
Figure 20	Complete Bouguer Gravity Map of a Portion of the Lower San Francisco River Area	(pocket)
Figure 21	Seismic Refraction Model of the Crust in the Lower San Francisco River Area	79
Figure 22	Pseudosections of Audiomagnetotelluric (AMT) Data, Clifton Area, Arizona	(pocket)
Figure 23	Temperature Logs of Drill Holes in the Clifton, Arizona Area	86
Figure 24	Lithology of Heat Flow Holes	87
Figure 25	Heat Flow Data for HF1 Drill Hole	89
Figure 26	Temperature vs Temperature Gradient HF2	91
Figure 27	Temperature Gradient Hole 80W6, Clifton, Arizona	92
Figure 28	Temperature vs Temperature Gradient, Clifton 1	95
Figure 29	Heat Flow vs Depth Clifton 1	96

TABLES

		Page
Table 1	Tertiary Volcanic Stratigraphy in Lower San Francisco River Area	108
1A	Tertiary Volcanic Stratigraphy in the Clifton Area	108
1B	Tertiary Volcanic Stratigraphy in the Glenwood-Mogollon-Lower Frisco Hot Springs Area	109
1C	Tertiary Volcanic Stratigraphy in the Blue Range Primitive Area (North)	111
1D	Tertiary Volcanic Stratigraphy in the Blue Range Primitive Area (South)	112
1E	Tertiary Volcanic Stratigraphy in the Juan Miller Basin	113
1F	Tertiary Volcanic Stratigraphy in the Bonita-Eagle Creek Area	114
1G	Tertiary Volcanic Stratigraphy in the Blue Creek Basin	115
Table 2	Chemical Analyses of Groundwaters in the Lower San Francisco River Area	117
2A	Analyses of Clifton Hot Springs	118
2B	Analyses of San Francisco River near Clifton Hot Springs	119
2C	Analyses of Gillard Hot Springs	119
2D	Analyses of Gila River near Gillard Hot Springs	120
2E	Analyses of Eagle Creek Hot Springs	120
2F	Analyses of Hanna Creek Hot Springs	120
2G	Analyses of Lower Frisco Hot Springs	121
2H	Analyses of Warm Springs (Martinez Ranch Area)	121
2I	Analyses of Non-Thermal Groundwater	121
Table 3	Geothermometry of Clifton Hot Springs	123
Table 4	Heat Flow Data in the Lower San Francisco River Area	124

ACKNOWLEDGEMENTS

Geothermal studies in the Clifton-Morenci area have benefited from discussions with numerous people. Yuram Eckstein, Kent State University, pointed out the probable mixed nature of the hot springs. Claudia Stone, ABGMT, measured rock thermal conductivities. Bruce Taylor and Rob Roy, University of Texas El Paso, provided assistance to Claudia and the use of the UTEP divided bar thermal conductivity apparatus. Paul Damon, University of Arizona kindly loaned his copy of Robert Berry's Thesis on the White Mountains volcanic province. Phelps Dodge geologists Ken Bennett, Mike Shearn, Fred Meinzer and Warren Niemi are thanked for their discussions and interest in this study. John Cunningham, Western New Mexico University, is thanked for his discussions concerning the geology east and north of Clifton. Clyde McBride of Clifton is thanked for the use of a horse and assistance in studies along the San Francisco river.

SUMMARY

Geologic Setting

The lower San Francisco River area lies in a "transition zone" between the Colorado Plateau and the Basin and Range physiographic provinces. Immediately north of the study area, on the southern margin of the Colorado Plateau, extensive Quaternary basaltic volcanism and high regional conductive heat flow (>2.0 HFU) are observed.

Paleozoic rocks overlie Precambrian granite and Pinal Schist and depict a time of relative tectonic quietude. A basal arkosic sandstone is overlain by interbedded shales and carbonate rocks; carbonate rocks become dominant higher in the Paleozoic section. At Clifton, sediments are exposed from all Paleozoic periods except Silurian and Permian (Lindgren, 1905).

Mesozoic uplift and erosion exposed potentially permeable upper Paleozoic carbonate rocks which were later covered by impermeable Cretaceous shales. Laramide (Paleocene) plutonism emplaced stocks and porphyry copper deposits in the Clifton area (Langton, 1973). After a period of erosion during Eocene, volcanism of Oligocene to early Miocene age buried the area beneath 1 to 5 km of mostly andesitic to basaltic flows, breccias, localized but important dacitic to rhyolitic lavas and tuffs, and volcano-clastic sediment. The only identified large silicic cauldrons in the region occur on the east boundary of the study area. Mid-Tertiary volcanic rocks comprise two suites, an older andesite to dacite suite called the Datil Group

and a younger bimodal suite of basaltic andesite and latite-rhyolitic lavas. The rhyolitic plugs, domes and dikes are aligned in WNW and NE trending zones. Four small nonresurgent cauldrons, Mule Creek, Red Mountain, Enebro Mountain and Horse-Maple cauldron dome complex, occur in the WNW trending zones (Ratte and others, 1969; Berry, 1976; and Rhodes and Smith, 1972). Studies of the volcanic sequence east of Clifton and seismic refraction studies identified a Tertiary basin, the Blue Creek basin, which is filled with up to 5 km of early Oligocene to late Miocene volcanic rocks (Seager and Clemons, 1972; Wahl, 1980; Gish, 1980). Volcano-tectonic subsidence or a broad Tertiary syncline may be responsible for the Blue Creek basin. No definitive ring fracture zone or fault was identified on the Blue Creek basin boundaries.

During and after the last stages of early Miocene volcanism, low lying areas between volcanic centers filled with course clastic sediments. These sediments are exposed in Eagle Creek Canyon and Juan Miller Basin.

Late Miocene to Pliocene faulting broke the crust along high-angle normal faults to form horsts and grabens. Subsequent erosion and sedimentation filled in the grabens to form the Duncan basin and the Glenwood-Mangas basins and the present day topography. Three major hot springs discharge from fault zones oriented transverse to the drainage of the San Francisco and Gila rivers. Two other hot springs discharge from or adjacent to Tertiary rhyolitic intrusions.

Hot Springs

Five widely separated hot springs representing surface discharge of geothermal convective systems occur in the lower San Francisco River area. Clifton Hot Springs flow from numerous springs and seeps along the San Francisco River in sections 18, 19, 30, Township 4 South, Range 30 East. Discharge from individual springs is small and observed temperatures range between 30°C and 70°C. Spring waters have sodium chloride chemistry with total dissolved solids (TDS) between 7000 and 1400 milligrams per liter (mg/l). These waters have mixed significantly with shallow cold water. Silica concentrations have reequilibrated with quartz as mixing and cooling occurred, suggesting an inhomogenous, with respect to temperature and chemistry, shallow- to intermediate-depth (<2.5 km) reservoir. Quartz geothermometry predicts 90°C to 150°C, shallow- to intermediate-depth subsurface temperatures. A chloride enthalpy diagram and the Na-K-Ca geothermometer predict 150°C to 190°C, deep (>2.5 km) reservoir temperatures. The natural flow rate of the Clifton Hot Springs system is 75.6 liters/sec with a natural heat loss into the San Francisco River of 18 to 27 megawatts of heat energy. Clifton Hot Springs occur on a major fault zone(s) that crosses the San Francisco River.

Gillard Hot Springs, the highest temperature springs in Arizona, discharge 80°C to 84°C water along the banks of the Gila River in Section 27, Township 5 South, Range 29 East. These springs are sodium chloride waters with equal concentrations of sulfate and bicarbonate. Total dissolved solids range between 1200 and 1500 mg/l. These waters have not mixed with shallow cold water. Quartz and Na-K-Ca geothermometers predict 130°C to 139°C subsurface temperatures,

respectively. Silica is in equilibrium with alpha-cristobalite at spring temperatures which suggests only minor silica precipitation as the waters cool. A chemically homogeneous reservoir with a natural discharge rate of 29.9 liters/sec is inferred. Convective heat loss into the Gila River is 7.8 megawatts of heat energy.

Eagle Creek Hot Springs in Section 35, Township 4 South, Range 28 East discharge 42°C sodium rich water with nearly equal concentrations of bicarbonate and chloride. These geothermal waters have total dissolved solids less than 1000 mg/l. Geothermometry of these waters is not reliable due to low discharge rates, probable mixing with cold water, and precipitation of silica and calcite. Silica is in equilibrium with alpha-cristobalite at measured spring temperatures while the Na-K-Ca geothermometers suggest a 115°C subsurface temperature. Eagle Creek Hot Springs is adjacent to the same zone of faults associated with Gillard Hot Springs.

Hanna Creek Hot Springs flow from a rhyolite dome complex in the Blue Range Primitive Area. These springs are sodium chloride waters with 670 mg/l TDS. The chalcedony geothermometer predicts a 60°C temperature while discharge temperature is 55.5^{o}C.

Lower Frisco Hot Springs, New Mexico, are sodium chloride waters with maximum measured temperatures of 49°C. They occur on the banks of the San Francisco River south of Pleasanton adjacent to a major fault zone traversed by the river. These waters are mixed with cold, near-surface water. Geothermometry predicts an 83°C to 102°C shallow- to intermediate-depth (<2.5 km) reservoir. Further work is needed to determine potential deep reservoir conditions and estimate natural flow rate and heat loss.

A warm spring near the Martinez Ranch seeps from a gravel bar of the San Francisco River, adjacent to a small latite intrusion and a fault zone striking NE. A 26.6°C surface temperature, sodium chloride chemistry, and 6594 mg/l TDS suggest the spring is a cooled geothermal water. The chloride/lithium ratio and geothermometry are correlative to Clifton Hot Springs; in fact, both occur on the same northeast-trending structural zone.

Thermal Regime

Seven heat flow measurements are available in the area for interpretation. Analysis of the heat flow data shows significant movement of groundwater, which largely masks the regional conductive heat flow. However, two conductive heat flow measurements from holes near Clifton, in Precambrian granite and Cambrian quartzite, have heat flows of 2.25 HFU and 2.35 HFU. Therefore, the regional conductive heat flow appears to be 2.30 HFU which is somewhat higher than normal for the southern Basin and Range province. Since the youngest silicic volcanism in the area is early Miocene and heat production of the Precambrian granite is tentatively less than 6×10^{-13} cal/cm^{3}sec, the high heat flow, assuming steady state conditions, results from either an anomalously thick, heat-producing crustal layer, the preferred explanation, or high mantle heat flow.

The low measured-heat-flow values, compared to the regional heat flow, result from lateral and downward water flow. In order to conserve energy, the heat losses due to groundwater recharge are apparently balanced by heat gains in discharge areas of the lower San Francisco River area. Hot springs in the lower San Francisco River area are a part of the conservation of mass and energy process.

Available data suggest that the hot springs result from circulating water heated by the high regional heat flow. Deep circulation is facilitated by forced convection induced by the region's highly variable topography and precipitation. In this region, free convection is not believed to be a dominant driving force for the hot spring systems because free convection generally requires great quantities of heat such as with igneous intrusion. Plumbing for the forced convective systems is believed to be vertically permeable fault zones, and brecciated silicic intrusions hydrologically connected below to deep laterally permeable lithology which is overlain by an aquiclude or cap rock. Potentially permeable rocks include the Precambrian rocks and the Coronado sandstone (in fault zones) Paleozoic carbonate rocks, and andesitic or basaltic flows and breccias. Impermeable cap rocks are the Morenci shale, Cretaceous shales, silicic tuffs, and highly indurated volcano-clastic sediments. Because the area is intersected by several major lineaments (Titley, 1976, and Chapin and others, 1978) and is adjacent to the rigid and inferred Tertiary Mogollon batholith (Rhodes, 1976), deep fractures may be dilated by present-day stress to allow deep (>2 km) water circulation.

INTRODUCTION

Five discrete and widely separated hot springs discharge geothermal water in the Lower San Francisco River region. Three of the hot springs are in federal Known Geothermal Resource Areas (KGRA's). The KGRA's are: Lower Frisco Hot Springs KGRA (New Mexico), Clifton KGRA (Arizona), and Gillard Hot Springs KGRA (Arizona). The remaining hot springs occur in Eagle Creek (Eagle Creek Hot Springs) and along Hanna Creek (Hanna Creek Hot Springs). Maximum discharge temperatures recorded at the hot springs range from 42°C (108°F) to 84°C (183°F).

Figure (1) shows the location of the Lower San Francisco River area, hot springs, and KGRA's. The study area straddles the New Mexico and Arizona border at about latitude 33°North. In New Mexico, the study area's eastern extent begins where the course of the San Francisco River changes from south to southwest. In Arizona, the San Francisco River flows south for a short distance then turns southwest again before it empties into the Gila River. Topography in the region is very rugged, creating poor access to many areas by motor vehicle.

This report summarizes the principal featues pertaining to the geothermal potential in the Lower San Francisco River area and recommends additional exploration methods and targets.

The purpose of the investigation is to define areas in the Lower San Francisco River area that may have geothermal resources suitable for direct use, desalination, or electrical generation.

Several requirements must be met to make geothermal energy feasible, the most important of which is the availability of a resource.

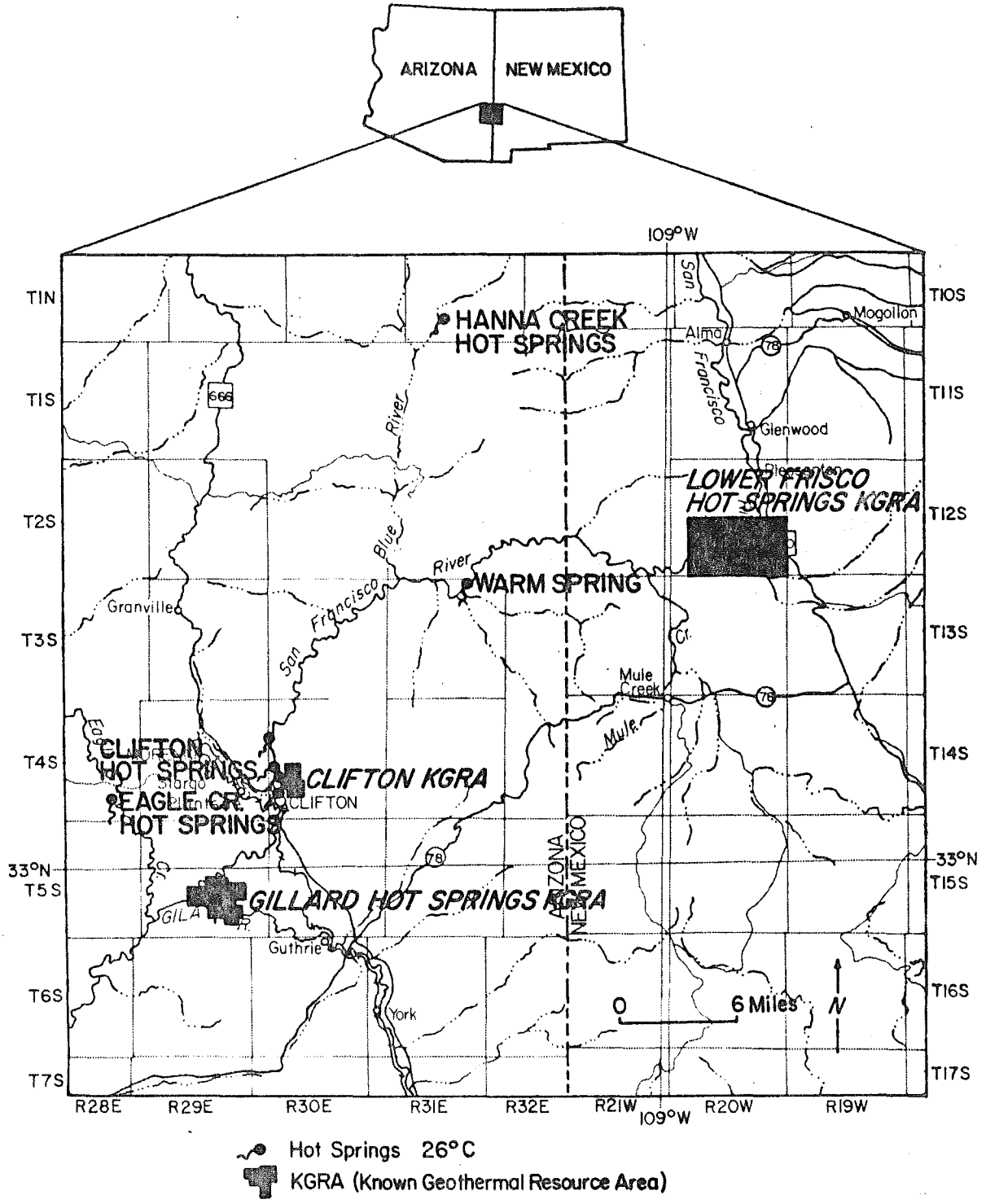

FIGURE I.
LOWER SAN FRANCISCO RIVER STUDY AREA

Additionally, several questions have to be answered concerning the potential resource before development can proceed: Is the potential resource beneath land that is favorable for development? In other words, what are the land ownership, topography, and access? What depth is the reservoir? What production temperatures are likely? What is the chemical quality of the geothermal water? What are the probable reservoir rocks and their reservoir properties? What are the structural geologic controls on the permeability and location of the reservoir? What is the geothermal heat source and the natural heat loss of the geothermal system?

The hot springs in the Lower San Francisco River area target the region for exploration to delineate and define potential geothermal resources.

Geothermal desalination and electrical production using present-day technology require temperatures greater than 180°C (350°F). Direct use applications may use lower temperature water between 30°C and 180°C. Geothermal reservoir production requirements vary depending on the type of utilization.

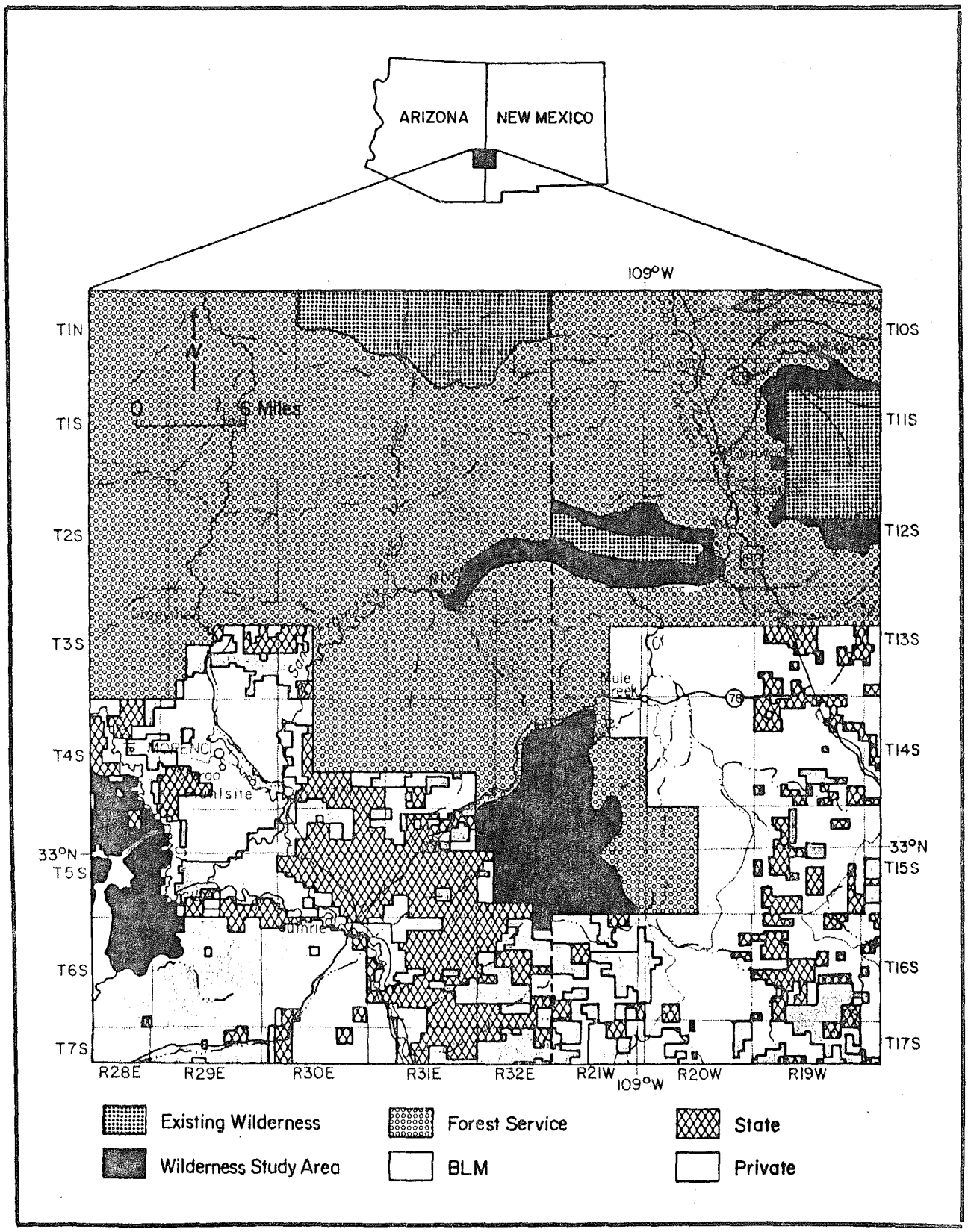

FIGURE 2.
LAND STATUS OF THE LOWER SAN FRANCISCO RIVER AREA

Land Ownership

Predominantly private land ownership occurs in the Mule Creek and Mangas Valley areas (Fig. 2). Private land interspersed with federal BLM land exists in the Clifton-Morenci area and in the Duncan Basin. Most of the lower San Francisco River area is administered by the U.S. Forest Service. Several areas are being studied by the U.S. Bureau of Land Management and U.S. Forest Service for inclusion in the national wilderness system (Fig. 2). Two wilderness study areas are situated on or adjacent to land that is highly prospective for geothermal resources. They include areas west of Gillard Hot Springs KGRA, Arizona, and the lower Frisco Hot Springs KGRA, New Mexico. Portions of the San Francisco River between Clifton, Arizona, and the New Mexico border are under study for designation as a Wild and Scenic River area. The wilderness studies are a serious impediment to exploration and development of the potential geothermal resources in the lower San Francisco River because they will not be completed for many years and they lie on or adjacent to land with high potential for discovery of significant geothermal resources.

REGIONAL SETTING

The lower San Francisco River area lies in a "transition zone" separating the Colorado Plateau and the Basin and Range physiographic provinces (Fig. 3). The Basin and Range province in southeastern Arizona is further divided into two subprovinces, the easternmost of which is the Mexican Highland section.

The Mexican Highland section is high in overall elevation (>914 m) (>3000 ft) and is further characterized by significant topographic relief (>1829 m) (>6000 ft). Great topographic relief and high elevation

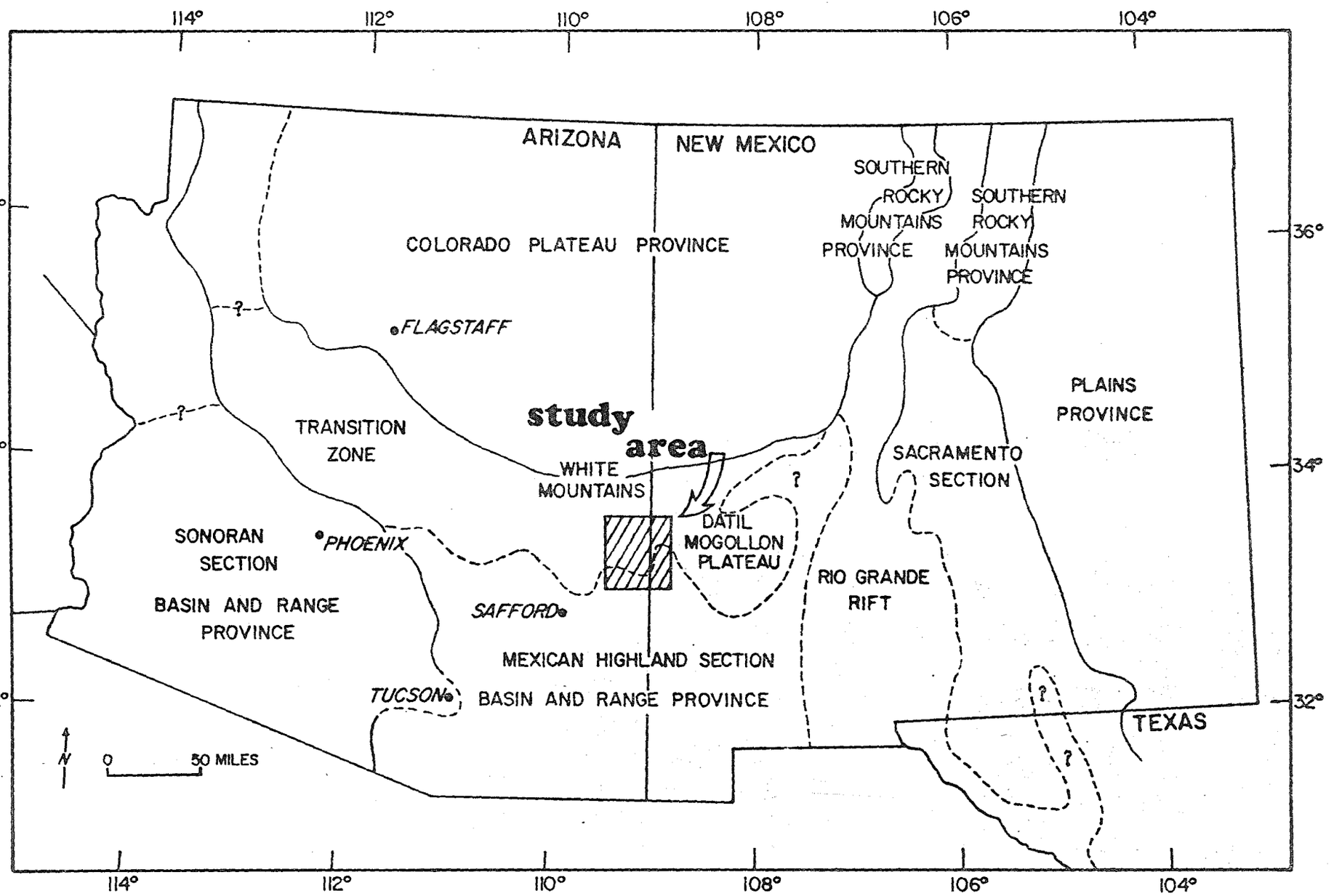

Figure 3: Location map the Lower San Francisco River Area physiographic-tectonic provinces and

may signify young and large-scale tectonism (mountain building), or young epiorogenic (regional) uplift in this region. Numerous through-going rivers and washes flowing north and west cut deeply into sediment-filled valleys. These entrenched streams may result from uplift of the Mexican Highland section relative to the Sonoran Desert section; or they may result from newly acquired communication of the streams into the lower Sonoran Desert section.

The Sonoran Desert section is low in overall elevation (<1067 m) (<3500 ft), subdued in topographic relief (<609 m) (<2000 ft), and characterized by relatively flat valleys. In the Sonoran Desert section, alluvial sediment covers broad erosional pediments and conceals all but the peaks of mountain ranges.

The Mexican Highland section in southeastern Arizona lies in a zone of seismicity that traverses Arizona from northwest to southeast (Sumner, 1976) and may indicate continued tectonism. Active tectonism is frequently accompanied by higher crustal heat flow, which favors increased geothermal phenomena.

North of the lower San Francisco River area on the Colorado Plateau, the overall elevation is over 1524 m (5000 ft) and the topography is relatively subdued except where erosion has cut canyons or shaped mesas in nearly flat-lying sediments. Quaternary basaltic volcanism occurs on the southern boundary of the Colorado Plateau immediately north of the study area (Luedke and Smith, 1978). Topography there is dominated by Mount Baldy, an eroded stratovolcano of late Miocene to Pliocene age (Merrill and Pewe, 1977). The volcanism suggests anomalous subsurface heat or release of pressure to cause melting in the lower crust or upper mantle. An upper mantle heat source or a crustal flaw that has dilated in a recent regional stress field may account for this volcanism

(Stone, 1979). Heat flow studies in the White Mountains have found anomalously high heat flow (>2.0 HFU)[1] for the Colorado Plateau (Stone, 1979; Reiter and Shearer, 1979).

A volcanic pile extruded during Oligocene and Miocene borders the Lower San Francisco River area on the east. This pile, the Mogollon-Datil Plateau, was created by eruptions of andesite followed by voluminous eruptions of silicic lavas and tuffs (Elston and others, 1973). The silicic tuffs and lavas are capped by basaltic andesite flows. The sources for the silicic tuffs and lavas are identified as large (>20 km diameter) resurgent cauldrons (Elston and others, 1973; Elston and others, 1976; and Rhodes, 1976).

A regional gravity low, overlapping resurgent cauldrons, radially oriented dikes (striking toward the Datil-Mogollon Plateau), petrology and chemistry of silicic volcanics, and a circling of graben structures around the Datil-Mogollon Plateau suggest that a large batholith was emplaced during mid-Tertiary beneath the Datil-Mogollon Plateau (Rhodes, 1976B; Elston and others, 1976). The hypothesized batholith appears to be mechanically competent because the Datil-Mogollon Plateau does not exhibit widespread, major post-Miocene faulting (Elston and others, 1976). Structurally competent crust such as a large batholith may affect present day stress fields and tectonics in adjacent areas.

The Lower San Francisco River area lies in the southwestern terminous of a northeast-trending structural zone, which forms the San Augustin Plains in New Mexico. The plains, a sediment-filled graben that forms the northern margin of the Datil-Mogollon Plateau

---

(1) HFU - Heat flow unit - 1×10^{-6} cal/cm^2 sec

and separates it from the Colorado Plateau, is interpreted to be an "arm" of the Rio Grande Rift, a Cenozoic continental rift trending north-south through the centers of New Mexico and Colorado (Chapin and Seager, 1975; Woodward and others, 1975). The Rio Grande Rift differs from the Basin and Range province in its Quaternary faulting, greater volume and distribution of Quaternary basaltic and silicic volcanism, and regional heat flow anomaly (>2.5 HFU). The rift may result from crustal thinning due to local upwarp of the mantle, inferred from high heat flow, chemistry of volcanic rocks, high residual gravity, and anomalous electrically conductive lower crust and upper mantle (Reiter and others, 1975; Decker and Smithson, 1975; Seager and Morgan, 1979; Bridwell, 1976).

Another regional feature with potential significance for geothermal exploration in the Lower San Francisco River area is the Texas Zone which refers to a west-northwest oriented belt crossing southern Arizona through the Basin and Range province (Schmitt, 1966). The belt is defined by west-northwest to west striking outcrop patterns. Evidence for major west-northwest basement structural flaws is circumstantial in most of the belt. However, in a few areas major west-northwest oriented faults occur along the traces of elements of the Texas Zone (Lutton, 1958; Titley, 1976; Drewes, 1971; Drewes, 1972). These elements or linear discontinuities have been involved in numerous tectonic and depositional events since Precambrian. Differential uplift and left-lateral strike slip are documented along portions of the linear discontinuities. Today, the grain of the Texas Zone is observed in outcrop patterns that are elongated trans-

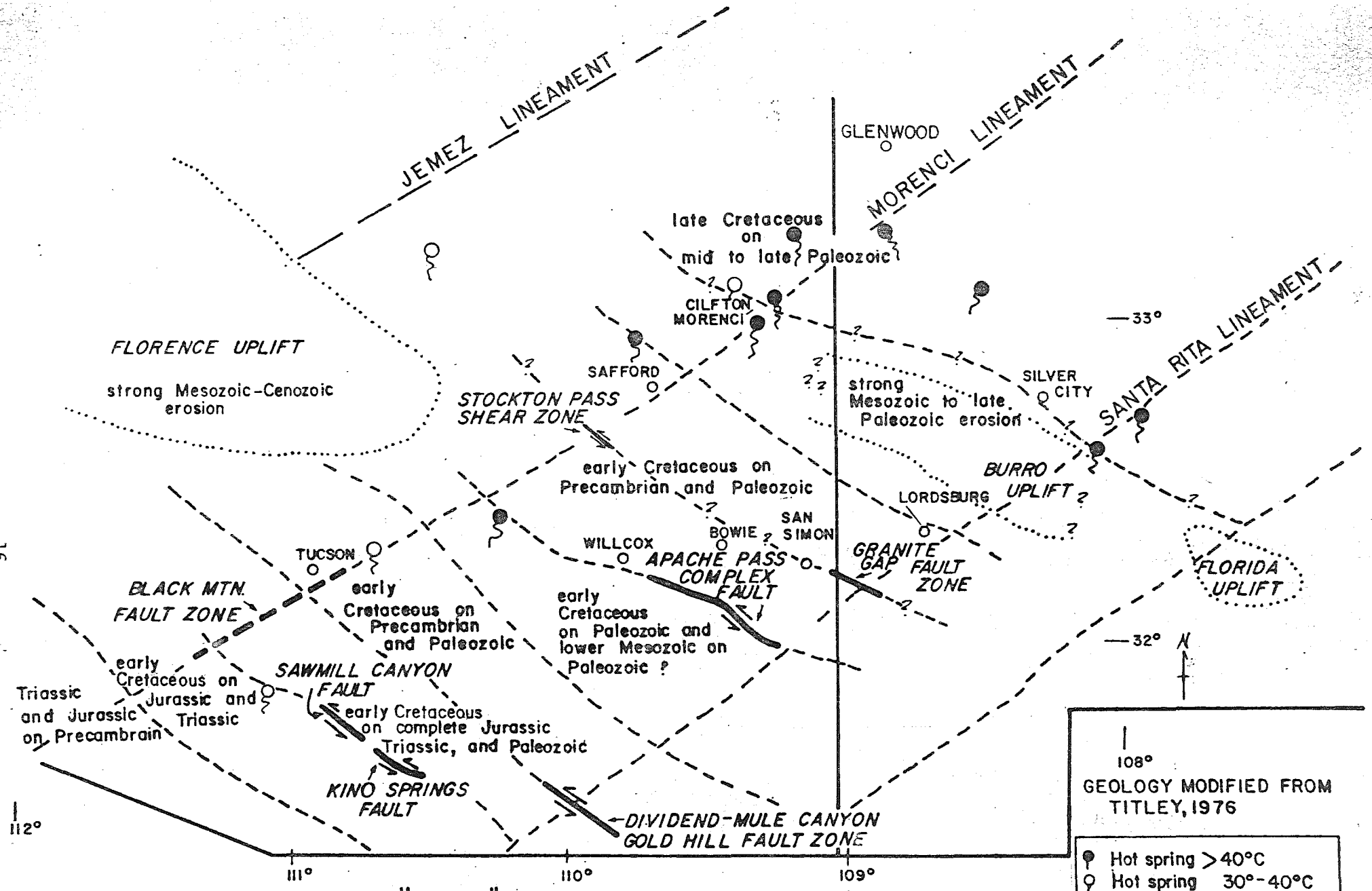

Figure 4: Map showing "Texas" zone discontinuities and lineaments

versely to present landforms (Titley, 1976) (see Fig. 4). Titley (1976) states, "the grain is revealed in at least six presently recognized faults or linear discontinuities which border northwest trending blocks of some 30 to 40 kilometer width. Each block bears its own signature by virtue of unique stratigraphic relationships and by distinctive relationships to adjoining blocks." The Texas Zone linear discontinuities may have originated during the Precambrian and may represent fundamental flaws in the crust of southern Arizona. The Texas Zone discontinuities appear to correlate with late Paleozoic and Mesozoic tectonic and sedimentation patterns in southern Arizona (Elston, 1958; McKee, 1951; Peirce, 1976; Ross, 1973). Elements or linear discontinuities of the Texas Zone that traverse the Lower San Francisco River area may play a role in localizing geothermal activity especially where they intersect north and northeast-trending crustal flaws and structure.

A major northeast-striking feature, the Morenci lineament, crosses the Lower San Francisco River area on a line approximately from Glenwood, New Mexico to Clifton, Arizona. In New Mexico, magma may be localized by the Morenci lineament in the shallow crust beneath Socorro (Chapin and others, 1978). Geologic mapping in the Socorro region defines structure that is interpreted to show the lineament acting as a transform fault where it crosses the Rio Grande Rift. Separated by the trace of the lineament through the Socorro region, normal faults have equivalent strikes but dip in opposing directions, suggestive of left-lateral movement along the lineament. The Morenci lineament is not expressed as a fault per se, but as a

linear zone marked by a variety of geologic and physiographic anomalies. Features of the Morenci lineament in New Mexico are as follows:

(1) Right lateral apparent offset of grabens forming the Rio Grande Rift (Chapin and others, 1978).

(2) A northeast oriented shear zone in the Socorro area separates fields of tilted blocks undergoing rotation and faulting in opposite directions (Chapin and others, 1978).

(3) Localization of the magma beneath Socorro by an inferred shear zone that prevents southward magma migration (Chapin and others, 1978). The shear zone may also bleed magma from depth into shallow, "dike" reservoirs beneath Socorro (Chapin and others, 1978).

(4) Hot springs discharge from the shear zone at Socorro (Summers, 1976; Chapin and others, 1978).

(5) Northeast alignment of at least five Miocene stratovolcanoes along the north margin of the Datil-Mogollon Plateau (Elston and others, 1973).

In Arizona the lineament is characterized as follows (see Figure 4):

(1) The San Francisco River changes direction near Glenwood and follows the lineament.

(2) The Gila River changes course south of Clifton and follows the lineament through the Peloncillo Mountains.

(3) Nearly every mountain range and basin show a "dog leg" at the lineament intersections in southeastern Arizona.

(4) Every other mountain block is structurally high--three of four of these blocks are metamorphic core complexes (Davis and Coney, 1979), with the easternmost in Arizona.

(5) Sediment-filled basins traversed by the Morenci lineament have the lowest and most intense residual Bouguer gravity anomalies in southeastern Arizona (Lysonski and others, 1980). These anomalies are on or immediately adjacent to the lineament. The anomalies are interpreted to indicate that these basins have the greatest thicknesses of basin-filling sediments, which may signify the greatest structural displacements.

(6) Every hot spring with a temperature greater than 40°C in southeastern Arizona occurs within 19 lateral kilometers of this lineament. Sixty percent of all reported warm and hot springs (>30°C) in Arizona occur within 48 kilometers of this lineament (see Figure 4).

(7) An inferred, northeast-striking structural zone crosses the Tucson area on trace of the Morenci lineament. Gravity and resistivity data suggest a fault on the north side of the Sierrita Mountains (Vroman, 1976; Davis, 1971). En echelon faults are observed along the northeast-trending Black Mountain (Percious, 1968). An aeromagnetic anomaly follows the same trend across the Tucson basin (Sauck and others, 1971). A groundwater "fall" also occurs along this trend in the Tucson basin and suggests an impermeable fault boundary (Davidson, 1973). All of these features are on strike with one another.

(8) Three different clusters of major Laramide copper deposits occur within 24 kilometers of the Morenci trend where it transects linear discontinuities of the Texas Zone; they are the Pima Mining District, Safford Mining District, and the Morenci Mining District.

The lower San Francisco River area lies on the northern and western flanks of the Mesozoic Burro Uplift (Elston, 1958), a west-northwest trending basement uplift that may be an element of the Texas Zone (Turner, 1962). All Paleozoic and Mesozoic rocks except for Late Cretaceous deposits are stripped from the center of the uplift (Elston, 1958; Hewitt, 1959). The Burro Uplift has very important implications concerning the location and extent of potential geothermal reservoirs in the Lower San Francisco River area. These implications will be discussed in detail later in this report.

The poorly defined "transition zone" in which the study area lies is relatively high in elevation and is cut by several deep canyons. Geologically, the transition zone is not as structurally complex as the Basin and Range province, nor as simple as the Colorado

Plateau.

Generally, the Lower San Francisco River area more closely resembles the Basin and Range province than the Colorado Plateau because the area has undergone a series of complex Cenozoic tectonic events characterized by faulting and extensive volcanism. From a regional stand point, this region is most favorable for geothermal exploration because:

(1) The Colorado Plateau north of the area is geothermally anomalous as evidenced by high heat flow and Quaternary basaltic volcanism.

(2) The Basin and Range province (Mexican Highland section) to the south and west may be tectonically more active than the Sonoran Desert section of southwestern Arizona. If epirogenic uplift is occurring, heat flow may also be higher in this area.

(3) The mechanically competent Datil-Mogollon Plateau may cause dilation along old structures in the Lower San Francisco River area because the present day stress fields are modified by the rigid batholith beneath the plateau. Dilated crust may host magmatic intrusions or geothermal reservoirs.

(4) The Lower San Francisco River area lies in the intersection(s) of the Morenci lineament and elements of the Texas Zone. These lineaments may be fundamental flaws in the crust, creating vertical permeability or structurally favorable reservoirs. Magma may also bleed upward through these flaws.

STRATIGRAPHY

A great variety of rock types and ages are found in the lower San Francisco River area. Granite, granodiorite, and diorite comprise the bulk of Precambrian and late Cretaceous-early Tertiary age crystalline rocks exposed in the Clifton area. Outcrops of Precambrian schist and metaquartzite, probably correlative to the Pinal Schist, were identified by Lindgren (1905), Moolick and Durek (1967), and Langton (1973). Paleozoic rocks, which depict a time of relative tectonic quietude, unconformably overlie the Precambrian rocks. Within the Paleozoic section, a basal arkosic sandstone is overlain by a sequence of interbedded sandstones, shales, and carbonate rocks that become increasingly carbonate rich as they go upsection and become younger in age. All Paleozoic periods except the Silurian and Permian are represented by the local stratigraphic column (Lindgren, 1905). Silurian rocks are not found in Arizona because they were never deposited or were stripped away by erosion during late Silurian or early Devonian (McKee, 1951). Permian rocks are not exposed; but they may exist in structural lows where they would be protected from erosion and concealed by Tertiary sedimentary and volcanic rocks. Unconformable relationships are observed between the Ordovician and Devonian rocks (the missing Silurian rocks) and between the Devonian shales and the Mississippian carbonates (Lindgren, 1905). Deeply eroded Pennsylvanian carbonate rocks are exposed north of Clifton, Arizona, along Highway 666 in the vicinity of Mitchell Peak (Lindgren, 1905; Ross, 1973).

The region is greatly disturbed by Mesozoic and Cenozoic tectonism. Mesozoic and Tertiary uplift and erosion exposed lower Paleozoic rocks and Precambrian rocks in the Clifton area. Triassic, Jurassic, and early Cretaceous rocks are not observed in the Clifton area, which may indicate that no deposition occurred during these periods or that Cretaceous erosion removed them (Lindgren, 1905). Late Cretaceous fine-grained clastic rocks of shallow marine and terrestrial origin overlie Paleozoic and Precambrian rocks in the Clifton area, in the Silver City, New Mexico area, and in the northern Big Burro Mountains southwest of Silver City near Redrock (Lindgren, 1905; Hewitt, 1959; Kottlowski, 1963). Tertiary stratigraphy is dominated by middle Tertiary volcanic rocks. Continental clastic sediments comprise the remaining volume of Tertiary rocks in the lower San Francisco River area.

Hot springs in the area may result from groundwater circulating through rocks heated by a young and still-hot intrusion or through hot rocks at great depth that are heated by the normal regional flux of heat conducting out of the earth's interior. In either case, permeable rocks are required for the water to circulate. Permeability is accomplished in two ways or their combination. A rock may be inherently permeable or the rock may have been mechanically fractured during tectonism or magmatism. Thus, the stratigraphy and structure in a region are exceedingly important factors to observe when searching for geothermal resources.

Limited exposures of Precambrian and Paleozoic rocks make it difficult to evaluate them as potential reservoirs. Since Paleozoic tectonics are rather subdued in Arizona and New Mexico, reliable in-

ferences may be drawn by studying the limited outcrops at Clifton in reference to regional Paleozoic stratigraphy. This is because drastic facies changes are exceptional during tectonic quiescence; thus, applying the stratigraphic relationships of the Clifton area to the larger lower San Francisco River area is justified.

Precambrian metaquartzites striking east and dipping very steeply south crop out north of Clifton (Lindgren, 1905; Moolick and Durek, 1966). Tightly overturned folds are observed in the metaquartzite, which is possibly correlative to the Pinal Schist of Ransome (1903). A coarse red granite comprises the bulk of the Precambrian rocks around Clifton. A possibly younger and less widespread Precambrian granodiorite also occurs there. Younger Precambrian sedimentary rocks found elsewhere in south-central Arizona, which would include the Apache Group, are not observed in this area.

The base of the Paleozoic section of rocks in the San Francisco River area is represented by the Coronado Sandstone, called the Coronado Quartzite by Lindgren (1905) and believed to be middle Cambrian to late Cambrian age (Hayes, 1978). The Coronado Sandstone is an arkose at its base, which includes a discontinuous basal conglomerate derived from the underlying Precambrian granitic terrain. The upper part of the Coronado Sandstone is mostly quartz sand. Some shales and silts are interbedded in the formation but they comprise less than 30 percent of the formation. Quartz is the most important cement although dolomitic cement is locally important in the upper part of the formation. The Coronado is interpreted to

represent beach sands of the eastward migrating Abrigo seashore. The Coronado Sandstone is correlative with the Bliss Sandstone in New Mexico and the Abrigo Formation to the west in south-central Arizona. Primary reservoir characteristics of this formation are very poor due to the pervasive quartz cement, which has destroyed the primary porosity. However, fracture permeability is potential because the formation is very brittle. Thus, where the Coronado Sandstone is structurally deformed very good fracture permeability may result. Chalcocite secondary copper enrichment occurs in the fractured Coronado at Morenci. The thickness of the Coronado ranges from 45.7 m to 76.2 m at Clifton.

Conformably overlying the Coronado is the El Paso Limestone or the Longfellow Formation of Lindgren (1905). The El Paso Limestone is comprised of two members (Hayes, 1978; Hayes and Cone, 1975). The lower member consists of sandy or silty dolomite interbedded with dolomitic sandstone and is probably equivalent to the Copper Queen member of the Abrigo Formation to the west. The upper member consists of thin-bedded cherty limestone or dolomite that was dated with fossils as early Ordovician. The El Paso Limestone represents shallow near-shore marine deposition in the eastward transgressing Abrigo sea. The El Paso Limestone is equivalent to the upper Bliss Sandstone and El Paso Group in New Mexico and west Texas (Hayes and Cone, 1975). Porosity of the lower member averages about 3.1 percent in New Mexico and west Texas and was described as being dominantly primary porosity with some vuggy and fracture porosity (Hayes and Cone, 1975). Porosity in the upper El Paso Lime-

stone averages 1.9 percent in New Mexico (Hayes and Cone, 1975). Thickness of the El Paso Limestone ranges from 61 m to 122 m in the Clifton area (Lindgren, 1905).

The El Paso Limestone is disconformably overlain by the Ordovician Second Value Dolomite of the Montoya Group (Hayes, 1978). A dark gray, partly dolomitized, coral-bearing, crinoidal, marine limestone comprises the Second Value Dolomite at Clifton. Lindgren (1905) includes the Second Value Dolomite, 4.6 m thick, in the Longfellow (El Paso) Limestone. Measured porosities of the Second Value Dolomite in New Mexico and west Texas average 4.8 percent and have average effective porosities around 3 percent, indicating moderate permeability (Hayes and Cone, 1975).

The El Paso Limestone does not appear to be a good reservoir host although isolated aquifers may exist in the lower member. The Second Value Dolomite has moderate porosity and permeability and may have geothermal reservoir potential where it is fractured in structural zones. In the lower San Francisco River area, the Second Value Dolomite is overlain by dark shales of Devonian age, which could serve as an aquaclude or "cap rock."

A relatively thin upper Devonian strata, 30-50 m, disconformably overlies the early Ordovician rocks. These rocks evidence two major depositional cycles separated by epeirogenic uplift and erosion (Schumacher, 1978). In the Clifton area, the Morenci Limestone, lower member of Lindgren's (1905) Morenci Formation, is a 23 meter thick representative of the lower depositional cycle (Schumacher, 1978). This black and knobby argillaceous limestone is equivalent to the

Martin Formation southwest of the study area and the Ready Pay Member of the Percha Shale Formation in New Mexico (Schumacher, 1978). The cessation of the first depositional cycle and withdrawal of the seas to the west coincided with a pulse of orogeny west of the Clifton area. The second depositional cycle began as a result of intensified orogeny to the west, which displaced a Devonian seaway eastward, flooding the lower San Francisco River area. Sediments deposited during this last Devonian cycle are represented by the Morenci Shale, which is equivalent to the Percha Formation on the west and the Box Member of the Percha Shale in New Mexico (Schumacher, 1978; Kottlowski, 1963). The Morenci Shale, upper member of the Morenci Formation, is an olive-brown to reddish-brown fissile, 31-m thick, rock that is a potentially very important aquiclude or "cap rock" in the lower San Francisco River area.

Mississippian carbonate rocks overlie the Devonian clastic rocks. The Modoc Formation of Lindgren (1905) is a 52-m thick gray, fossiliferous limestone with minor dolomitic limestone and calcareous quartzite beds. A thick, massive cliff forming crinoidal limestone (26 m thick) that is almost pure calcium carbonate comprises the bulk of the formation (Lindgren, 1905). The Modoc is part of an extensive depositional unit of a shallow, mostly sediment free sea. In New Mexico, the Lake Valley Limestone of the lower Magdalena group is equivalent to the Modoc; in Arizona, the Modoc is equivalent to the cliff-forming Escabrosa Limestone of southern Arizona and the Redwall Limestone of the Grand Canyon Region of northern Arizona (Armstrong and Mamet, 1978). The Mississippian limestones are poten-

tially very significant aquifers as evidenced by tremendous springs discharging several hundred liters of water per second in the Grand Canyon and the Mogollon Rim areas (Feth and Hem, 1963). Havasu Springs in the Grand Canyon discharge from the Redwall Limestone. Numerous caverns and solution cavities are observed in the Mississippian limestones throughout the Southwest. Mississippian limestones are also important hosts to hydrothermal ore deposits (fossil geothermal systems) in the Southwest (at Morenci, the Modoc is mineralized and silicified). Clearly, the Modoc Limestone is a potentially very important geothermal aquifer given the right combination of structural setting and deep burial.

Lindgren (1905) described a cherty limestone that was locally called the Blue limestone by miners at Morenci. This formation that Lindgren (1905) called the Tule Springs Limestone unconformably overlies the Modoc Limestone. Ross (1973) designated a 91 m thickness of this limestone as the Pennsylvanian Horquilla Limestone.

In the Clifton area, the Horquilla Limestone is between 40 and 50 percent carbonate. The Horquilla Limestone is also a potential reservoir rock due to secondary porosity resulting from solution and vuggy porosity, and fracture porosity in structural zones.

Permian rocks are not observed in the lower San Francisco River area. Continuation of regional Permian isopach contours across the area suggests that up to 457 meters of Permian strata may have been deposited (Peirce, 1976). Permian rocks were either stripped away by erosion or they are concealed by volcanic rocks in structural depressions. If they are present, red siltstones and clay probably

comprise the bulk of Permian strata in the lower San Francisco River area. Red siltstones of the Abo Formation outcrop in the Silver City area east of the lower San Francisco River area while the Supai Formation, mostly red clay and siltstone, crops out to the northwest (McKee, 1951; Kottlowski, 1963; Peirce, 1976). If the Permian rocks are present in the structural depressions of the area, they will not be good aquifers due to their probably argillaceous lithology. However, if present in the subsurface, they may serve as a cap rock or aquiclude over potentially permeable Pennsylvanian and Mississippian carbonate strata.

Late Paleozoic (Pennsylvanian-Permian) was a time of increasing tectonic activity, which evolved into orogeny during the Mesozoic and Cenozoic.

Jurassic or Triassic age rocks are not observed in the area. At Clifton, Late Cretaceous clastic rocks unconformably overlie the Mississippian Modoc Limestone and the Devonian Morenci Shale. Lindgren (1905) named these sediments the Pinkard Formation. Black shale interbedded with yellow-brown sandstone comprises the Pinkard Formation. At least 61 m of the Pinkard Formation remains in an outcrop southwest of Clifton (Lindgren, 1905). Over 305 m of Late Cretaceous sandstone and shale are observed in New Mexico south and east of the Lower San Francisco River study area. These sediments, called the Beartooth Sandstone and the Colorado Shale, overlie Precambrian rock in exposures on the Burro uplift and overlie Paleozoic rocks north of the Burro uplift (Elston, 1958; Hewitt, 1959; Kottlowski, 1963). The Late Cretaceous rocks are not good aquifers. However,

they are good aquicludes and may act as excellent cap rocks on possible Paleozoic carbonate and sandstone aquifers.

Paleocene (Laramide) magmatism intruded diorite, quartz monzonite, and granite into the area of the Morenci copper mine and mineralization is associated with these intrusions. This plutonism intruded Precambrian, Paleozoic and Cretaceous rocks as stocks and laccoliths.

Tertiary stratigraphy in the Lower San Francisco River area is dominated by volcanic rocks. Subordinate clastic rocks are interbedded in the volcanic flows. In areas deformed by Miocene and Pliocene faulting, relatively thick sequences of clastic rocks overlie the volcanics.

Even though Tertiary volcanic rocks have long since lost their heat content, they have an important impact on the geothermal potential of the region because these rocks may act as host aquifers.

Volcanic eruptions differing in source, style, and time have resulted in a thick pile of volcanic rocks in the area. Andesite and basaltic andesite flows that originated from probably mid-Tertiary stratovolcanoes comprise 80 to 90 percent of the observed volcanic sequences. An additional 10 to 20 percent of the volcanic section is represented by felsic lavas, tuffs, and breccias erupted in association with cauldron collapse or dome extrusion.

Andesites extruded 37 m.y. ago occur in the Blue Range Primitive Area just north of the Lower San Francisco River area (Ratte and others, 1969). In the Blue Creek basin, a 2- to 3-km thick sequence of interbedded rhyolite ash flow tuff and andesite (Virden Dacite, of Elston, 1960) is overlain by andesite porphyry flows dated at 34.7 m.y. (Seager and Clemons, 1972; Berry, 1976). At Clifton, an

ash flow tuff dated at 32.9 m.y. unconformably overlies Paleozoic rocks (Damon and associates, 1966). Andesite flows overlying the 32.9 m.y. ash flow tuff at Clifton are correlated with a red vesicular andesite deposited on an ash flow tuff resting on the 34.7 m.y. andesite flows in the Blue Creek basin (Berry, 1976). These andesites and contemporaneous rhyolite flows and ash flow tuffs are considered equivalent to the 40 to 28 m.y. old Datil Group volcanics of Elston (1968).

On the eastern margin of the Lower San Francisco River area, between 27.5 and 25 m.y. cauldron collapse occurred to form the Bursum cauldron (Rhodes, 1976). Volcanism associated with the Bursum cauldron subsidence and resurgence resulted in deposition of a thick pile of ash flow tuff and extrusion of rhyolite domes in the cauldron moat and ring fracture zone. These rhyolite tuffs and lavas are interbedded with andesite that flowed into the cauldron moat from the south and west (Rhodes, 1976). A "turkey track" andesite overlying the Datil Group in the Blue Creek basin area (Seager and Clemons, 1976) may be correlative to the andesites in the Bursum cauldron moat. In Arizona, most "turkey track" andesites are 25 to 28 m.y. in age; however, it should be noted that a few "turkey track" andesites are 35 to 43 m.y. in age

After an apparent 5 to 7 m.y. quiescence of volcanism in the western three quarters of the Lower San Francisco River area, basaltic andesite and minor felsic volcanism began. In the southern half of the Blue Range Primitive Area, quartz latite and rhyolite ash flow tuffs, breccias, and lavas dated at 23 to 24 m.y. are associated with

small cauldrons and dome complexes (Ratte and others, 1969). Basaltic andesite lavas and breccias were erupted from several possible stratovolcanoes to bury the entire Lower San Francisco River area. The basaltic andesites range in age from 25 to 20 m.y. (Ratte and others, 1969; Berry, 1976; Strangway and others, 1975).

Near the close of basaltic andesite volcanism, rhyolite tuffs, lavas, and breccias were erupted in a zone trending northwest across the area north of Clifton. Two probable nonresurgent cauldrons, Mule Creek and Enebro Mountain occur along this zone (Rhodes and Smith, 1972; Berry, 1976). Numerous northwest trending felsic dikes are observed along with rhyolite domes in the San Francisco River Canyon north of Clifton. Thickness and physical character of these volcanic rocks will determine their role in influencing the geothermal environment of the area.

Great thicknesses of volcanic rocks bury potential Paleozoic aquifers and older mid-Tertiary volcanic rocks at depths where temperatures are high. Water heated in these aquifers may flow to the surface or to shallow depths through vertically permeable zones. Brecciated zones along faults or dikes and plugs can provide vertical permeability.

Excellent aquifers are known to occur in volcanic rocks. Highly productive aquifers occur in basalt flows in the Snake River Plain, Idaho, and the Columbia Plateau, Washington. Mid-Tertiary volcanic rocks host excellent aquifers in the Dateland-Hyder area and Bonita Creek area in Arizona (Heindl, 1967).

Basaltic and andesitic flows are probably the best potential

volcanic aquifers. These lava flows are typically fractured and brecciated and occur as individual flows 5 to 20 m thick in sequences up to 700 m thick. Usually the surfaces of individual flows are very scoriaceous and brecciated. Thick flows frequently have vertical cooling fractures that traverse most of the flow interior. Thin and permeable alluvial gravel deposits frequently overlie individual flows. Depending on the degree of fracture permeability and vesicularity, and lack of cavity filling from diagenesis, these rocks make very good potential geothermal aquifers when deeply buried.

Other potential aquifers and recharge areas are felsic domes and dikes because they are sometimes highly fractured.

A known low-temperature ($48^{o}C$-$56^{o}C$) geothermal reservoir occurs in basaltic andesite flows at a depth less than 100 m in Eagle Creek Canyon, just west of Clifton (Heindl, 1967). The hot water in this aquifer has artesian pressure and rises in the wells nearly to the surface. Wells tapping these aquifers are reported to pump up to 60 liters/sec (Heindl, 1967).

Figure 5 shows composite sections of the volcanic stratigraphy in the Lower San Francisco River area. Table 1 lists by stratigraphic section the location of each volcanic unit with pertinent information and references.

Cenozoic sediments in the area may be separated into two broad groups. The first and older group includes those sediments that are interbedded with or overlain by mid-Tertiary volcanic rocks. The younger group are sediments that overlie volcanic rocks or that fill Late Cenozoic structural basins. Cenozoic sediments in the Clifton area

are predominately coarse-grained clastic rocks of non-marine origin. Gilbert (1875) applied the term "Gila Conglomerate" to these rocks.

Subsequent studies (Heindl, 1958) have shown that the Gila Conglomerate is actually several noncontinuous conglomerates with different ages, compositions, tectonic positions, origins and extents; therefore, the Gila Conglomerate is actually the entire sequence of Cenozoic sediments in the study area and are not a laterally extensive and mapable stratigraphic unit or formation (Heindl, 1962).

In the Clifton-Morenci area, Heindl (1958) studied excellent exposures of Cenozoic sediments along the Gila River, San Francisco River, and Eagle Creek.

In Eagle Creek, a dark red-brown boulder conglomerate composed of basaltic boulders set in a matrix of basaltic and rhylolitic pebbles unconformably overlies Tertiary basaltic andesite. This basal conglomerate, called the Bat Beds by Heindl (1958), is discontinuous and observed only in Eagle Creek Canyon.

Unconformably overlying the Bat Beds and the volcanic rocks are the Gold Gulch Beds (Heindl, 1958). This unit was mapped by Lindgren (1905) as a rhyolite tuff breccia; however, the presence of cross-bedding, cut and fill channeling, and rounded clasts attest to alluvial deposition as opposed to a pyroclastic origin. The Gold Gulch Beds dip gently northeast and are in fault contact with pre-Tertiary rocks east of Eagle Creek. Rhyolite clasts predominate over minor basaltic clasts in the 300-meter thick Gold Gulch Beds.

Relatively flat-lying sediments, which fill the Duncan Basin, are observed in unconformable depositional contact with the older and

tilted sediments (Gold Gulch Beds) near the confluence of the Gila and San Francisco Rivers (Heindl, 1958). These younger sediments are fluvial deposits consisting of mostly basaltic gravels with a few distinctive red granite clasts. Heindl (1958) named the basin-filling sediments the Greenlee Beds. A basal and basaltic boulder conglomerate forms the base of the Greenlee Beds at Gillard Hot Springs where it is observed to be in depositional and fault contact with the older Gold Gulch Beds. The basal conglomerate is well cemented as is the Gold Gulch unit while the upper and middle Greenlee Beds are less indurated. The Greenlee Beds appear to be an excellent shallow, cold-water aquifer at the Clifton 1 heat flow drill site at Three Way, near the Gila River.

The Gold Gulch Beds do not make good aquifers because they are very indurated by calcareous cement and very few springs are observed in this unit.

Northeast of Clifton, a gray to reddish conglomerate with gentle dips is interbedded with minor ash flow tuff and basaltic andesite flows. In the Juan Miller basin, these sediments are 600 to 700 m thick (Berry, 1976). Faulting has displaced the conglomerate up to 100 m and numerous basaltic dikes are observed in the lower part of the unit but not in the upper part (Berry, 1976; Ratte and others, 1969). The conglomerate in the Juan Miller Basin area is capped by basaltic flows along U. S. Highway 666 on 4 Bar Mesa (Berry, 1976). These sediments are probably equivalent to the Gold Gulch Beds or are older.

STRUCTURE

Geologic structure of the lower San Francisco River area ultimately controls the location and lateral extent of the geothermal resources. Structures in the area have evolved episodically through geologic time. Different tectonic and depositional environments existing at different times have created a variety of potentially favorable structures for geothermal reservoirs. Frequently, these structures are superimposed, enhancing their size and potential as reservoirs. Known geothermal resources frequently occur in the intersections of structures.

Geologic structures in the area create favorable vertical and lateral permeability and they displace permeable rocks to sufficient depth for significant heating to occur by normal flow of heat from the earth's interior. If cap rocks exist, the temperature of the deep-downward displaced reservoir will remain high because fluid leakage out of the reservoir will occur in limited flows only along vertical fracture zones or faults that exist in the overlying formations. Thus, faulted and fractured zones can become shallow geothermal reservoirs where upward leakage occurs. These shallow reservoirs may manifest themselves as hot springs where the topography and water table (piezometric surface) intersect.

Structural geometry resulting from tectonic movement and post and syn-tectonic sediment deposition or erosion may provide favorable combinations of reservoir host rocks and cap rocks to form "stratigraphic traps." One such tectonic event has occurred in the Clifton area during the Cretaceous. Similar traps may also evolve during volcanism where episodic and changing styles and compositions of vol-

canic eruptions result in mud flows and unwelded tuffs overlying permeable volcanic sequences such as fractured basaltic flows and fractured welded tuffs.

Very deep structural features occur in the Precambrian rocks of this region. The apparent regional crustal discontinuities evidenced by the Texas Zone and the Morenci lineament are possibly the result of reactivation of major Precambrian structures. The Morenci lineament direction correlates with the northeast direction of major Precambrian structures in Arizona. Elsewhere in southeastern Arizona, the oldest Precambrian rocks, the Pinal Schist, are believed to represent major northeast-trending regional structural deformation (Silver, 1978). Near the trace of the Morenci lineament in northwest Cochise County, the Pinal Schist is highly deformed and forms a large (40 km) wide anticlinorium that exhibits strongly overturned folds (Silver, 1978). The schist is intruded by granite and granodiorite plutons in a relationship that is similar to those seen at Clifton. Due to the intense tectonic deformation, it is reasonable to infer the existence of deep Precambrian structures in the Clifton area, which could allow deep forced convective flows of water if dilated by present day stresses.

Paleozoic structural deformation was limited to broad epiorogenic movements. While these movements may cause favorable stratigraphic sequences for reservoirs, they do not cause favorable fracture zones for reservoirs or vertical water movement. Langton (1973) reported the existence of an interformational conglomerate of Ordovician age resting on Precambrian rocks north of Clifton. This would

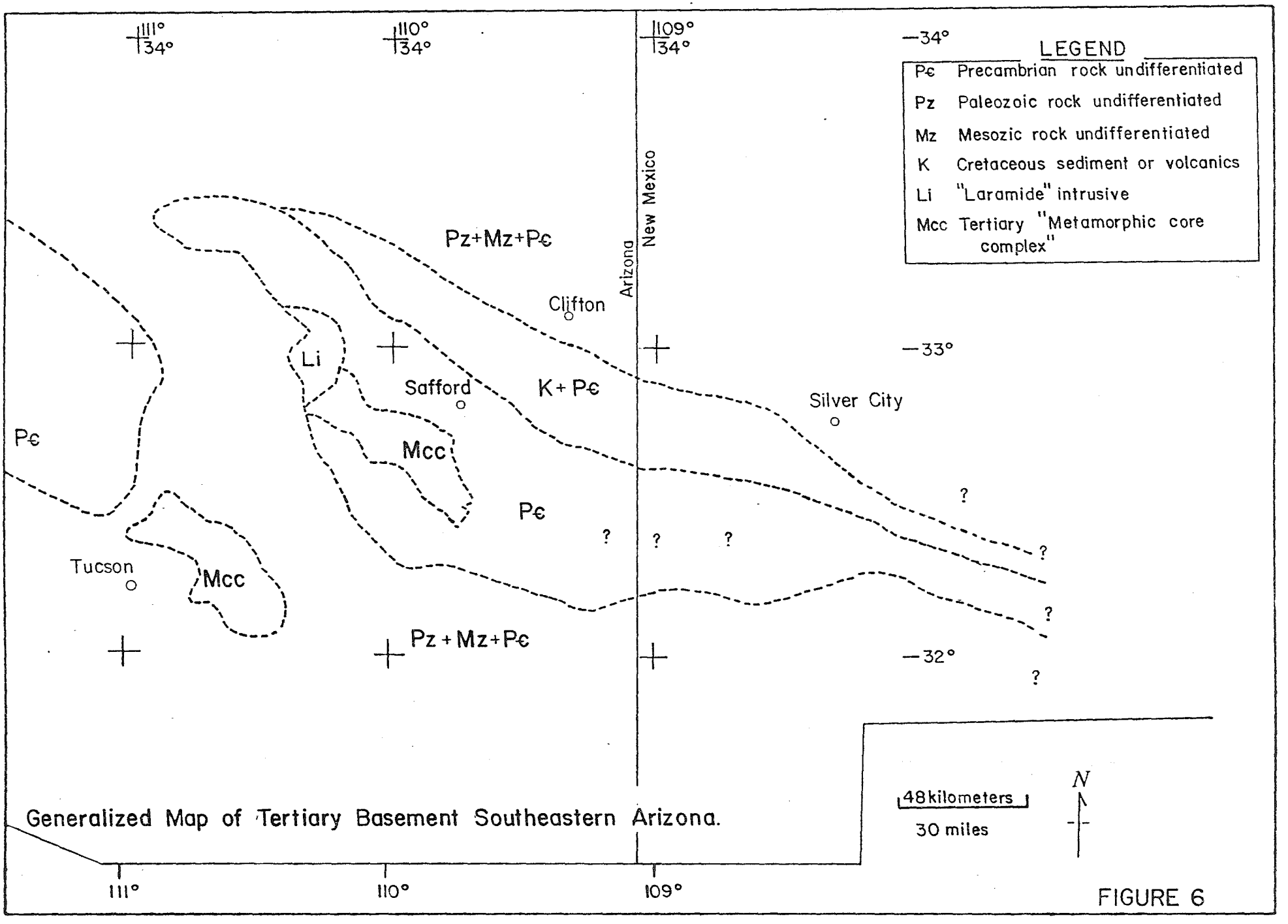

Generalized Map of Tertiary Basement Southeastern Arizona.

FIGURE 6

suggest possible early Paleozoic fualting. However, recent mapping in the area suggests that Langton (1973) was observing a thrust fault (Cunningham, 1979). This fault is described in the following discussion on Mesozoic deformation.

The Mesozoic was a time of orogeny. Uplift of the area south of the San Francisco River area and subsequent erosion has evidently stripped away the Paleozoic stratigraphic section. Elston (1958) named this Mesozoic orogenic feature the Burro uplift. North of the uplift, which is centered in the present day Burro Mountains, progressively older Paleozoic rocks are observed in outcrop as the uplift is approached. Late Cretaceous sediments are observed unconformably overlapping both the Precambrian rocks on the uplift and the Paleozoic rocks on the uplift margins. Thus, the uplift is post Permian and pre-Late Cretaceous.

The actual extent of the uplift is uncertain due to a widespread cover of Tertiary sedimentary and volcanic rocks; however, it is believed the uplift trends west-northwest in conformance with the trend of Mesozoic tectonic features inferred to comprise elements of the Texas Zone. Figure 6, a generalized map of the Tertiary basement in Arizona and southwestern New Mexico, shows that the Pinaleno Mountains may be a western extension of the Burro uplift. However, this is uncertain because Tertiary tectonism may have removed the Paleozoic rocks. The Pinaleno Mountains are a Tertiary metamorphic core complex (Davis and Coney, 1979). Listric normal faulting merging into an inferred dislocation surface near the top of the core complex may have shed the Paleozoic cover off the Pinaleno Mountains as a set of

shingle-like blocks into the lowlying surroundings. It is not known for certain if these relationships exist in the Pinaleno Mountains.

The relationship of the Burro uplift to the location of potential Paleozoic reservoir rocks is of primary importance. In areas overlying the uplift most of the Paleozoic cover is absent. However, it may have exposed Paleozoic limestones to chemical solution on its margins creating secondary permeability. Later burial of these rocks by Late Cretaceous shales provides a cap rock over the Paleozoic limestones. Southwest of Morenci, Cretaceous shales disconformably overlie the Mississippian Modoc Limestone.

Compressional tectonism is evident in the Clifton area. A thrust fault has been mapped on the east side of the San Francisco River north of Clifton (Cunningham, 1979; Lindgren, 1905). Geologic cross sections of the Clifton quadrangle (Lindgren, 1905) show additional low-angle faults in upper Chase Creek between Metcalf and Pinal Point. The extent and origin of these faults is uncertain.

The thrust fault north of Clifton displaces Ordovician El Paso Limestone into low angle fault contact with the Precambrian granite. Brecciation and shearing is observed at the contact. Sheared lenticular carbonate lenses are inbedded in a sheared sandstone immediately overlying the fault. This shear zone may represent Langton's (1973) interformation conglomerate. Hydrothermal alteration has locally removed the carbonate lenses to give the sandstone a "compressed Swiss cheese" appearance. The contact between the overlying sheared El Paso Limestone and the granite is folded, suggestive of post-faulting compression.

The thrust may be intimately associated with Paleocene intrusions that are associated with mineralization at Morenci or it may be associated with earlier tectonism that formed the Burro uplift. Bennett (1975) tentatively identifies Paleozoic quartzite (Coronado) and shale in the Morenci breccia pipe in the Morenci mine. Bennett also pointed out that these rocks may be fragments of Pinal Schist or altered zenoliths from Laramide intrusions.

Origin and extent of the low-angle faults are speculative and require further geologic mapping and geophysical investigation. It is an important question concerning geothermal potential because an overthrust in the Clifton area could profoundly control geothermal convection systems.

The first Laramide (Paleocene) intrusion is a hypobysal tonalite porphyry southwest of Morenci (Langton, 1973). The largest and most widespread intrusion is a quartz monzonite-monzonite porphyry complex. The quartz monzonite intrusion is elliptically shaped in a northeast direction (Langton, 1973). It forms an apparent laccolith in the Paleozoic sediments, but appears to be passively intruded into the Precambrian granite (Langton, 1973). Diabase dikes and sills intrude the monzonite intrusions and Precambrian granite.

A Paleocene granite porphyry is intruded into the older intrusions (Langton, 1973). The breccia pipes at Morenci are associated with this last phase of Paleocene magmatism (Bennett, 1975).

Analysis of U-2 black and white aerial photography reveals numerous close-spaced "fracture" lineaments oriented N. 25°-45° E. in the Precambrian granite immediately north and east of the Paleocene

intrusions and in conformance with the elongation of the Paleocene plutons and associated dikes.

No record of tectonic and depositional events exists between 55 and 33 m.y. at Clifton. An ash flow tuff dated as 32.9 m.y. (Damon and associates, 1966) unconformably overlies Paleozoic sediments at Clifton; therefore, it is believed that the Clifton area was structurally high and underwent erosion during this time period.

Between 40 and 34 m.y.B.P. volcanism began in the Lower San Francisco River area with the eruption of andesites in the Blue Range primitive area, Blue Creek basin, and in the Datil-Mogollon area. The largest and most important structure to evolve during this time was the Blue Creek basin.

The existence of the Blue Creek basin is inferred from studies of the volcanic sequence (Seager and Clemons, 1972; Wahl, 1980). The basin is oriented north-northwest and is about 50 km long. Its northern end is in the Big Lue Mountains east of Clifton and its southern end is the Burro Mountains in New Mexico. Up to 4 km thickness of andesites and ash flows tuffs may be deposited along its axis. In the northern part of the depression, rhyolite domes and breccias form the western boundary of the depression in the Black Jack Canyon area. The rhyolite extrusives may be evidence of a ring fracture zone suggesting a volcano-tectonic origin for the basin (Seager and Clemons, 1972). Due to the great thickness of the volcanic pile, potential Paleozoic and Tertiary volcanic reservoir rocks may be buried to great depth in the northern end of the basin. If the Paleozoic and Cretaceous stratigraphic relationships observed at Clifton are true in

the northern Blue Creek basin, significant, deep geothermal reservoirs may occur in fault zones in the Horquilla Limestone (Pennsylvanian), Modoc limestone (Mississippian), the Second Value Dolomite (Ordovician) and the Coronado Sandstone (Cambrian).

Post-30 m.y. volcanics have uniform maximum thickness of about 1 km in most of the area except around Lower Frisco Hot Springs. They are dominantly basaltic andesite. Maximum thickness of the volcanic rocks occurs in the eruptive centers and thins outward. Major faulting is not identified with the volcanism. However, geologic mapping is incomplete for much of the area. Depositional basins existed in the Eagle Creek area and the Juan Miller Basin during the waning stages of volcanism as evidenced by highly indurated clastic sediments interbedded with basaltic andesite flows in the lower sections of these basins. The structural relations of these Miocene basins is uncertain due to poor exposures. Faulting may have played a key role. More likely, these basins were low lying areas between volcanic centers. This interpretation is based on the apparent onlap of the sediments on the basaltic volcanics and the basaltic flows interbedded in the lower sediments. Also, in Eagle Creek the Gold Gulch Beds of Heindl (1958) consist of mostly felsite clasts with minor basaltic clasts interbedded with minor basaltic flows in basal sections. East of Eagle Creek, Paleozoic and Precambrian rocks are exposed and are in fault contact with the Gold Gulch Beds. These lithologic incongruities suggest that major faulting is both post-basaltic volcanism and post-Gold Gulch Beds.

Two west-northwest trending zones of felsic volcanism are ob-

served in the lower San Francisco River area. North of Clifton rhyolite domes and dikes are intruded in a N55^{o}W zone and are associated with the waning stages of basaltic volcanism. East of these felsic volcanics on the same trend is the Mule Creek Cauldron. The Mule Creek Cauldron is nonresurgent and was dated as 20 m.y. old (Rhodes and Smith, 1972). The other late Oligocene-early Miocene felsic volcanic trend occurs in the southern Blue Range wilderness (Ratte and others, 1969). Hanna Creek Hot Springs discharges from a large rhyolite dome complex in this area (Ratte and others, 1969).

A large Oligocene resurgent cauldron, Bursum Cauldron, is a major structure in the eastern San Francisco River area. The Lower Frisco Hot Springs occur west of the ring fracture of the Bursum Cauldron. The ring-fracture zone of the Bursum Cauldron may provide vertical permeability for deep circulation of water. Since water recharge in the ring fracture system would occur at high elevations in the Mogollon Mountains, significant forced convection may exist in the Glenwood Graben where large fault zones with normal displacement intersect the older ring-fracture zones.

The large normal faults in the lower San Francisco River area are the manifestation of a major post-volcanism tectonic event characterized by rifting of the crust along steeply dipping faults. Scarborough and Peirce (1978) named this last episode of faulting the Basin and Range disturbance. Basin and Range faulting has created much of the present-day topography of the region. The faulting displaced crustal blocks downward as much as 2 to 3 km to form deep grabens that filled with sediments derived from the surrounding high

terrain. Several earthquakes have been felt in the Clifton area during the last 50 years, which may indicate continuing Basin and Range faulting (DuBois and Smith, 1980).

Faults of the Basin and Range disturbance appear to be the most important localizer of shallow geothermal convection systems because all hot springs except the Hanna Hot Springs occur on or adjacent to these faults. At least three dominant trends are observed for these faults: N. 30° E., N-S, and N. 40° W. ($\pm 5^{\circ}$). Hot springs are observed on all orientations of faults; however, N. 40° W. appears to be the preferred fault orientation. Eagle Creek Hot Springs, Gillard Hot Springs, and Clifton Hot Springs occur on or adjacent to major northwest trending faults. This interpretation may be incidental because these faults are transverse to local groundwater flow. Faults may force water to flow vertically by acting as a sort of "groundwater dam." This follows the hypothesis of Harder and others (1980) who showed that shallow geothermal systems in the Rio Grande rift, New Mexico correlate with large scale structures transverse to regional water flow at the discharge points of hydrologic basins. In any case the Basin and Range faults are important because they provide vertical permeability or act as groundwater dams that force convection; and they may tap deep reservoirs.

In summary, the structure and tectonics in the Clifton area have created favorable geologic conditions for geothermal systems because they:

(1) provide conditions for deposition of favorable reservoir-lithology and overlying cap rocks;

(2) buried potential reservoirs to great depth;

(3) provide vertical permeability or structural groundwater dams for forced convection;

(4) may have created significant fracture permeability in zones of intense faulting; and

(5) created topography that enhances recharge (high precipitation in mountainous areas) and potential for deep forced convection.

Additional geologic and geophysical studies are needed to confirm, identify, and quantify specific structures associated with potential geothermal resources in the lower San Francisco River area. While much of the discussion of structure with respect to geothermal potential is speculative, it is a guide for future exploration.

HOT SPRINGS

Studies of hot springs are very important because the springs represent leakage of hot water at the surface from a geothermal system. Hot springs are caused by complex hydrologic conditions at depth. They may result from two basic conditions: (1) very high temperature gradients causing density differences between shallow cold water and deeper hot water, which result in upward hot-water flow if vertical permeability is sufficient (free convection); and (2) upward leakage of hot water from a deep confined or artesian aquifer (forced convection). Many hot springs probably result from a combination of free and forced convection. Free convection requires great quantities of heat. Therefore, most of these types of geothermal systems are associated with hot igneous intrusions or very high regional heat flow (>3.0 HFU). In other areas forced convection is the predominant cause of hot springs.

By studying the discharge, temperature, and chemistry of hot springs, predictions about the subsurface reservoirs are possible. Such predictions are necessary because hot water loses heat by conduction to shallow rocks, by mixing of hot water with shallow cold water, or both.

Temperature predictions are accomplished by utilizing chemical geothermometry. Fournier and others (1974) discussed the assumptions made when applying these techniques to hot spring chemistry. These assumptions are:

(1) Temperature-dependent reactions between water and rock

determine the amounts of the chemical constituents used in geothermometry.

(2) There is an adequate supply of the required chemical constituents in the reservoir rock.

(3) There is reaction equilibrium of the specific chemical constituents at the reservoir temperature.

(4) No temperature-dependent reequilibration occurs after the hot water leaves the reservoir and cools conductively.

(5) No mixing of hot water with cold, near-surface water occurs after the hot water leaves the reservoir.

Mixing, assumption 5, may not be a road block to interpretation; mixing fractions of hot and cold water can be calculated and subsurface conditions determined if mixing can be shown from the chemical constituent ratios of hot springs. To test for mixing, non-reactive chemical constituents are used with the assumption that their concentrations reflect mixing and not reactions or solution after the hot water leaves a subsurface reservoir.

The water solubility of quartz, chalcedony, and opal are directly temperature dependent (Fournier and Rowe, 1966). Minimum subsurface temperature may be calculated using the silica concentration. The technique is advantageous because silica approaches solution equilibrium slowly at lower temperatures (Fournier, 1977). Thus, a cooled geothermal water will retain most of its originally high silica concentration after leaking from the reservoir. Silica geothermometry is most applicable where hot water has not cooled by mixing with cold, low-silica concentration water.

Besides the silica geothermometers, the Na-K-Ca geothermometer is commonly used. The molal concentrations of sodium, potassium and

calcium are used to calculate the Na-K-Ca geothermometer. The Na-K-Ca geothermometer is based on an empirical relationship between the proportions of potassium to sodium, the square root of calcium to sodium, and measured temperatures in geothermal wells. Utilization of the Na-K-Ca geothermometer is more complicated than the silica geothermometers. The cations used in this calculation may be involved in many non-temperature dependent reactions, after the hot water leaks out of the geothermal reservoir, such as ion exchange or precipitation of calcium carbonate. However, the Na-K-Ca geothermometer is less affected by mixing if the chemical concentrations of sodium, potassium, and calcium are high in the hot water compared to the concentrations in the cold water. This means the ratios of sodium, potassium, and calcium in the mixed water will be roughly those of the hot unmixed water.

Clifton Hot Springs

Clifton Hot Springs discharge from gravel in the San Francisco River channel and along the river banks. Hot springs and warm springs are observed during low river flows in sections 18, 19, 30, Township 4 South, Range 30 East. Discharge from individual springs is small but the cumulative discharge is significant. Most of the discharge probably occurs into the river in the bottom of the channel. The temperatures of individual springs are variable and range between $30^{o}C$ to $70^{o}C$.

Mariner and others (1977) presented deuterium versus chloride data that suggest that these springs originate from a single geothermal system whose waters mix with cold waters before discharge at the

surface. In order to test their conclusions, all chemistry reported in the literature, on these springs, was gathered, and additional geochemical sampling was performed. Table 2 is a compilation of the Clifton Hot Spring data.

Since chloride, lithium and boron are the least likely elements to be involved in rock-water reactions, their solubility is high, and their concentrations in hot waters are high relative to cold water, these elements were used to confirm mixing of the geothermal water with cold waters. If mixing is taking place, plots of chloride versus lithium and chloride versus boron should have a linear relationship. Figures 7, 8 and 9 substantiate Mariner and others' (1977) suggestion that mixing occurs and that the hot spring waters probably originate from the same source. Interestingly, the slopes of the linear, fitted data are nearly identical when the concentrations of lithium, boron, and chloride are scaled to the same order of magnitude.

Figure 10 is a plot of Chloride versus Measured Temperatures and silica geothermometer temperatures of these springs. The measured temperature versus chloride data show no correlation. Conductive cooling of the spring water after mixing with cold water could explain this lack of correlation with chloride. Silica geothermometers were calculated also for the springs and plotted against chloride in figure 10. The best linear fit was obtained with the quartz geothermometer temperatures, using high concentration chloride springs. The slope obtained with the quartz geothermometers versus chloride concentration is nearly the same as the slope of chloride versus boron! This is interpreted to show that mixing occurs in an intermediate tem-

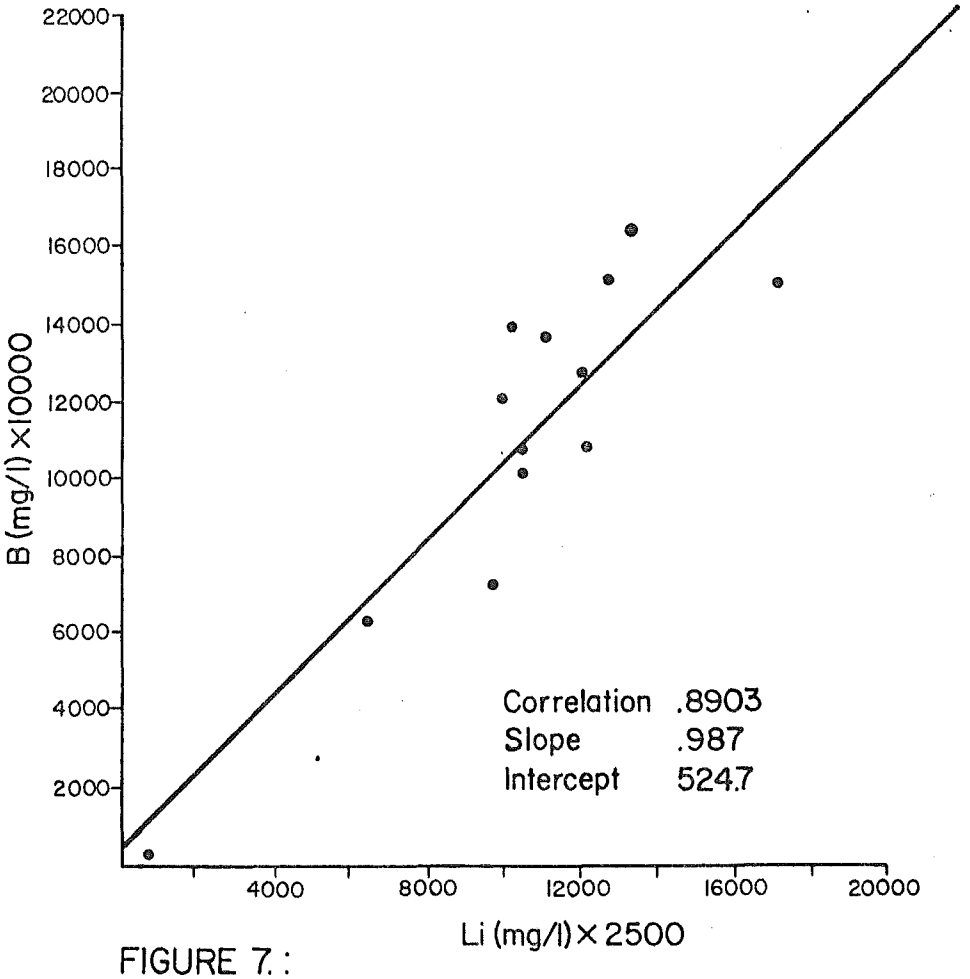

FIGURE 7.:
LITHIUM vs. BORON
CLIFTON HOT SPRINGS

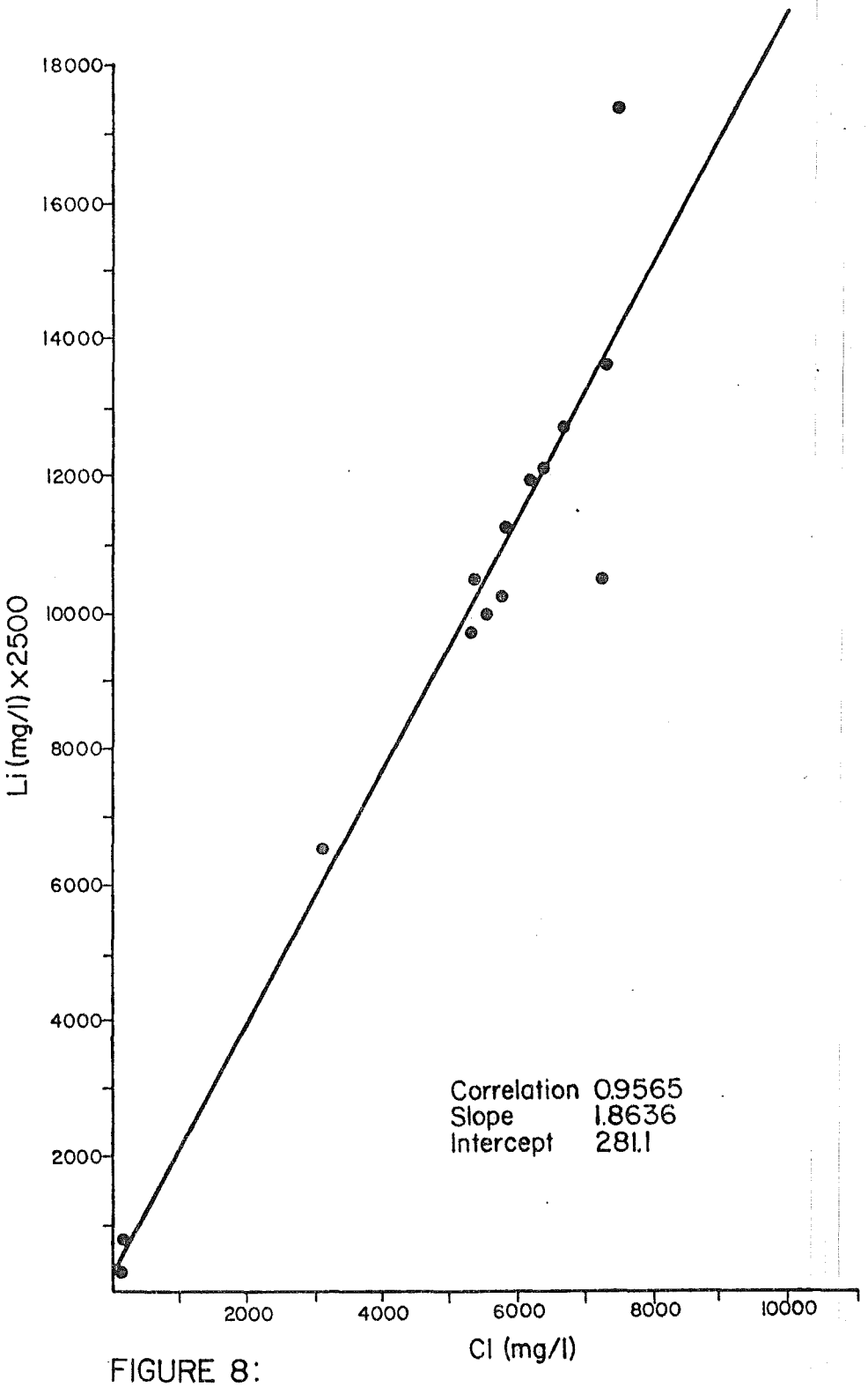

FIGURE 8:
LITHIUM vs. CHLORIDE
CLIFTON HOT SPRINGS

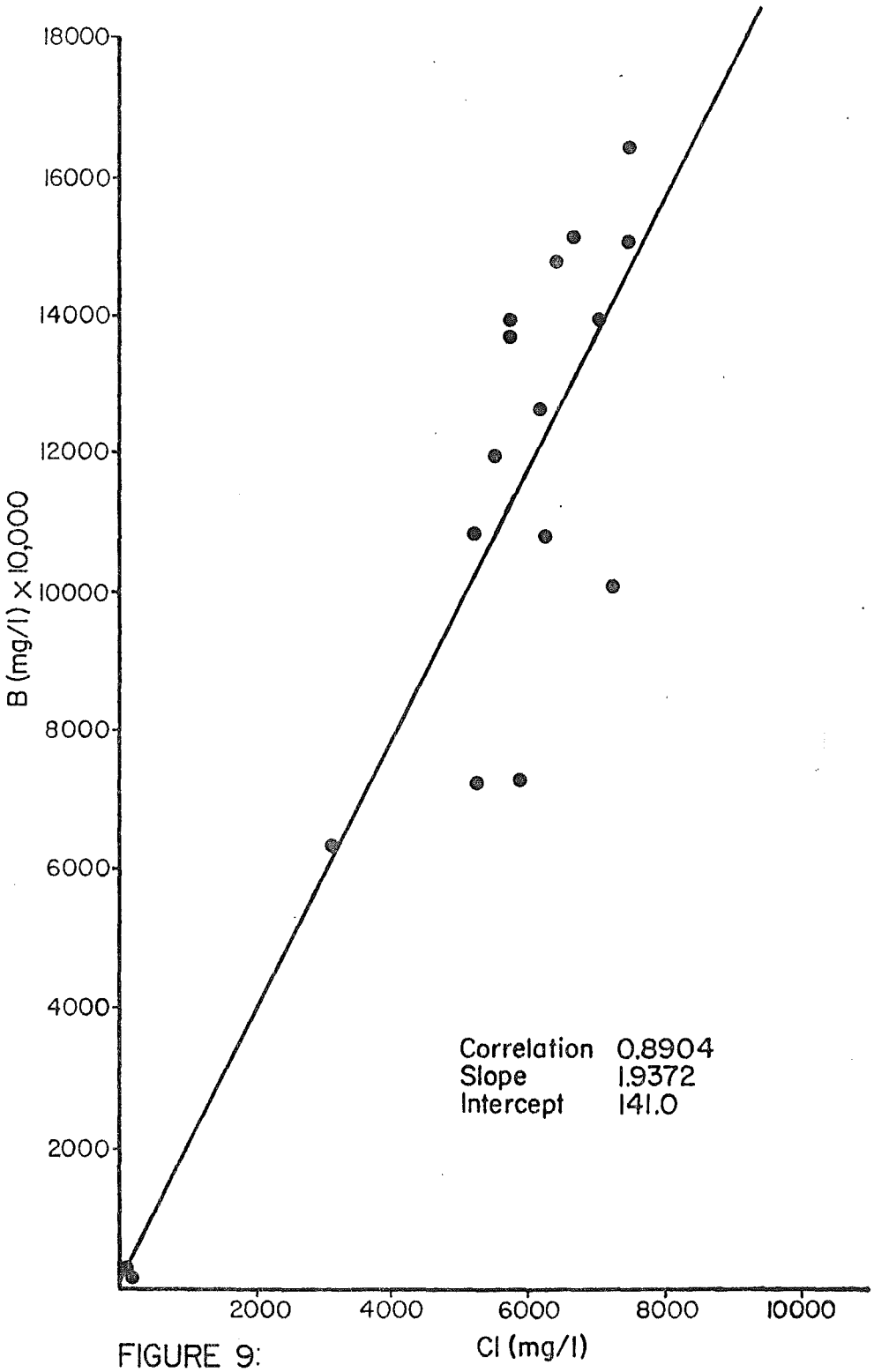

FIGURE 9:
BORON vs. CHLORIDE
CLIFTON HOT SPRINGS

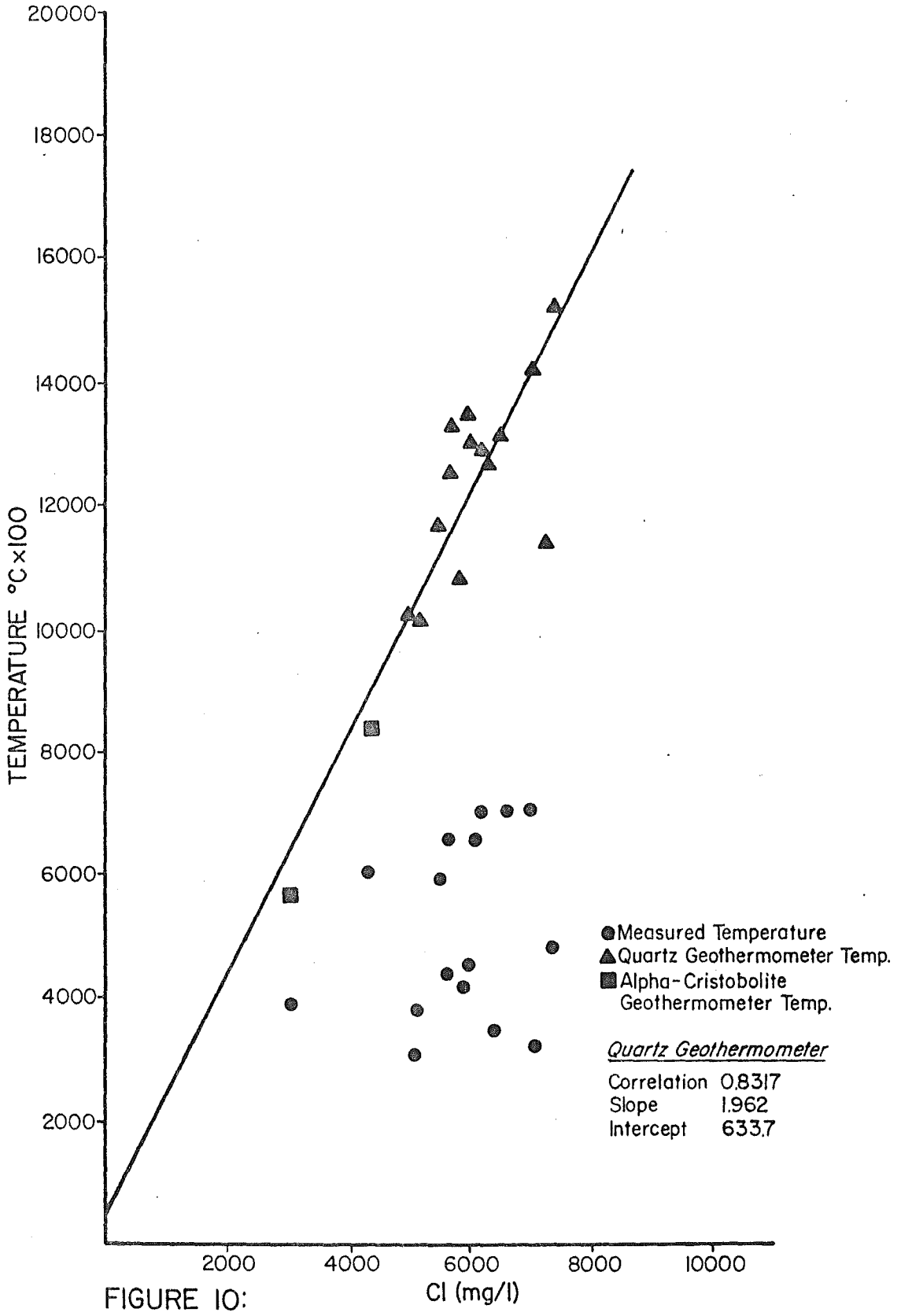

FIGURE 10:
TEMPERATURE vs. CHLORIDE
CLIFTON HOT SPRINGS

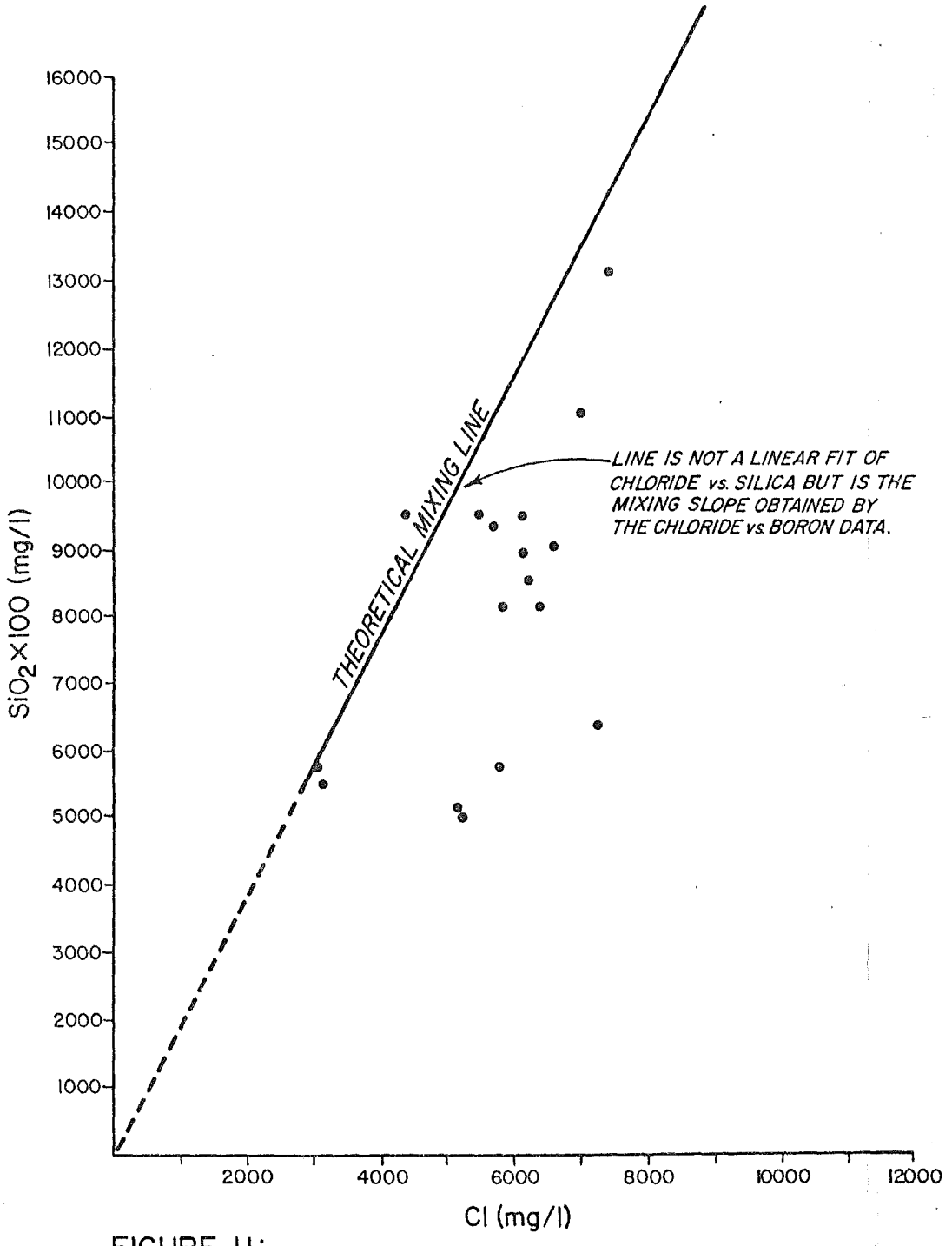

FIGURE 11:
SILICA vs. CHLORIDE
CLIFTON HOT SPRINGS

perature geothermal reservoir and temperature dependent reequilibration with quartz results after mixing. Temperatures in the intermediate reservoir range between 105 and 150°C.

Lower-concentration chloride springs are in silica equilibrium with alpha cristobalite, suggesting silica reequilibration at 55 to 85°C. It is reasonable to assume that the low chloride springs have retained most of their original silica contents after mixing. It is also possible that they did not reequilibrate with respect to quartz after mixing. This would cause these waters to be highly supersaturated with respect to alpha cristobalite after they cool conductively. In this situation, precipitation of alpha cristobalite results at the measured spring temperatures.

A Silica versus Chloride plot of the Clifton Hot Springs data is shown in Figure 11. The slope of the boron versus chloride data from Figure 9 is included to show the theoretical mixing line of the silica versus chloride data. This is reasonable because the slope of this line is interpreted as the mixing ratio of the cold and hot waters of this geothermal system. Note that all the springs shown to have reequilibrated with respect to quartz after mixing (Figure 10) fall below the mixing line. Springs that show equilibration with alpha cristobalite plot slightly above or on the theoretical mixing line in conformance with the assumptions of no reequilibrium with quartz after mixing and minor precipitation of alpha cristobalite.

Observed maximum discharge temperatures of the springs is 70°C. Due to the high temperature of some of the springs, possible subsurface boiling should not be ignored. Since boiling, cooling by mixing,

and conduction all may occur, the quartz geothermometry temperatures may predict only the shallow reservoir temperatures since silica appears to have reequilibrated with quartz in most springs. Mixing models, Na-K-Ca geothermometers, and chloride/enthalphy diagrams are useful to predict deeper subsurface temperatures where mixing is known to occur.

A silica mixing model was done on the Clifton Hot Springs (Witcher, 1979), using the method described by Fournier and Truesdell (1974). A temperature of 188°C was obtained. Subsequent work on the hot springs has shown that significant conductive cooling occurs. Therefore, the subsurface temperature predicted by the mixing model is probably not valid. Mixing models using silica and temperature work best on springs having large flow rates, little conductive cooling, and no silica reequilibration as the water flows to the surface. This is not the case for the hot springs at Clifton.

Table 3 lists the Na-K-Ca geothermometers calculated from selected, representative analyses of the Clifton Hot Springs. A magnesium correction to the Na-K-Ca geothermometer (Fournier and Potter, 1978) is not applicable to these data because of relatively low magnesium concentrations. Subsurface temperatures between 159 and 191°C are predicted, with the majority in the 170 to 180°C range. Modification or effect of mixing on the geothermometer temperatures is seen in Figure 12, a plot of Chloride versus Na-K-Ca Geothermometer Temperatures (dot symbols) and Silica Geothermometer Temperatures (cross symbols). Note that the pattern of the Na-K-Ca geothermometers versus chloride is the same as the silica geothermometer versus chlo-

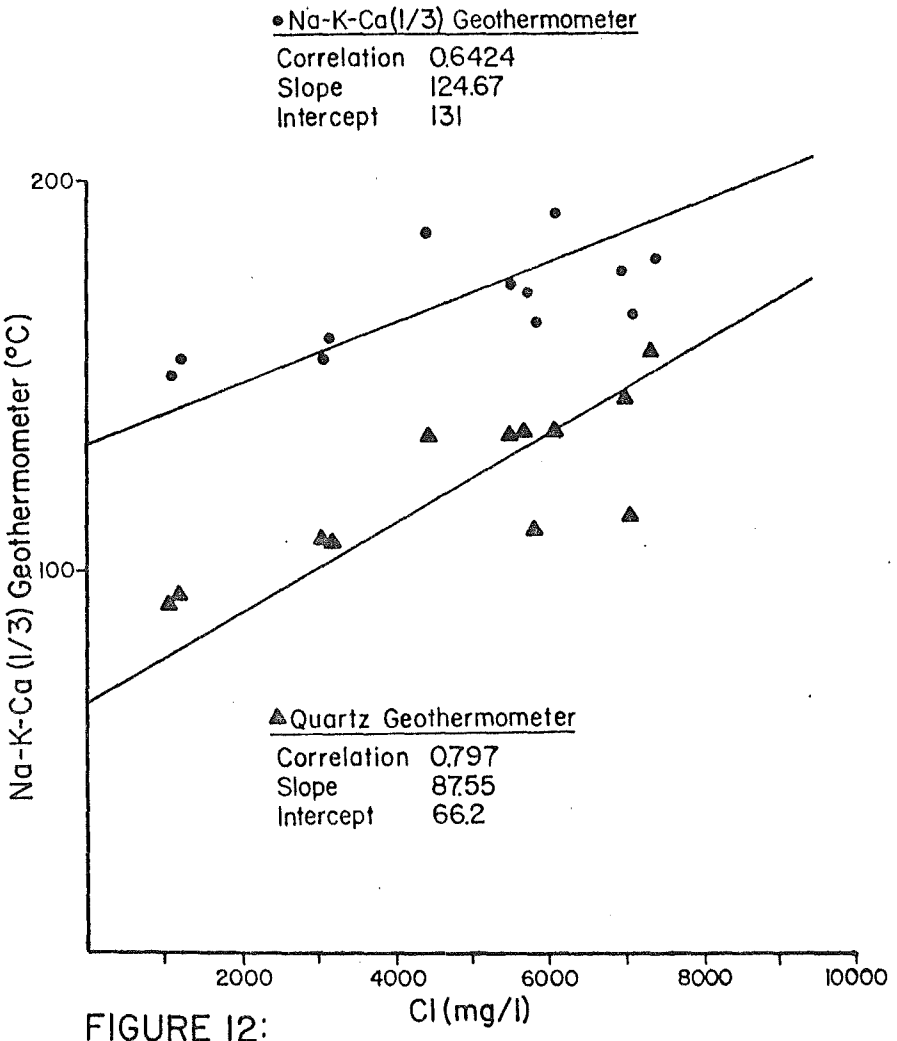

FIGURE 12:
Na-K-Ca (1/3) GEOTHERMOMETER vs. CHLORIDE
CLIFTON HOT SPRINGS

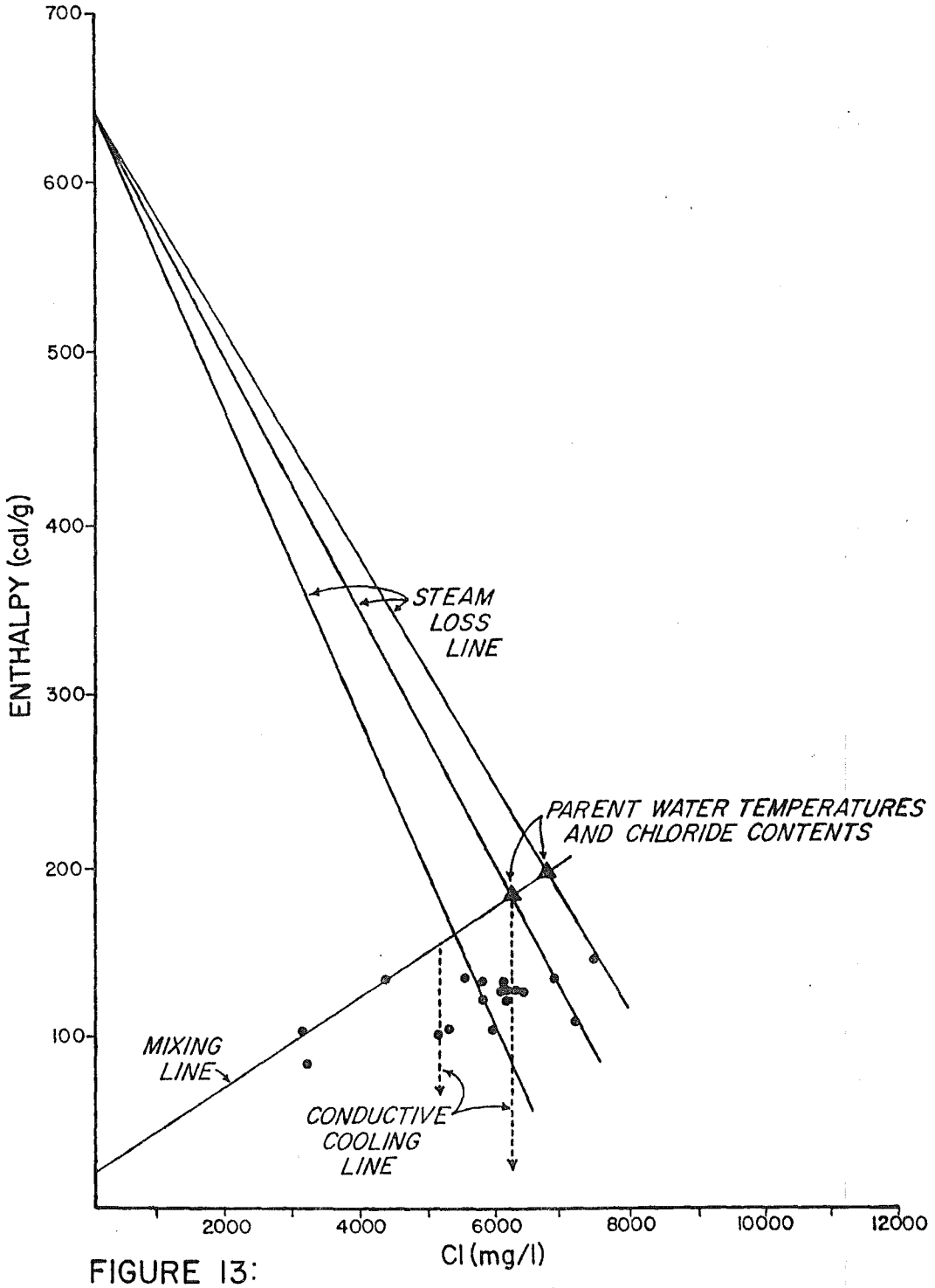

FIGURE 13:
ENTHALPY/CHLORIDE DIAGRAM
CLIFTON HOT SPRINGS

ride and in both cases a correlation with chloride exists. It is evident that the Na-K-Ca geothermometer is much less affected by mixing because it changes less than the quartz geothermometer. The similarity in pattern of the two geothermometers suggests that subsurface conditions are more complex than required by simple mixing to cool these waters. Minor conductive cooling and chemical reequilibration are apparently also involved. The Na-K-Ca/chloride relationship is probably not linear, as shown in Figure 12, at higher Cl concentrations. Thus, the 170°C to 180°C temperatures may actually predict deep unmixed reservoir temperatures.

The Silica versus Chloride plot in Figure 11 suggests that lower chloride waters have retained most of their silica concentrations and have not reequilibrated (precipitated silica) since mixing. If this assumption is correct, a Chloride/Enthalpy Diagram may be used to predict the deep unmixed reservoir temperature (Figure 13). Enthalpy is determined by using the quartz geothermometer. Lower chloride waters would define the mixing line that intersects the Y axis at about 20°C (which is near the mean annual temperature of Clifton). Also, since these waters probably have lost a minor amount of silica due to precipitation of alpha cristobalite (see Figures 11 and 12) the temperatures predicted by this diagram are treated as minimum, deep-reservoir temperatures. All other enthalpy and chloride data are plotted in the diagram to facilitate interpretation, which may account for the combined effects of boiling, mixing, and conductive cooling. For instance, water compositions and enthalpy controlled by mixing will plot on the mixing line; water compositions and enthalpy influ-

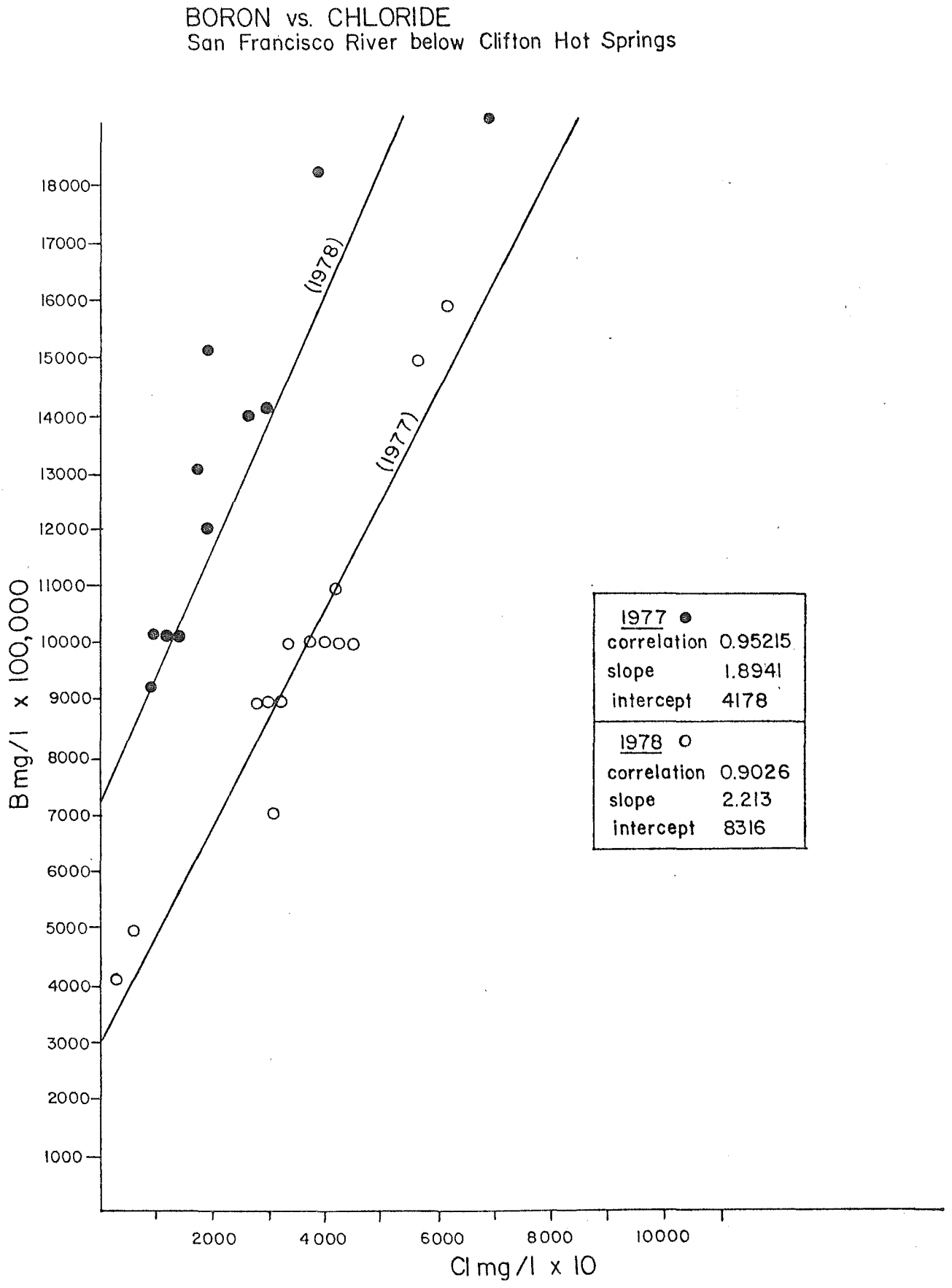
BORON vs. CHLORIDE
San Francisco River below Clifton Hot Springs
B mg/l x 100,000
Cl mg/l x 10
(1978)
(1977)
1977 ●
correlation 0.95215
slope 1.8941
intercept 4178
1978 O
correlation 0.9026
slope 2.213
intercept 8316

Figure 14.

enced by boiling will plot on the line of maximum steam loss. For a complete description on the use and interpretation of Chloride/Enthalpy Diagrams, consult Fournier (1979). Triangles on the Chloride/Enthalpy Diagram lie on the steam loss lines passing through the highest concentration chloride waters at the intersect of the mixing line. The triangles represent "parent" reservoir waters that have not mixed, boiled, or cooled conductively. The temperatures and chloride contents of the deep reservoir vary between 180°C to 195°C and 6000 mg/l to 7000 mg/l. Comparatively, the Na-K-Ca geothermometer predicts 160°C to 190°C deep reservoir temperatures.

The wide range in subsurface temperatures and chloride contents suggests a fracture controlled and inhomogenous geothermal reservoir. A relatively shallow (110°C to 150°C) reservoir seems likely to exist over the very deep high-temperature reservoir(s) (160°C to 190°C).

Figure 14 shows the relationship between boron and chloride concentrations in the San Francisco River below Clifton Hot Springs for the years 1977 and 1978. The slopes of the boron versus chloride concentrations are almost the same as the rate of change in the hot springs. This is expected because the concentrations of chloride and boron in the river are contributed by the hot springs that discharge into the river; therefore, the different concentrations are a function of river flow provided the spring discharge remains constant. The river waters are the end members in the system of mixed geothermal water. Natural volume discharge of the hot springs is calculated in Figure 15. The average chloride content in the geothermal water is 6500 mg/l. Thus a mean volume discharge from the reservoir is calcu-

CHLORIDE vs. FLOW OF SAN FRANCISCO RIVER BELOW CLIFTON HOT SPRINGS

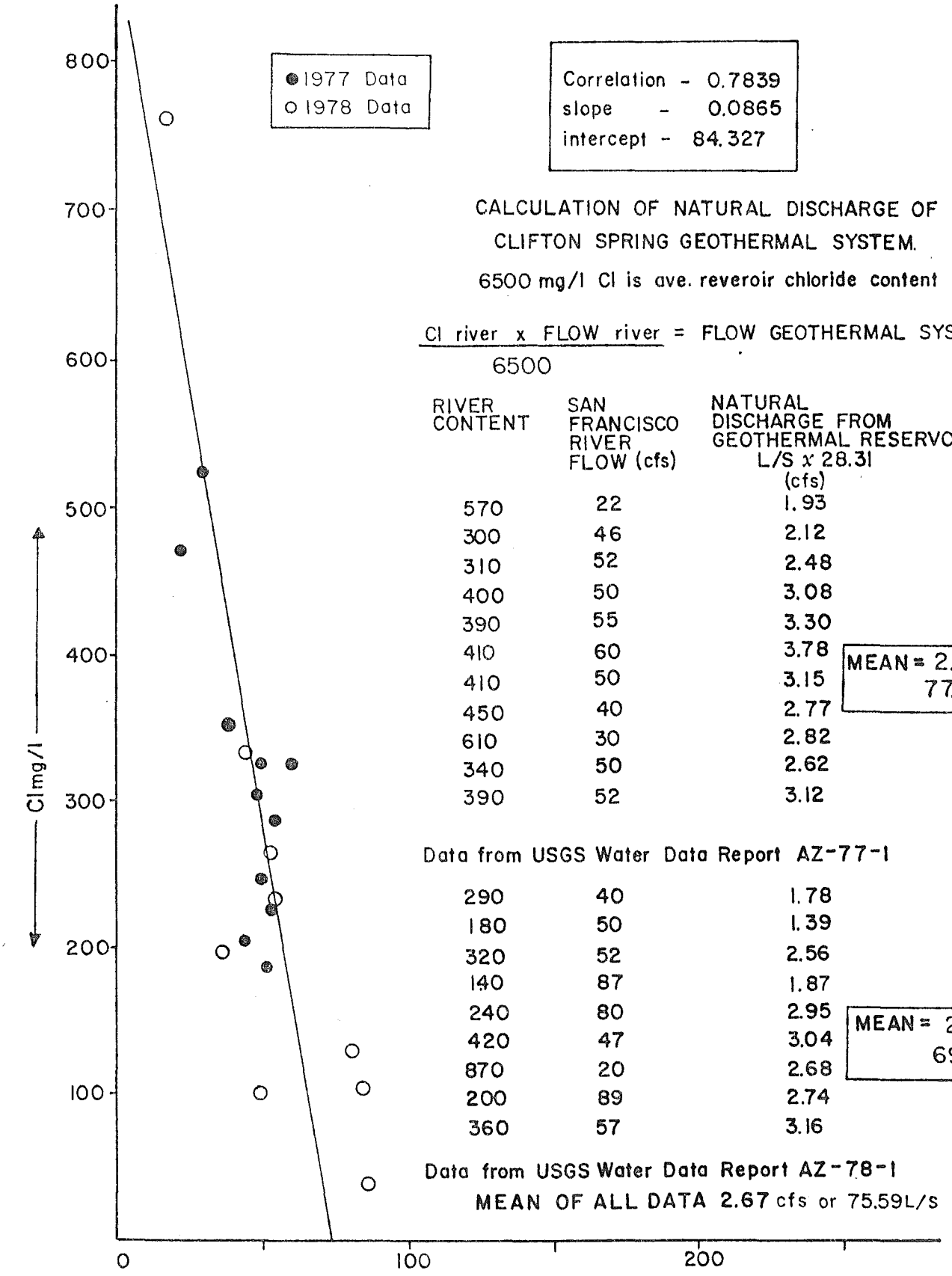

Correlation - 0.7839
slope - 0.0865
intercept - 84.327

CALCULATION OF NATURAL DISCHARGE OF CLIFTON SPRING GEOTHERMAL SYSTEM.

6500 mg/l Cl is ave. reveroir chloride content

$$\frac{\text{Cl river} \times \text{FLOW river}}{6500} = \text{FLOW GEOTHERMAL SYSTEM}$$

RIVER CONTENT	SAN FRANCISCO RIVER FLOW (cfs)	NATURAL DISCHARGE FROM GEOTHERMAL RESERVOIR L/S x 28.31 (cfs)
570	22	1.93
300	46	2.12
310	52	2.48
400	50	3.08
390	55	3.30
410	60	3.78
410	50	3.15
450	40	2.77
610	30	2.82
340	50	2.62
390	52	3.12

MEAN = 2.46cfs
77.57L/s

Data from USGS Water Data Report AZ-77-1

290	40	1.78
180	50	1.39
320	52	2.56
140	87	1.87
240	80	2.95
420	47	3.04
870	20	2.68
200	89	2.74
360	57	3.16

MEAN = 2.46cfs
69.64L/s

Data from USGS Water Data Report AZ-78-1

MEAN OF ALL DATA 2.67 cfs or 75.59L/s

Figure 15.

lated at 75.588 liters per second (l/s).

Heat discharged by the Clifton hot springs geothermal system was calculated using the 180°C deep-reservoir temperature and the natural flow rate of the system, 75.588 l/s. Both convective and conductive heat flow is included in this calculation. The total natural heat flow from the system is approximately 51 megawatts of heat energy. The estimate assumes 1 gram of water equals 1 cm^3 of water, and temperature (^{o}C) is equal to enthalpy (cal/g). The calculation is:

$$75.588 \text{ l/s} \times 1000 = 75588 \text{ cm}^3\text{/sec}$$

$$75588 \text{ cm}^3\text{/sec} \times (180\text{-}20^{o}\text{C}) = 12{,}094{,}080 \text{ cal/sec}$$

$$12{,}094{,}080 \text{ cal/sec} \times 4.186 = 50.6258 \text{ megawatts}$$

The Temperature versus Chloride plot (Figure 10) shows two possible discharge temperature groupings for the hot springs; however, the scatter is too large to accurately determine the mean surface discharge temperature of the Clifton Hot Springs. Temperature increases of the San Francisco River downstream from the hot springs are therefore used to estimate the convective heat loss of the system. Because most of the discharge apparently occurs in the river bottom the springs on the river banks may not accurately reflect the mean discharge temperature into the river bottom.

This temperature can be estimated when the temperatures upstream and downstream from the hot springs and the downstream chloride content are known. Using Figure 15, the downstream chloride content of the river (350 mg/l) is compared to the dilution line to determine a 1443.8 l/s river flow. Assuming that 1 gram of water equals 1 cm^3 of water and temperature ^{o}C is equal to enthalpy (cal/g) the following calculations estimate the average discharge temperature:

$$\text{fraction hot water to river water} = 0.0524 = \frac{75.588\ l/s}{1443.8\ l/s}$$

$$x = \text{temperature of discharge water}$$

$$x(0.0524) + 19\ (0.0524) = 22$$

$$x = 76.3^{o}C$$

The heat discharge into the river is calculated to be 18 megawatts or about 35 percent of the total heat loss of the system. Temperature and chloride data reported in Swanberg and others (1977) give a 108.5^{o}C discharge temperature and a heat loss of 27 megawatts or about 53 percent of total heat loss. The discrepancy in the calculated values is possibly due to uncertainty in factors controlling the temperature of the river. Heat loss due to evaporation or variations in spring discharge may also help explain the differences. Nearness of these values to the boiling temperature suggests that shallow adiabatic heat loss may be important. Conductive heat loss is certainly high and may be due to relatively shallow and extensive lateral flow of water after the hot water leaves the reservoir. If the flow is mostly vertical, very high conductive heat flow (>20 HFU) should be measured by shallow heat flow studies in the area immediately adjacent to the San Francisco River.

Gillard Hot Springs

Gillard Hot Springs, highest temperature springs in Arizona, discharge 80°C to 84°C water from gravel along the banks of the Gila River, Section 27, Township 5 South, Range 29 East. Total dissolved solids measured from these springs is between 1200 mg/l and 1500 mg/l. Chemically, the Gillard Hot Springs are sodium-chloride waters with

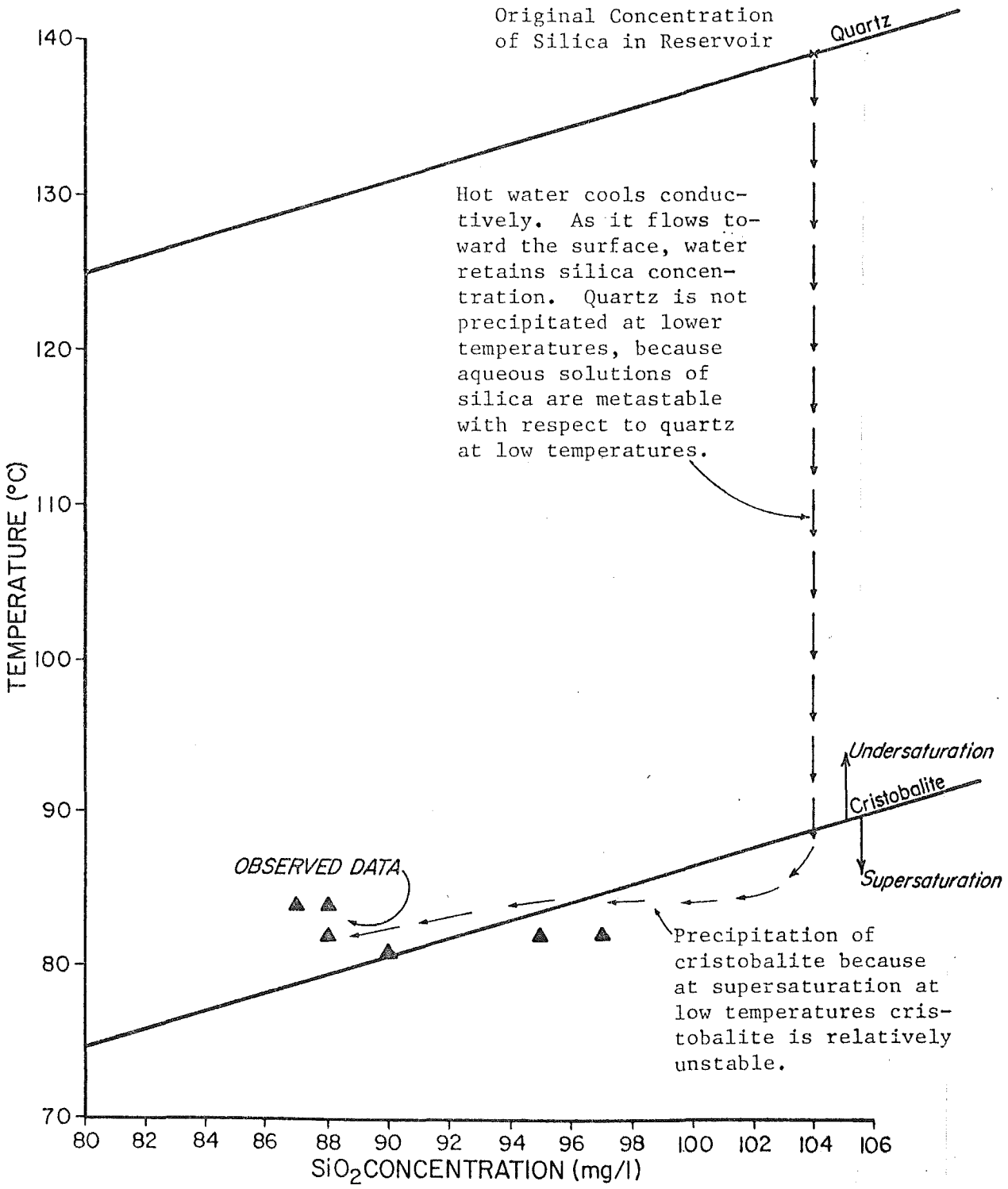

DIAGRAM SHOWING POSSIBLE MECHANISM FOR THE VARIATION IN SILICA CONCENTRATION OF GILLARD HOT SPRINGS

Figure 16.

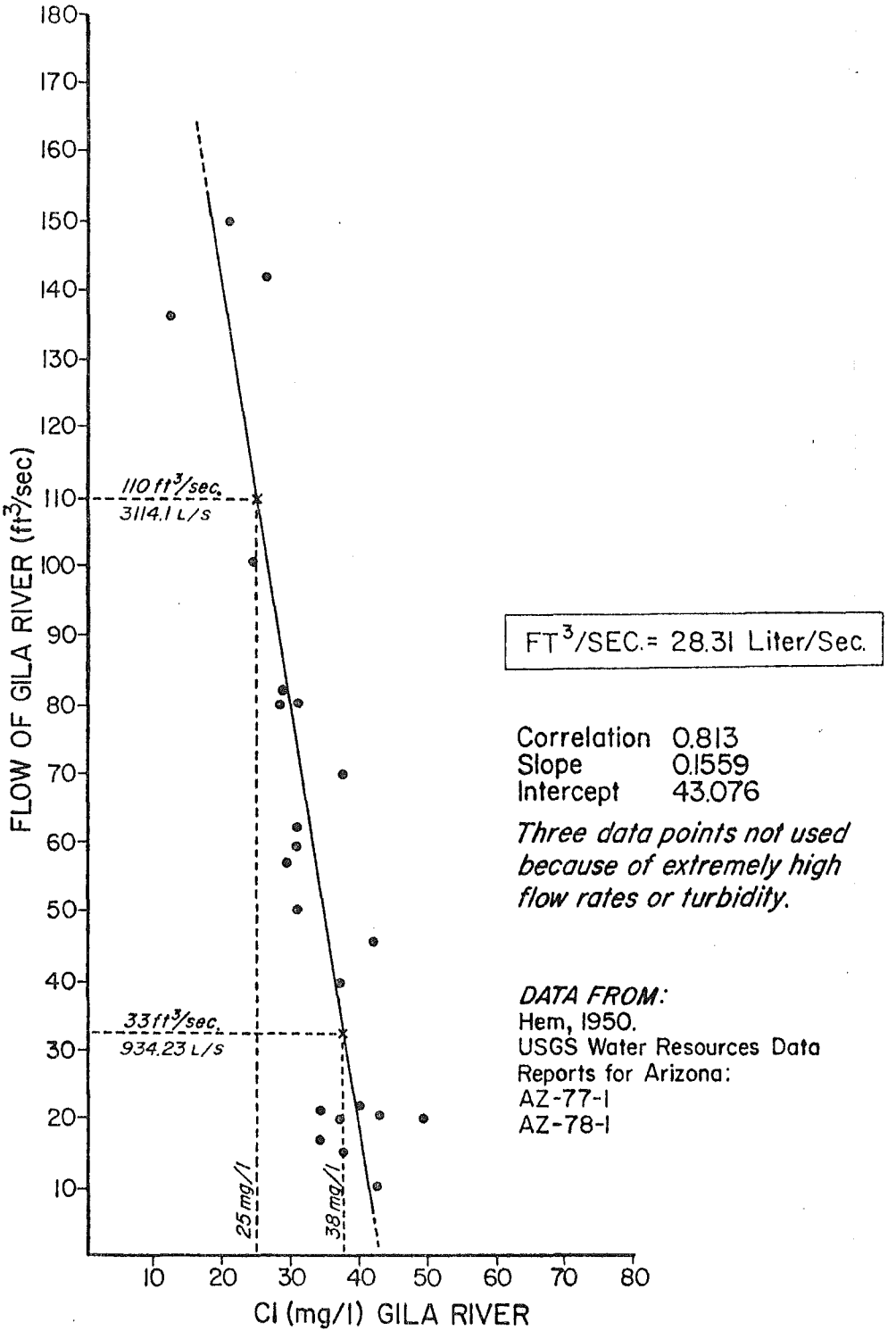

CHLORIDE CONTENT vs. FLOW RATE OF THE GILA RIVER 3 MILES ABOVE GILLARD HOT SPRINGS

Figure 17.

equal concentrations of sulfate and bicarbonate. The springs occur along a northwest-striking fault zone that displaces the Gold Gulch gravels into contact with the Greenlee Beds.

Chemical data reveal that no systematic variation of cations and anions occurs; therefore, significant subsurface mixing probably does not occur. Chemical geothermometry on these springs indicates a 130°C to 139°C reservoir temperature. The Na-K-Ca geothermometer predicts a 139°C reservoir temperature. No magnesium correction is necessary on the Na-K-Ca temperature prediction because the magnesium content of the springs is very low.

Silica geothermometry substantiates the Na-K-Ca geothermometer prediction. The quartz geothermometer predicts 130°C to 136°C reservoir temperatures. The lower and varied temperature prediction probably results from silica deposition after the waters have left the reservoir and cooled conductively. At the measured spring temperatures, silica is in equilibrium with cristobalite, which suggests that as the hot waters cooled their originally high silica contents (104 mg/l) became supersaturated with respect to cristobalite at 88°C and deposition of cristobalite occurred. As conductive cooling continued, additional cristobalite was deposited in order to maintain silica equilibrium. Figure 16 graphically shows this process.

Hem (1950) reported that the total discharge of the Gillard Hot Springs system is approximately 25.23 l/s (400 gallons per minute). Chloride and flow rates of the Gila River three miles above Gillard Hot Springs are shown in Figure 17. These data are from Hem (1950) and U. S. Geological Survey Water Resources Data Reports for Arizona,

AZ-77-1 and AZ-78-1. The chloride and flow data are useful to confirm and refine Hem's (1950) discharge estimate of Gillard Hot Springs. Hem (1950) reported a river flow of 2859.3 l/s (101 cubic feet per second) and a chloride content of 25 mg/l upstream from the hot springs. Downstream from the hot springs the chloride content is 30 mg/l. Using all available data (see Table 1), the mean chloride concentration of the hot springs is 488 mg/l ± 19 mg/l. The fraction of hot water and flow rate of hot water entering the river is calculated as follows:

$$488\ (x_1) + 25(1-x_1) = 30$$

$$x_1 = 0.010799$$

$$x_1(2859.3\ l/s) = 30.86\ l/s$$

If the river flow rate is determined graphically using Figure 17, the spring discharge is: $x_1(3114.1\ l/s) = 33.689\ l/s$.

Swanberg and others (1977) reported chloride contents of the Gila River above and below Gillard Hot Springs. Using Swanberg's data the hot water discharge rate is calculated:

$$488\ (x_2) + 38.3\ (1-x_2) = 50.0$$

$$x_2 = .0260173$$

The river flow rate graphically determined in Figure 17 is 934.23 l/s.

$$x_2(934.23\ l/s) = 25.196\ l/s$$

Chloride data collected from the Gila River upstream and downstream from the hot springs by the writer is apparently spurious and cannot be used to determine a spring discharge rate. The mean spring discharge rate is 29.899 l/s ± 4.289 or 474 gallons per minutes ± 68.

Temperature increase in the Gila River from 22°C upstream from

the hot springs to 24°C downstream requires that the average temperature discharge into the bottom of the river exceeds 90°C. Boiling may occur in the subsurface, but it is not readily apparent in the spring's chemistry.

The total natural heat loss of the Gillard Hot Springs geothermal system is 15 megawatts. Convective heat loss into the Gila River is approximately 7.8 megawatts.

The reservoir chloride content is probably around 500 mg/l and the reservoir chemistry is probably homogeneous because no large variations in hot spring chemistry are observed.

Eagle Creek Hot Springs

Eagle Creek Hot Springs (42°C) discharge from a tributary to Eagle Creek in Section 35, Township 4 South, Range 28 East. Location of the springs is apparently controlled by the contact between the Gold Gulch Beds and the underlying basaltic volcanics. No faults are observed at the springs; but prominent, vertical jointing oriented N. 35° W. and parallel to a fault zone 1 km west of the springs is seen in the Gold Gulch Beds.

The hot spring waters are sodium-rich, with nearly equal concentrations of bicarbonate and chloride. Total dissolved solids are less than 1000 mg/l. Local cold spring waters are calcium-bicarbonate rich, with high magnesium concentrations. Eagle Creek Hot Springs may be a mixed water; a high concentration of sodium chloride geothermal water mixing with the local cold water would result in a sodium-rich bicarbonate-chloride water.

Geothermometry of the Eagle Creek Hot Springs is probably not reliable due to potential precipitation of calcite, cristobalite, or amorphous silica and possible mixing. The silica concentration is saturated with respect to cristobalite at the measured spring temperature. The Na-K-Ca geothermometer predicts a temperature of 115°C.

The Eagle Creek Hot Springs may be related to the Gillard Hot Springs since both springs occur on or adjacent to the same zone of faults.

Hanna Creek Hot Springs

Hanna Creek Hot Springs are located in the Blue Range Primitive Area, about 40 km northeast of Clifton. Hot water flows from a northeast-oriented fault zone in flow banded rhyolite. The rhyolite comprises a complex rhyolite-latite dome eruptive center of mid-Tertiary age (Ratte and others, 1969).

Total dissolved solids of the Hanna Creek Hot Springs is 671 mg/l and it is a sodium chloride water. Measured surface temperature of the springs is 55.5°C. Chalcedony geothermometer predicts a 60°C subsurface temperature. Mixing is not believed to occur and the springs probably represent a low temperature geothermal reservoir.

Lower Frisco Hot Springs

The Lower Frisco Hot Springs in New Mexico discharge along the San Francisco River where the river direction changes from south to southwest. The springs' maximum observed temperature is 49.0°C. Most of the spring flow probably occurs in the river bottom and may be substantial. Tertiary gravels ("Gila Conglomerate") are in normal fault

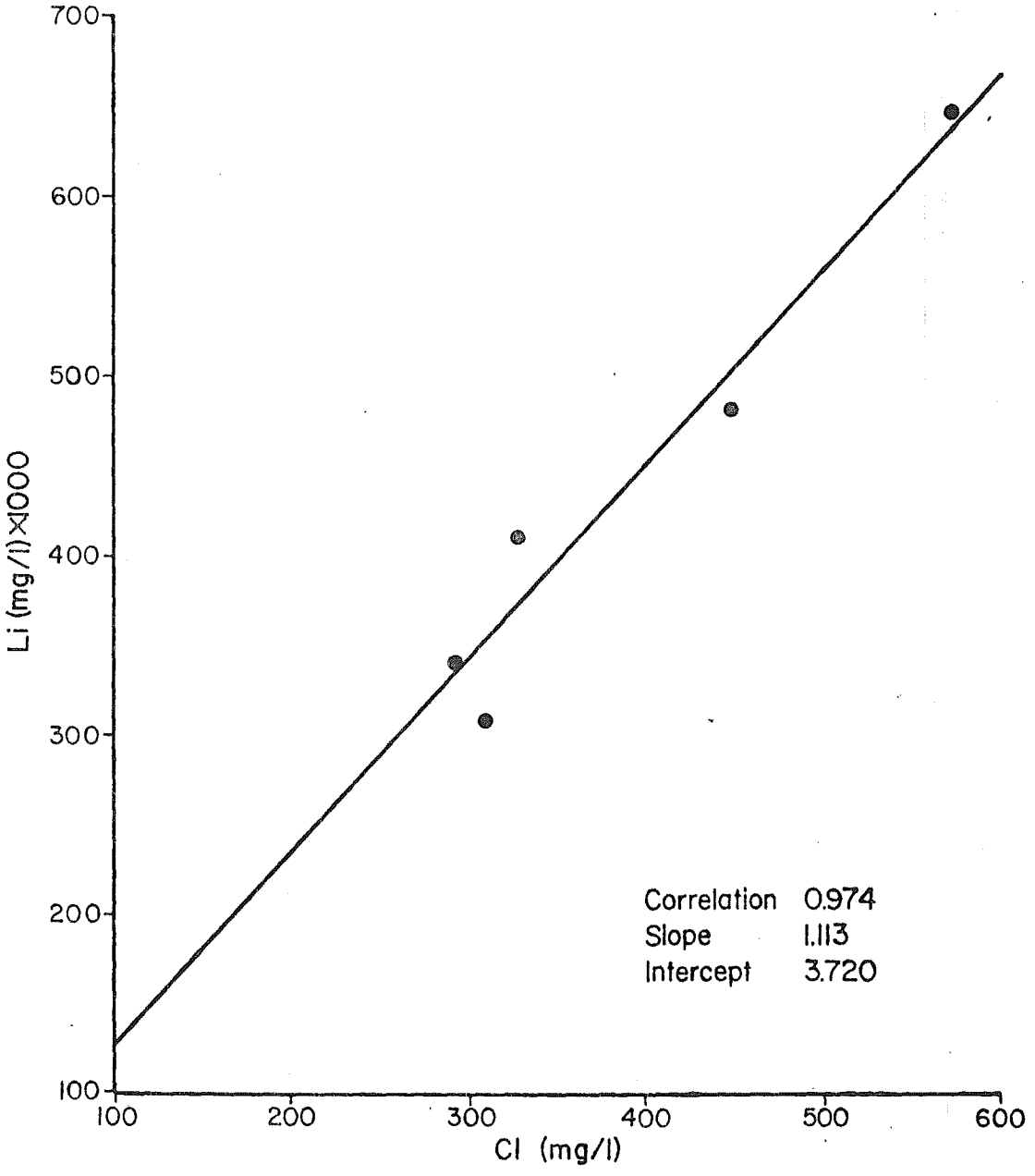

LITHIUM vs. CHLORIDE
LOWER FRISCO HOT SPRINGS (NEW MEXICO)

Figure 18.

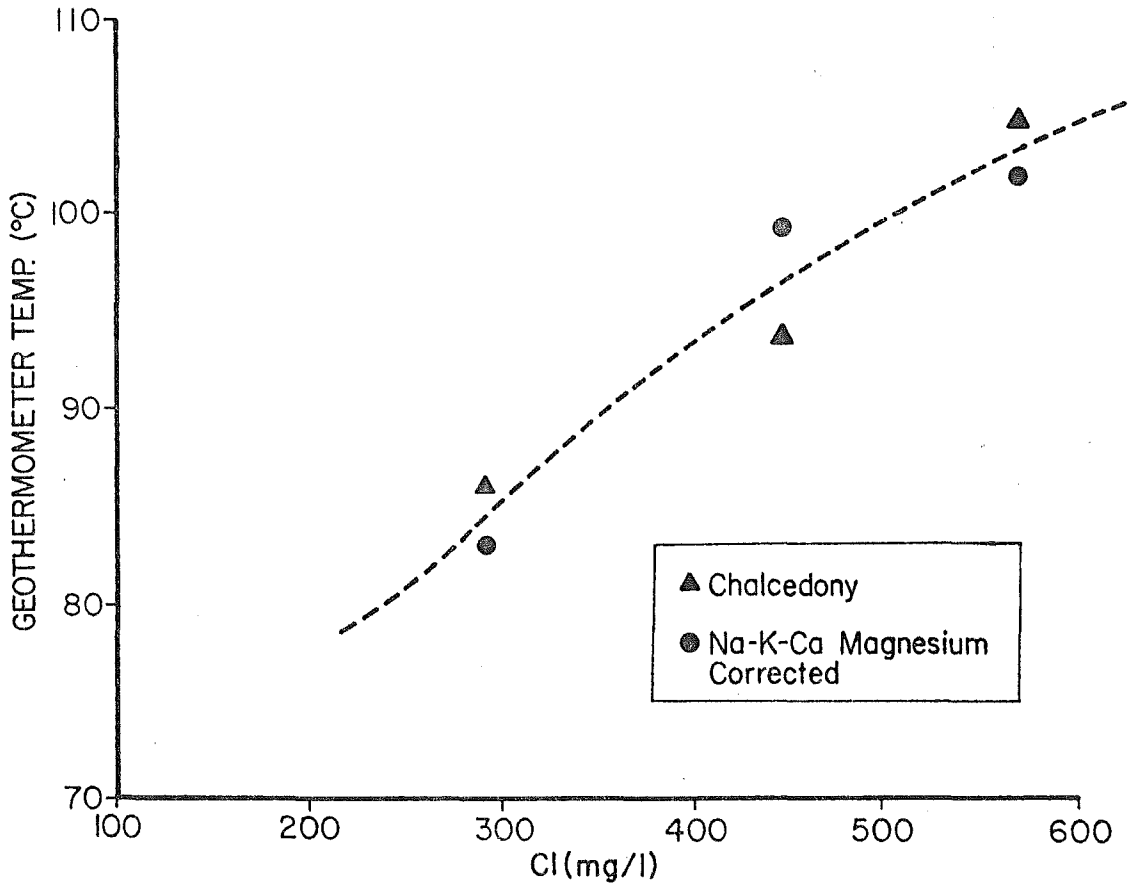

GEOTHERMOMETERS vs. CHLORIDE
LOWER FRISCO HOT SPRINGS (NEW MEXICO)

Figure 19.

contact with middle Tertiary basaltic andesite just west of the spring area. This suggests that the springs are localized by a major basin-and-range fault zone. Also of interest is a west-northwest lineament that crosses the San Francisco River just north and upstream of the hot springs. In black and white U-2 photography the lineament is quite striking because of very prominent tributary drainages on the lineament strike. The lineament roughly parallels the Mogollon Mountains' frontal escarpment. On the southeast end of this feature, displacement of an "old" Quaternary geomorphic surface is postulated from the aerial photos. No confirmation on the ground has been done. If this is in fact an early- or mid-Pleistocene fault, its intersection with the fault at the hot springs may control upward movement of water in the Lower Frisco Hot Springs geothermal system.

The Lower Frisco Hot Springs are sodium chloride waters of mixed origin. Figure 18 is a plot of lithium versus chloride. Lithium and chloride are highly soluble so the linear variation most likely indicates mixing of high concentration hot water with cold low chloride/lithium concentration waters.

Na-K-Ca magnesium corrected geothermometers agree with the chalcedony geothermometers for individual springs. The geothermometers also have a linear relationship to chloride (see Figure 19). This relationship suggests that as mixing occurs, temperature-dependent re-equilibration is occurring in a manner similar to that postulated for the Clifton Hot Springs. Geothermometry predicts an 83°C to 102°C reservoir. A high temperature deep reservoir may exist but the data are too few to determine if mixing model calculations or chloride/

enthalpy diagrams would be useful to predict the deep reservoir temperature. Detailed geochemical sampling of all spring discharges and the river below and above the springs should be done. Interpretation of this data in a manner analogous to what was done at Clifton Hot Springs should show deep subsurface temperatures, system flow rate, and natural heat loss.

Warm Spring

Geochemical reconnaissance along the San Francisco River has delineated an additional geothermal system (Witcher, 1979). A warm spring (seep) east of the Martinez Ranch in the Harden Cienega area occurs on the northwest bank of the San Francisco River. The spring temperature is 26.6^{o}C, which is about 8°C higher than the average temperature of springs in the area. Chemical analysis of the spring shows a sodium chloride water with a TDS of 6594 mg/l and a chloride content of 3391 mg/l. The chemical similarity to the Clifton Hot Springs is very close. The chloride/lithium ratio is nearly the same, and the chalcedony geothermometer temperature (69.9^{o}C) plots on the temperature versus chloride mixing line of the Clifton Hot Springs (see Figure 10). The Na-K-Ca magnesium corrected geothermometer (126.9^{o}C) plots close to the mixing line of the enthalpy/chloride diagram for Clifton Hot Springs. This is intriguing because the warm spring seep lies on a northeast-striking structure zone that intersects the Clifton Hot Spring area 24 km to the southwest. Further work is needed to confirm a relationship.

GEOPHYSICS

Geophysical data are highly useful for exploration of geothermal resources. Geophysical studies such as gravity, magnetic, electrical, and seismic surveys provide data that may be interpreted to define buried structures and lithologies, which control the location, extent and character of a geothermal resource. Most important, a few geophysical surveys are able to directly detect heat and provide information on the reservoir and its fluids. These latter surveys include heat flow studies, electrical studies and, in some cases, microearthquake (passive seismic) studies. Electrical surveys are able to detect heat because hot water heated to temperatures greater than 180°C has resistivities less than 1 ohm-meter. Electrical survey data, like nearly all geophysical data, may not give unique solutions; for example, not all 1 ohm-meter anomalies are hot water. Salt water or water-saturated clays frequently have resistivities less than 1 ohm-meter. However, if geophysical data are interpreted using geology, hydrogeologic, and other geophysical surveys, reliable and unique solutions to subsurface problems are possible.

In the lower San Francisco River area, several reconnaissance geophysical surveys have been accomplished and their results and preliminary interpretations published. Most recently, gravity and electrical (audio-magnetotelluric AMT) surveys were done by the U. S. Geological Survey as part of their reconnaissance evaluations of potential economic geothermal resources in the Gillard and Clifton Hot Springs Known Geothermal Resource Areas (KGRAs). Passive seismic

studies by the University of Arizona, New Mexico State University, and the University of Texas at El Paso and funded through the Arizona Bureau of Geology and Mineral Technology, Geothermal Group, by the U. S. Department of Energy and the U. S. Water and Power Resources Service were completed recently. In addition, several heat flow studies have been published that have measurements in the area.

Gravity Surveys

Gravity data are useful to obtain subsurface structural and lithologic information. Since different rocks vary in density, gravity surveys are useful to map and model subsurface rock density variations. Gravity surveys are able to detect subsurface density changes because anomalous gravitation acceleration, the quantity measured in a gravity survey, is directly proportional to the anomalous mass (density and volume of material) beneath the gravimeter and inversely proportional to the square of the distance from the center of the anomalous mass beneath the gravimeter.

Figure 20 is a complete Bouguer gravity map of the Clifton area. Generally, the southern three quarters of the area is a gravity high, while the northeast quadrant is a gravity low. A band of steep gravity gradient strikes west-northwest across the area just north of Clifton. The steep gravity gradient is the result of a north to south change in subsurface rock density. The steep gradient separates the generally high gravity to the south from the lower gravity in the northern area. On the surface, a west-northwest zone of probably Miocene rhyolite domes, small calderas, and west-northwest striking felsite dikes coincide with the zone of steep gravity gradient. Grav-

ity and geologic data are interpreted to indicate a significant crustal discontinuity in this west-northwest-trending zone.

A gravity low southeast of Clifton coincides with the northern end of the Duncan Basin. Thick and relatively low density basin-filling sediments (Greenlee beds) in the deeper parts of the basin probably create this low Bouguer gravity anomaly.

A broad gravity high occurs in the Blue Creek Basin area on the east margin of the map. The Blue Creek Basin is a thick pile (>4 km) of middle Tertiary volcanics filling a probable volcano-tectonic graben or depression (Seager and Clemons, 1972; Wahl, 1980; Gish, 1980). The gravity high probably results from either the thick pile of volcanics or from a probable intrusion of batholith dimensions emplaced beneath the area. On the west side of the map, another broad gravity high extends from just south of Morenci into the Peloncillo Mountains. Klein and others (1980) suggest that the closed gravity high anomaly south of Morenci results from a higher density Laramide (Paleocene) intrusion buried at depth. This interpretation is reasonable because known Laramide intrusions are exposed at the surface in the area and coincide with the northern end of this gravity high.

Seismic Surveys

A geothermal convective system may be defined as heat transfer via hydrothermal fluids, from a deep heat source to shallow depths in the earth's crust. Faults penetrating deep into the earth's crust may tap hot water. These faults have permeable breccia zones and open spaces which result from relative movement of mostly planar but irregular surfaces.

Geothermal fluids frequently transport large quantities of dissolved salts which are precipitated out of solution at shallow depth and changing physiochemical environments, thus sealing permeable fault zones. However, an active fault will maintain open conduits for flow of geothermal water, by refracturing sealed breccia zones and mineral-filled pores and vugs. Active faults frequently have continuous or episodic seismic activity in the form of microearthquakes.

Many high temperature (>150°C) geothermal systems occur along active faults exhibiting microearthquake activity. In general, the best geothermal reservoirs occur on the sections of a fault zone characterized by the most intense microearthquakes. Near-surface heat and increased pore pressure resulting from hot water flow along the fault zone no doubt contribute to this phenomenon. Heated rocks lose fundamental strength [2] and increased pore pressure decreases normal stresses compared to shearing stresses on a fault zone because the pore pressure is in opposition to lithostatic pressure. Decreased normal stress relative to the shearing stress required for motion effectively reduces the static coefficient of friction in the rock, thus enhancing rock slippage potential and microearthquake activity.

During the summer of 1978, 19 portable seismographs were placed 10 to 15 km apart in the area surrounding Clifton, Arizona, by the University of Arizona, New Mexico State University, and the University

---

[2] fundamental strength - stress which a material is able to withstand, regardless of time, under given physical conditions, temperature, pressure, solutions, without rupturing or deforming (Billings, 1972, p. 31).

Seismic Refraction Model of Crust in the Lower San Francisco River Area

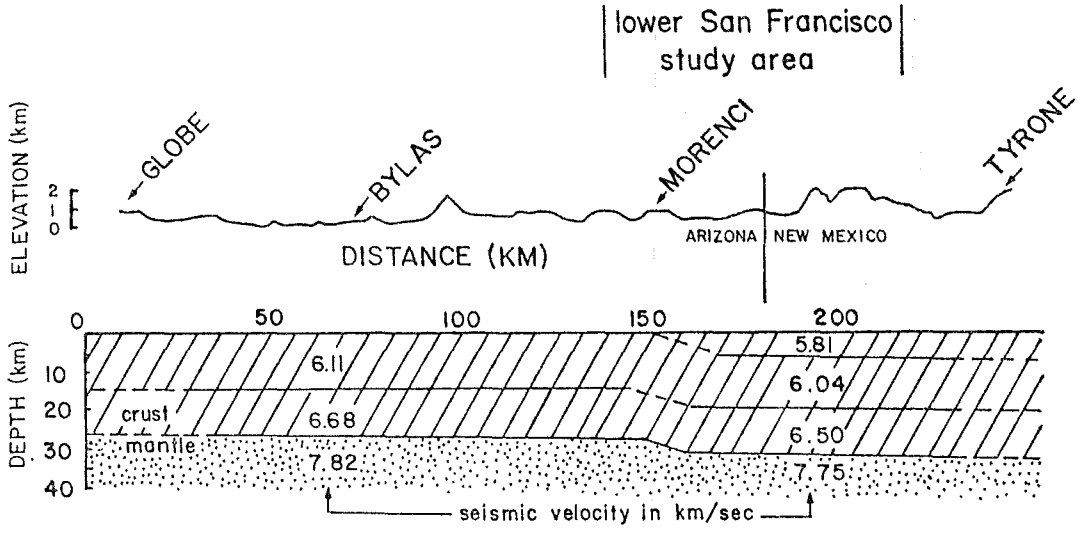

Data from Gish, 1980.

Figure 21.

of Texas at El Paso. The seismographs operated in the field for two weeks but no local earthquakes were recorded. Sbar (1979) stated that the regional tectonic stresses are possibly too low to create significant microearthquake activity. In addition, the short duration of the seismic records may have missed "swarm" type microearthquake activity frequently associated with shallow high temperature geothermal systems.

Mine blasts from large copper mines at Tyrone, New Mexico, and Globe, Arizona, were recorded with seismographs along a profile extending from Tyrone, New Mexico, through Clifton, Arizona, to Globe, Arizona (Gish, 1980). The seismic sources at both ends of the recording line enabled the University of Arizona survey to obtain a reversed refraction profile of the crust. More than 100 recording stations were occupied at approximately 3 km intervals in mostly quiet areas. Data collected by this survey from spring 1978 to summer 1979 were digitized for reduction and plotting by computer (Gish, 1980).

Interpretation of the refraction data shows a 28 km depth to the Moho in east-central Arizona and a 32 km depth to the Moho in western New Mexico and extreme eastern Arizona (Gish, 1980) (Figure 21). Delays in the refracted P wave in the upper mantle just below the Moho (Pn) are interpreted as evidence for an abrupt crustal thickening of 2.75 km in Arizona east of Clifton (Gish, 1980). The interpreted data show an overall decrease in velocity of the crustal layers in extreme eastern Arizona and western New Mexico, which may indicate increased crustal temperatures or a change in crustal compo-

sition between Clifton, Arizona, and Tyrone, New Mexico. Also, a surface low velocity layer 5.5 km thick between Clifton, Arizona, and Tyrone, New Mexico, was interpreted from the refraction data. This layer is not present in the Basin and Range province west of Clifton, Arizona. A thick pile of mid-Tertiary volcanics at least 4 km thick coincides with this low velocity layer (Seager and Clemons, 1972; Wahl, 1980). Open pores and fractures in the thick volcanic sequence may also contribute to the lower velocities interpreted for the upper crustal layer. The apparent decrease in overall seismic velocity of the crust between Clifton, Arizona, and Tyrone, New Mexico, has important implications for geothermal exploration because it indicates that the subsurface in this area may have higher crustal temperatures.

Electrical Surveys

Subsurface rock resistivity is influenced by several factors. Porosity, water saturation, and rock type are among the more important. A porous, water-saturated clay has very low resistivity, while a nonporous, dry granite has high resistivity. Salinity of subsurface water and temperature may also greatly affect subsurface resistivity. High salinity and high temperature (>180°C) may cause exceedingly low resistivity.

Subsurface apparent resistivity has been tentatively determined by the U. S. Geological Survey near Clifton and Gillard Hot Springs using the audio-magnetotelluric method (AMT).

Amplitudes of the orothogonal electric and magnetic components of the natural alternating electromagnetic (EM) fields are measured at different frequencies to determine subsurface resistivity. Elec-

tromagnetic (EM) waves measured by the AMT method are generated by thunderstorms occurring mostly in the tropics. Resistivity measurements at depths up to several kilometers are possible depending on the apparent resistivity of the shallow subsurface and the frequency of the measured EM wave. The maximum exploration depth (skin depth) is calculated using the following equation:

$$D = 503 \frac{\rho}{f}$$

where

D = depth in meters
p = apparent resistivity
f = frequency

From Parasnis, D. S., 1979.

Interpretive skin depth pseudosections were constructed using data presented by Klein and others (1980). The pseudosection interpretations are useful to show the main electrical properties beneath the Clifton and Gillard Hot Spring areas. The pseudosections are not unique layered models of subsurface electrical properties, but are quick graphical methods to see the general subsurface electrical character of the area.

Audio-magnetotelluric (AMT) stations Gillard 1 and Gillard 3 show relatively low apparent resistivities (Figure 22), which are probably indicative of hot sodium-chloride water at depth in fractured volcanic rocks and clastic sediments. Gillard 1 and Gillard 3 AMT stations were located near the northwest trending Gillard Hot Springs fault zone. The low measured apparent resistivities probably reflect hot geothermal waters rising in the fault zone and flowing laterally. Apparent resistivities at Gillard 2, which is north of the fault and also situated over well-cemented clastic sediments, are much higher.

The low apparent resistivities at Gillard Hot Springs do not indicate a high temperature resource at shallow depths. They do indicate an intermediate temperature (90-150°C) resource at very shallow depths along the northwest trending Gillard fault zone.

At Clifton, low apparent resistivities are observed in the Clifton 2 AMT site; they probably reflect hot sodium chloride water up to 10,000 mg/l TDS rising along faults and fractures beneath Clifton Hot Springs. North of Clifton Hot Springs, high apparent resistivities are measured in AMT station Clifton 1, which is situated on Precambrian granite. The resistivities are normal for granite except for anomalously low resistivities calculated for the 7.5 Hz through 27 Hz EM waves. Klein and others (1980) suggested that the lower apparent resistivity is probably due to groundwater, although they added that a zone of hydrothermal alteration may also cause this anomaly. Lateral flow of hot water that is less than 150°C may cause this anomaly also.

Heat Flow

Seven heat flow measurements in the lower San Francisco River area are available for interpretation. One of the heat flow calculations is detailed in this report. Roy and others (1968), Reiter and Shearer (1979), and Witcher and Stone (1980) reported the other heat flow measurements.

Many factors influence the temperature distribution within the upper crust of the earth. Heat flow from the earth's interior is the most important factor. Daily and annual solar heating has only minor importance and affects only the uppermost few meters. Temperature differences caused by pressure changes with depth (adiabatic

temperature) are insignificant and of no importance in shallow crustal studies because of the incompressibility of crustal rocks.

Heat flow is predominantly influenced by deep subsurface temperature, thermal conductivity of rock, and by ground water flow. Additional factors are also important, such as radiogenic and chemical heat production, and time (i.e., time since emplacement of a magma body or initiation of convection). Topography may also influence subsurface temperature distribution.

Conductive heat flow measurements are the easiest and most straightforward method to study the temperature distribution in the crust. Conductive heat flow depends mostly upon the rock thermal conductivity and the subsurface temperature. The equation for vertical conductive heat flow, assuming no radiogenic heat production, groundwater convection, or inhomogeneity in crustal rock is:

$$q = K \frac{\partial T}{\partial Z} \qquad (1)$$

where

q is heat flow
K is the rock thermal conductivity

$\frac{\partial T}{\partial Z}$ is the temperature gradient

Temperature at depth may be extrapolated to greater depth in a region of conductive heat flow if reasonable assumptions about rock thermal conductivity can be made. For this reason, regional heat flow studies seek drill holes that are located in nonpermeable, isotropic rock such as granite.

The objective of geothermal exploration is to locate and explore hydrothermal convection systems, at economically drillable depths. Since convective transport of heat from great to shallow (economic)

depths occurs in convection systems, geothermal studies are concerned with convective heat-flow measurements in addition to conductive heat-flow measurements. Also, convective heat flow contains information concerning the movement of ground water that may be useful for indirect estimation of flow rates, rock permeability, and heat budgets within the system. The equation for vertical heat flow with convection, but no heat production is:

$$q = K \frac{\partial T}{\partial Z} + \rho C v \partial T \qquad (2)$$

where

ρ is the density of water,
C is the heat capacity of water,
∂T is change in temperature through interval of the heat flow measurement,
v is the vertical component of water velocity,
other terms as in Equation (1)

The velocity of convective water flow is dependent upon the pressure (head), permeability, and fluid viscosity according to Darcy's Law.

Topographic relief in the lower San Francisco area can affect the thermal regime by causing complex hydrologic conditions. Because of the elevation differences the rainfall and mean annual temperature are quite varied. In the mountains up to 50 cm of precipitation per year and a mean annual temperature around 11°C to 12°C are recorded (Sellers and Hill, 1974). At lower elevations such as at Clifton, average annual rainfall is 25 cm or less and the mean annual temperatures range up to 19°C (Sellers and Hill, 1974). As a result of the climate contrasts, the vegetative cover changes radically from low to high elevations. Sparse creosote vegetation changes to dense forests of pinon, cedar, oak, manzanita, and ponderosa pine with increasing elevation. The areally variable climate and vegetative cover enhance complex hydrologic conditions. Lateral and vertical flow of water, which can

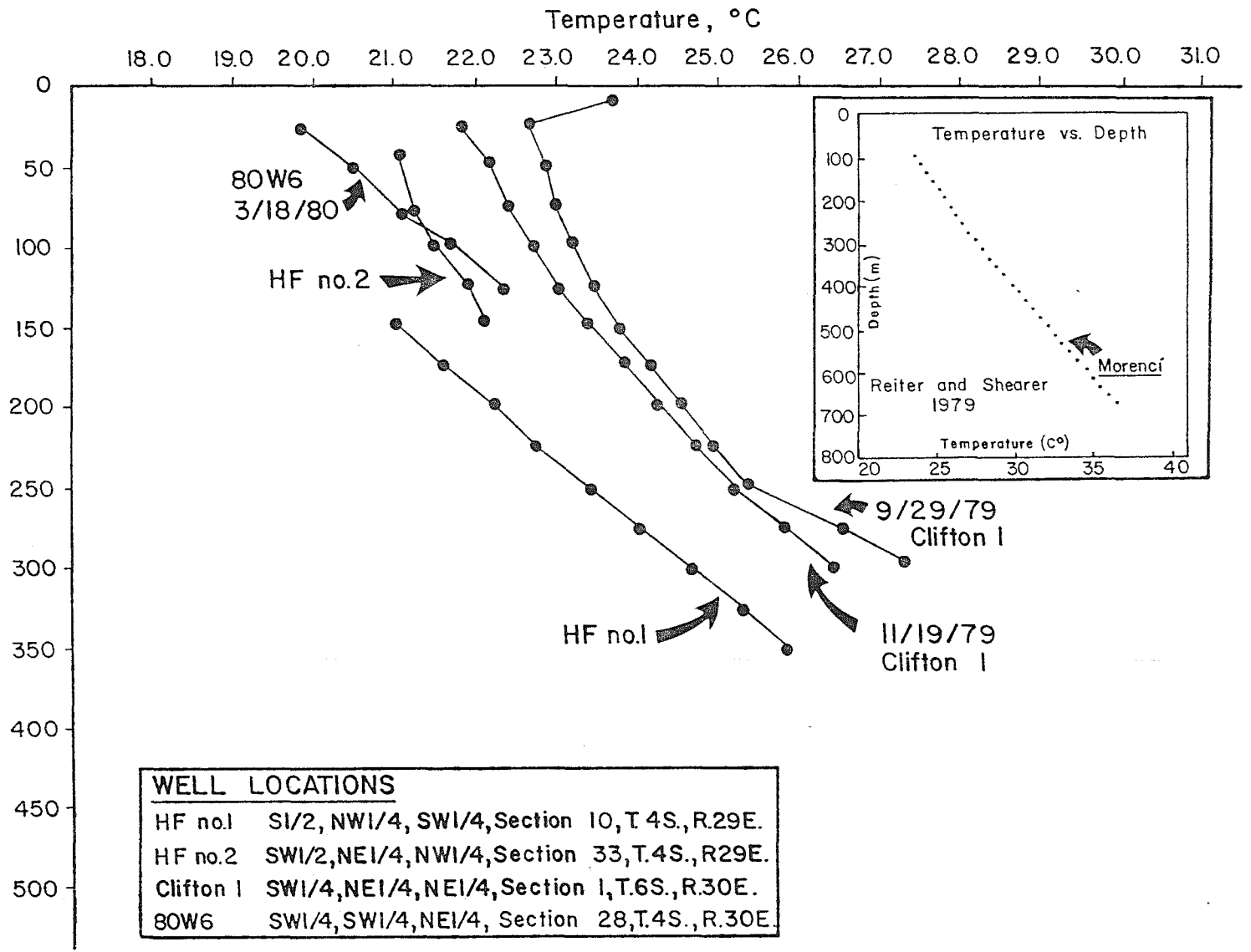

FIGURE 23:
Temperature logs of drill holes in the Clifton, Arizona area.

LITHOLOGY OF HEAT FLOW HOLES

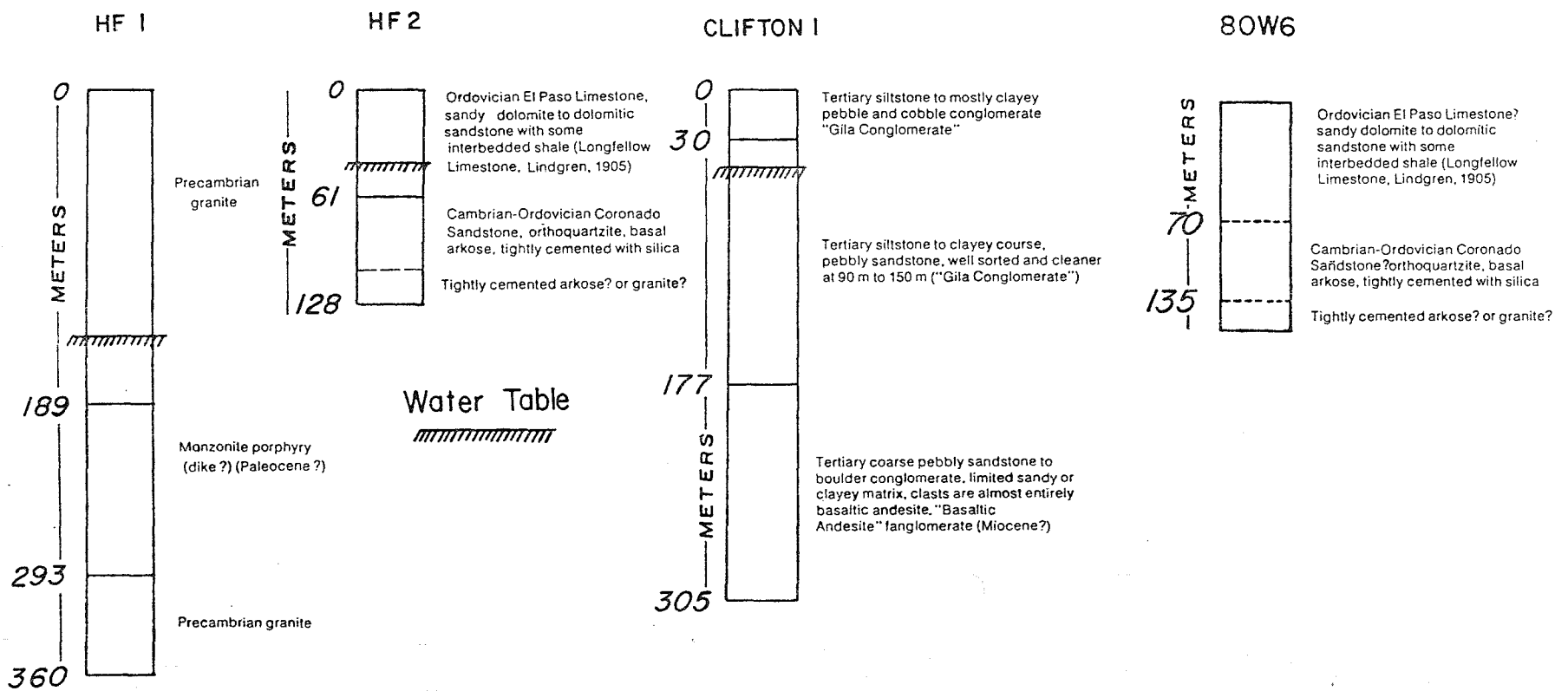

FIGURE 24

profoundly change the thermal regime, may result from complex hydrologic conditions.

Deep canyons formed by entrenchment of the Gila and San Francisco rivers and their tributaries have resulted from one or a combination of several post-Pliocene events, among which are regional uplift, acquisition of drainage outside of the Clifton area, or climatic change (Morrison, 1965, and Harbour, 1967). All of these factors may influence local and regional heat flow.

The first heat flow measurement reported for the lower San Francisco River vicinity was reported by Roy and others (1968). This heat flow hole, the Bitter Creek site southeast of Clifton in New Mexico, had a gradient of 45.7^{o}C/km between 240-390 ft, and a calculated heat flow of 3.07 HFU. Roy and others (1968) applied a topographic correction to the data and obtained a 2.77 HFU heat flow.

Reiter and Shearer (1979) published heat-flow data from Morenci, Arizona on a hole deeper than 600 m. A temperature-depth profile of this data is concave upward suggesting downward water seepage or progressively decreasing rock thermal conductivity (Figure 23). The low 1.4 HFU value from the thickest depth interval in the hole is significantly below the 1.9 to 2.0 HFU average southeastern Basin and Range province heat flow, and tends to substantiate modification of the thermal regime in this hole by water flow.

Heat-flow holes HF1 and HF2 are drill holes that the Phelps Dodge Corporation, Morenci, Arizona, kindly gave permission to log and provided rock samples for thermal conductivity measurements. Figure 24 shows the lithology of these holes. HF1 is in granite and monzonite

Heat Flow Data for HF1 Drill Hole

Depth Meters	Temperature Gradient °C/km	Temperature °C	Thermal Conductivity 10^{-3}cal/cm-sec-°C	Heat Flow 10^{-6}cal/cm^2-sec
75	28.7	19.07	8.74	2.10
105	24.0	19.80	8.26	1.98
180	25.7	21.78	7.48	1.92
220	22.7	22.62	8.24	1.87
240	24.3	23.09	5.92	1.44
280	25.3	24.18	7.04	1.78
290	24.7	24.43	6.52	1.61
320	23.7	25.19	8.72	2.06
355	20.0	25.89	11.13	2.23

Cross section of Hypothesized Geology in HF1

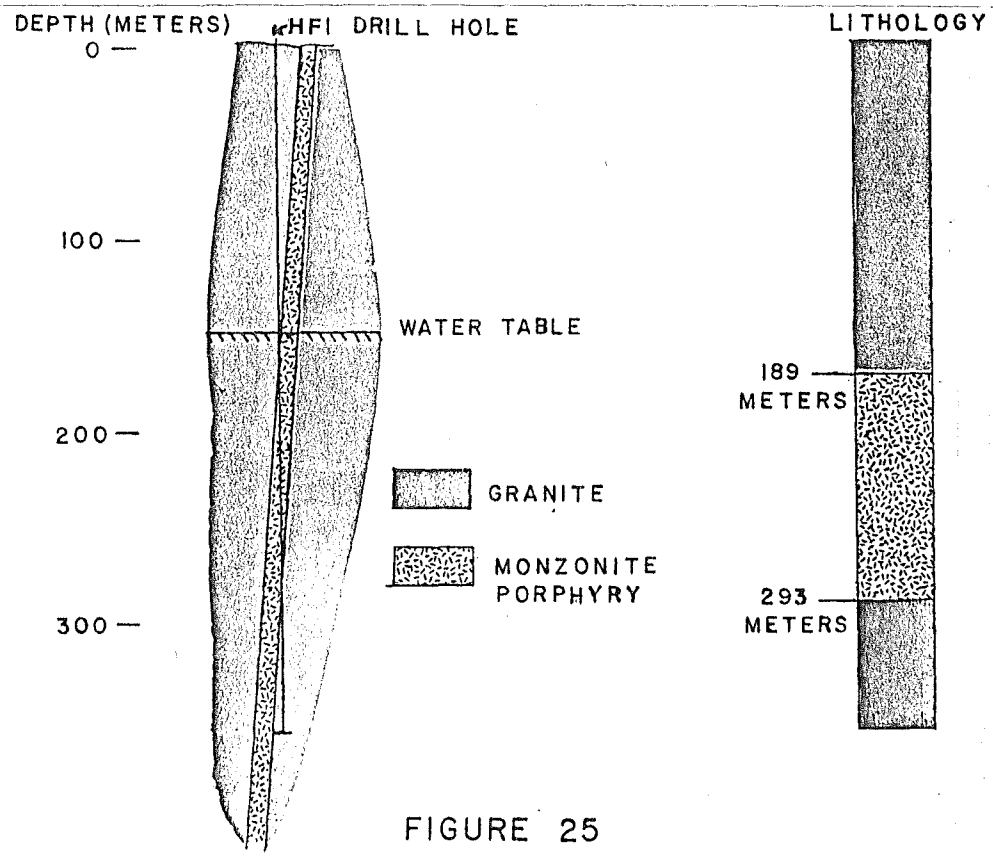

FIGURE 25

Note: The HF1 heat flow data in Table 4 are mean values for conductivities and temperature gradients calculated over the reported depth intervals. The heat flows in this figure are slightly different because they were calculated for each depth interval without averaging the data.

porphyry of Paleocene age. HF2 is in the lower Paleozoic section, which is exposed in the Clifton area. The upper 60 m of HF2 is in the Ordovician El Paso limestone (Longfellow Limestone of Lindgren, 1905), a sandy dolomite-to-dolomitic sandstone. The lower 70 m is in the Cambrian Coronado Sandstone, a tightly cemented arkose to orthoquartzite.

HF1 has a straight temperature-depth profile, usually indicative of a uniform lihtology with conductive heat flow and little change in rock thermal conductivity (Figure 23). HF1 probably represents a regional heat flow of 2.25 HFU for the Clifton area. However, this interpretation could be in error because the thermal regime may not result strictly from conductive heat flow as the straight temperature profile would initially suggest. The rock thermal conductivities that were measured for this hole probably are accurate because they are consistent with the subsurface lithology. However, the heat flow values within the hole change from over 2.0 HFU to less than 1.50 HFU (Figure 25).

The inconsistent section of this hole is associated with a section of monzonite porphyry between 189-293 m. The lowest heat-flow value is calculated at the middle of the monzonite interval. It is believed that the monzonite porphyry is a near-vertical dike that is an apophysis of a local northeast-striking monzonite intrusion(s), which is related in turn to the Paleocene magmatic activity that emplaced copper mineralization at Morenci (Langton, 1973). Downward seepage of cold water in the dike may "wash out" the conductive heat flow in the dike. Also, the monzonite dike may not be sufficiently

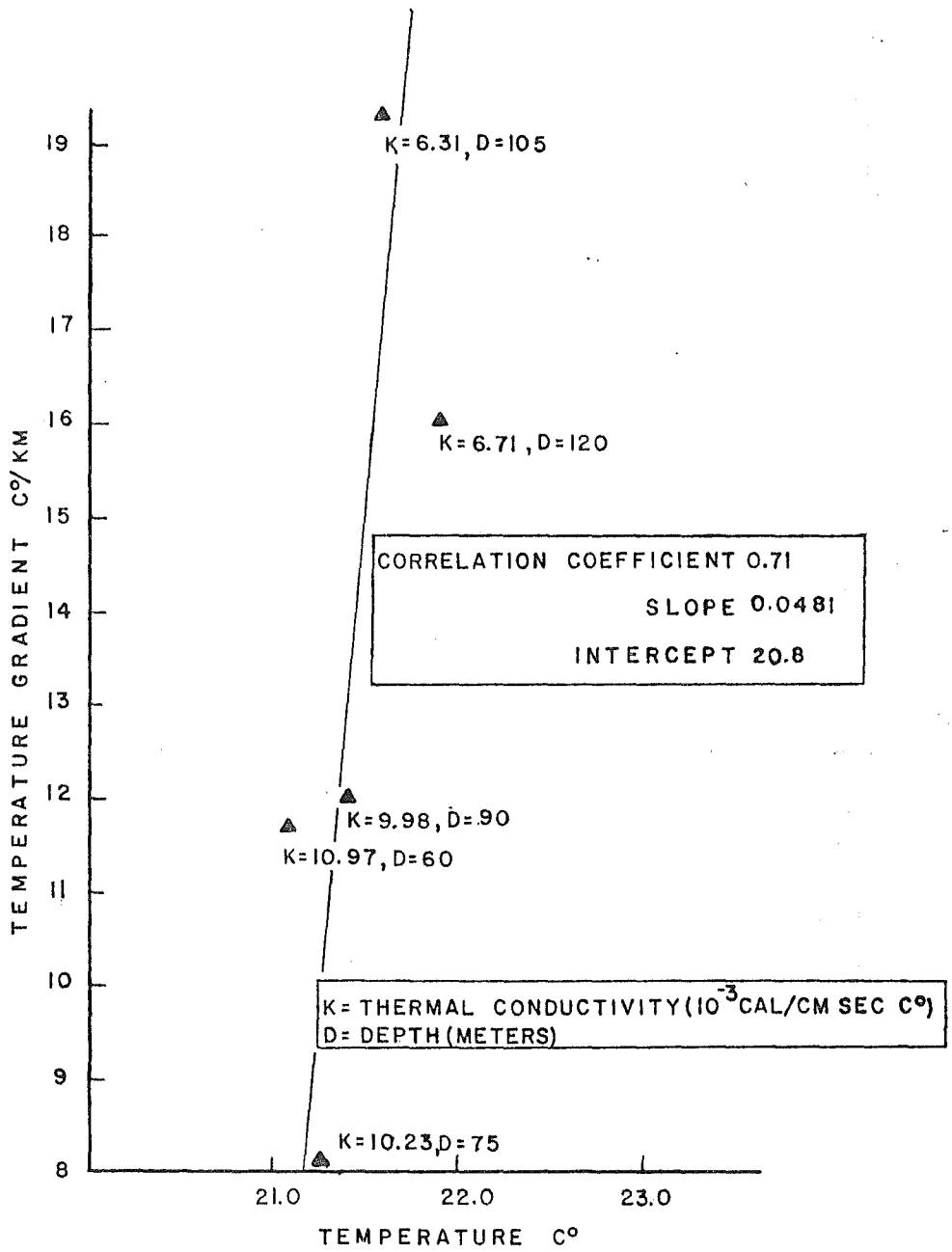

TEMPERATURE VERSUS TEMPERATURE GRADIENT
HF 2

FIGURE 26

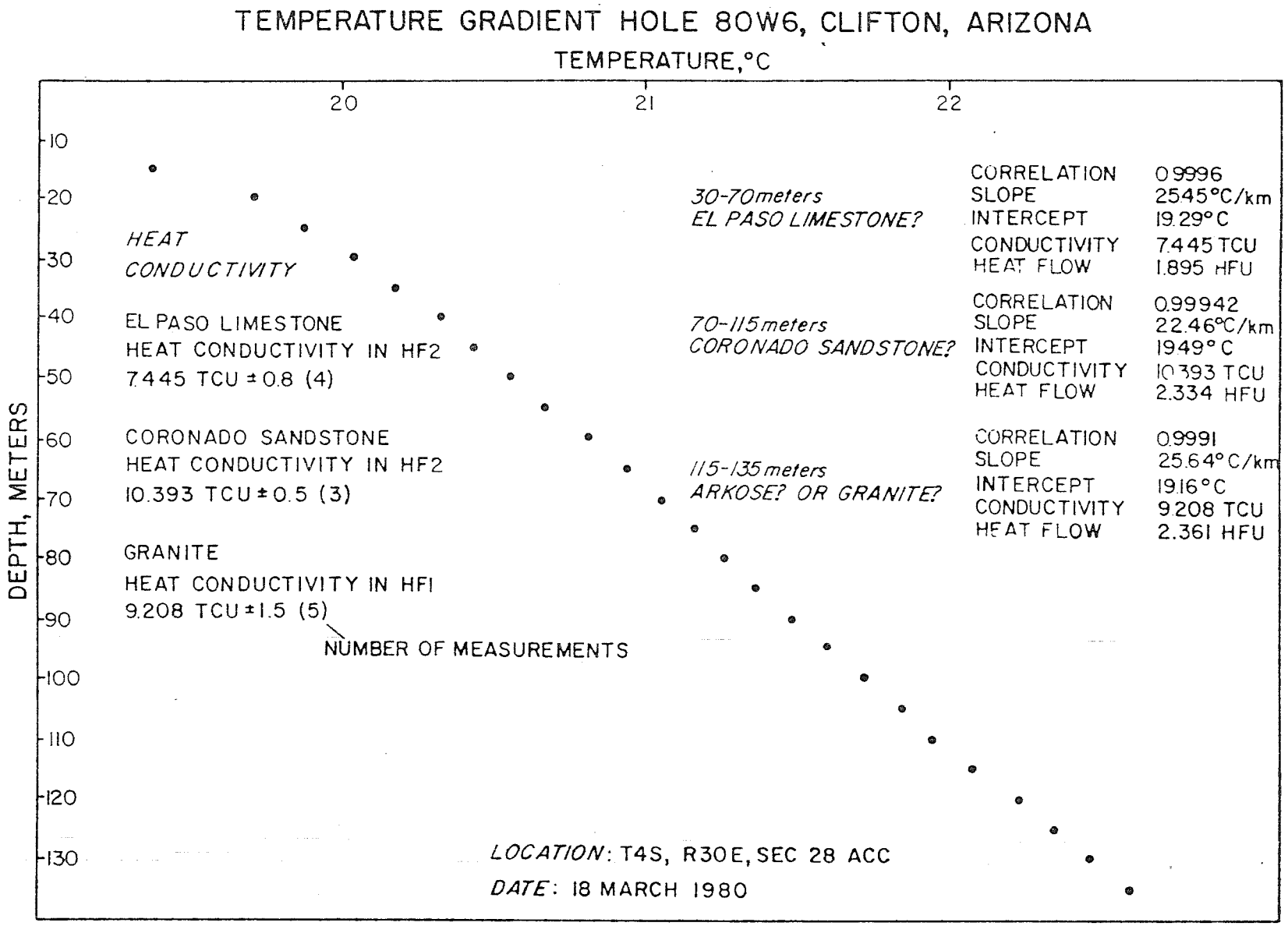
TEMPERATURE GRADIENT HOLE 80W6, CLIFTON, ARIZONA
TEMPERATURE, °C
20
21
22
DEPTH, METERS
10
20
30
40
50
60
70
80
90
100
110
120
130
HEAT CONDUCTIVITY
EL PASO LIMESTONE
HEAT CONDUCTIVITY IN HF2
7.445 TCU ± 0.8 (4)
CORONADO SANDSTONE
HEAT CONDUCTIVITY IN HF2
10.393 TCU ± 0.5 (3)
GRANITE
HEAT CONDUCTIVITY IN HFI
9.208 TCU ± 1.5 (5)
NUMBER OF MEASUREMENTS
30-70 meters
EL PASO LIMESTONE?
CORRELATION 0.9996
SLOPE 25.45°C/km
INTERCEPT 19.29°C
CONDUCTIVITY 7.445 TCU
HEAT FLOW 1.895 HFU
70-115 meters
CORONADO SANDSTONE?
CORRELATION 0.99942
SLOPE 22.46°C/km
INTERCEPT 19.49°C
CONDUCTIVITY 10.393 TCU
HEAT FLOW 2.334 HFU
115-135 meters
ARKOSE? OR GRANITE?
CORRELATION 0.9991
SLOPE 25.64°C/km
INTERCEPT 19.16°C
CONDUCTIVITY 9.208 TCU
HEAT FLOW 2.361 HFU
LOCATION: T4S, R30E, SEC 28 ACC
DATE: 18 MARCH 1980

FIGURE 27

wide to change the temperature profile in the hole even though the monzonite has different thermal conductivity (Paul Morgan, pers. commun., 1980). This situation results from the thermal diffusivity of the rocks. Figure 25 summarizes the pertinent data on HF1. No porosity or topographic corrections were applied to HF1 data.

HF2 has an upward concave temperature-depth profile and a very low overall temperature gradient (Figure 23). Temperature versus Temperature Gradient profile of the HF2 heat-flow hole is shown in Figure 26. At least two conditions are influencing the temperature distribution in this hole. First, very high thermal conductivities are contributing to very low temperature gradients, shown by the fact that gradients less than 12°C/km have conductivities greater than 9 TCU[3] and gradients greater than 16°C/km have conductivities less than 7 TCU. Second, ground-water flow at depth seems likely since the heat flow valves within the holes are internally consistent but the 1.0 HFU value is far below the average Basin-and-Range value of 2.0 HFU.

Hole 80W6 is an abandoned and open drill hole in SW¼, SW¼, NE¼, Section 28, Township 4 South, Range 30 East. While no core or cuttings from this hole are available, accurate lithologic inferences are possible by examining surface lithology, and comparing the temperature log (Figure 27) to the local stratigraphic section. The Ordovician El Paso limestone crops out on the surface at the drill site. At 70 m depth the temperature gradient changes from 25.46^{o}C/km to

---

[3] TCU - Thermal conductivity unit (1 x 10^{-3}cal/cm sec ^{o}C)

22.46^{o}C/km. The lower temperature gradient in the 70 m to 135 m interval is inferred to correlate with the Coronado Sandstone because that interval correlates with the measured thickness of the formation and because quartzite has a high thermal conductivity, which would cause a lower temperature gradient.

Temperatures in 80W6 were measured in air at 5-m intervals with a calibrated thermistor logging unit. Calibration accuracy of the temperatures is $\pm$ .01°C. Temperature data for 80W6 is shown in Figure 27. Since the readings were taken in air, the thermistor probe did not thermally equilibrate; so several readings were taken at specified times at each depth interval. These temperatures were used to extrapolate equilibrium or true temperature at each depth using the method of Parasnis (1971).

Since no core or cuttings are available and the Paleozoic and possibly Precambrian rocks encountered by the hole are laterally continuous for some distance, rock conductivities measured in HF1 and HF2 were used to calculate heat flow, where the temperature gradient intervals were inferred to correlate with HF2 stratigraphy.

Data for the heat flow calculations are summarized in Figure 27 and Table 4. The intervals 70-115 m and 115-135 m have essentially the same heat flow (2.33 and 2.36 HFU). This internal consistency gives credence to the lithologic and conductivity assumptions. The gradient interval that is correlated with the El Paso Limestone has an estimated 1.89 HFU heat flow. The heat flow of 80W6 is interpreted as 2.34 HFU. This value is in close agreement with HF1, which was 2.25 HFU. The slightly higher value in 80W6 may result

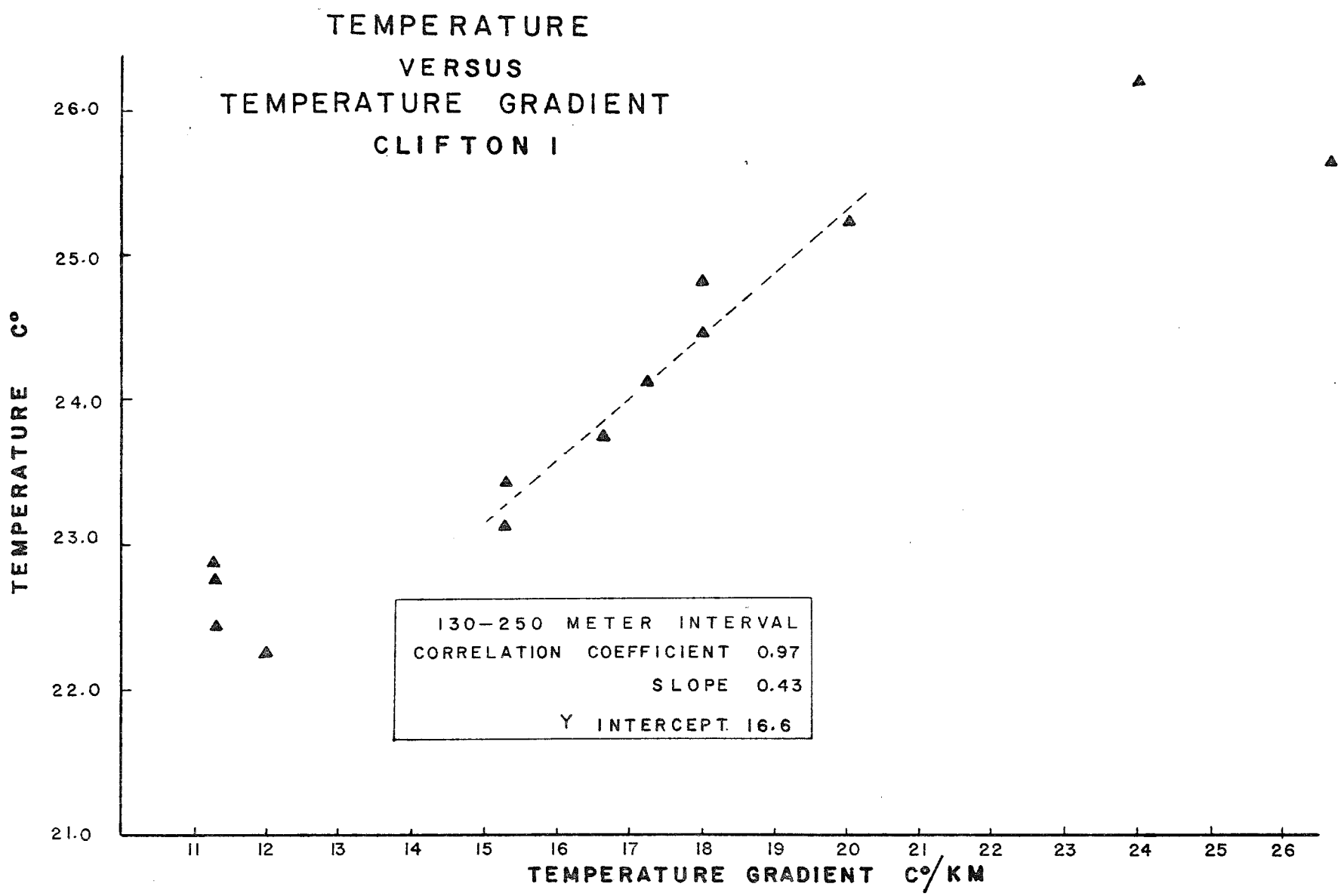
TEMPERATURE
VERSUS
TEMPERATURE GRADIENT
CLIFTON I
TEMPERATURE C°
26.0
25.0
24.0
23.0
22.0
21.0
11
12
13
14
15
16
17
18
19
20
21
22
23
24
25
26
TEMPERATURE GRADIENT C°/KM
130–250 METER INTERVAL
CORRELATION COEFFICIENT 0.97
SLOPE 0.43
Y INTERCEPT 16.6

FIGURE 28

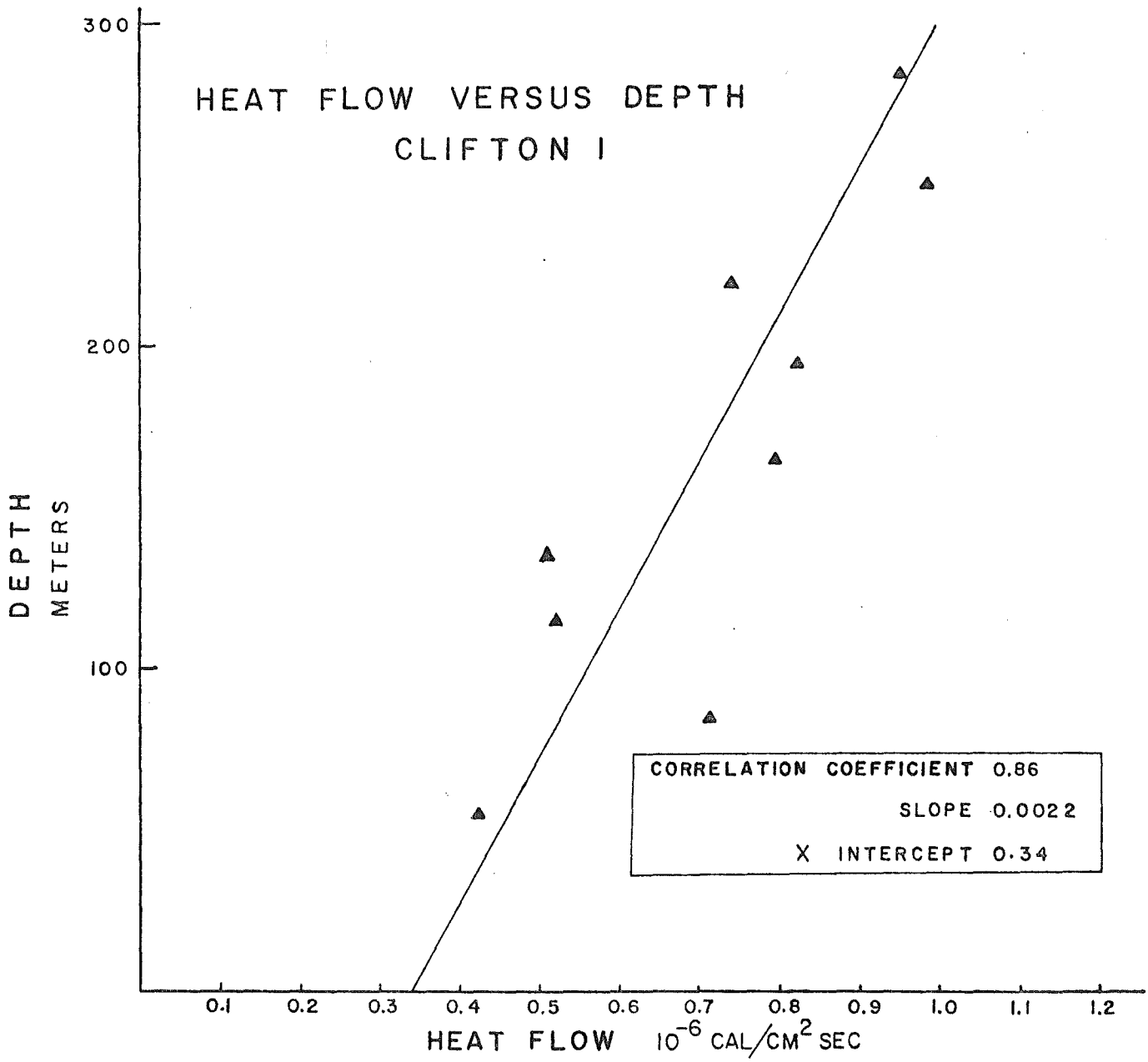
HEAT FLOW VERSUS DEPTH
CLIFTON I
DEPTH
METERS
300
200
100
0.1
0.2
0.3
0.4
0.5
0.6
0.7
0.8
0.9
1.0
1.1
1.2
HEAT FLOW 10^{-6} CAL/CM^2 SEC
CORRELATION COEFFICIENT 0.86
SLOPE 0.0022
X INTERCEPT 0.34

FIGURE 29

from its being 5.6 km (3.5 mi) from the Clifton Hot Springs. No topographic or porosity corrections were applied to 80W6 data.

Clifton 1 is in basin-fill sediments derived mostly from volcanic rocks. The lower 130 m appears to be boulder conglomerate consisting of basaltic andesite clasts. Some drill chips are rounded and slightly weathered on one side as if originally part of a large cobble or boulder. This lower conglomerate is tentatively correlated with the basal conglomerate in the Greenlee Beds of Heindl (1958). The water table at Clifton 1 is approximately 50 m deep and this depth approximates the level of the Gila River 0.8 km away.

Clifton 1 has very low heat flow. The Temperature versus Temperature-Gradient profile (Figure 28) between 130-350 m is nearly linear, suggesting a uniform vertical flow of water that could transport heat. The Heat Flow versus Depth plot (Figure 29) shows that the heat flow increases with depth, which confirms that vertical water flow is occurring in a downward direction. Where vertical water flow exists, the heat flow contributed or removed by this convective component (Δg) can be calculated by subtracting the component of heat contributed by conduction.

$$\Delta q = \rho C v \partial T = (\text{Equation (2)} - \text{Equation (1)})$$

For Clifton 1, Δq is - 0.22 HFU[4] and is obtained by subtracting the

[4] A negative sign indicates reduction of heat flow by loss of heat to downward flowing water. A positive sign indicates increased heat flow by addition of heat by upward flowing water.

heat flow at 250 m from the heat flow at 130 m. Assuming a heat capacity (C) of 1.0 cal/gm^{o}C and a density (ρ) of 1.0 g/cm^3 for water, a one cm^3 volume of water would require a downward velocity (v) of about 4.6 cm/year to lower the heat flow through an area of one cm^2, at the top of the 130 m to 250 m interval, by 0.22 HFU.

A column of water moving downward each year (4.6 cm/year) is 18 percent of the annual rainfall (26 cm/year). This percent of annual rainfall recharging subsurface aquifers may be too high for an arid region. Rantz and Eakin (1971) report recharge percentages of annual rainfall less than 7 percent in an arid and cooler region in Nevada. Therefore, flow of water resulting from rainfall recharge does not account entirely for the observed heat loss at Clifton-1. Lateral water flow associated with a sloping water table could account for the vertical water velocities and the heat loss observed at Clifton-1. With a sloping water table in an isotropic aquifer, the lateral water flow would have a downward component of flow at shallow depths. If the water flow is laminar and the water table is the piezometric surface for the 130 m to 150 m depth interval (unconfined), it is possible to approximate the average permeability of the sediments in the 130 m to 150 m interval. In order to do this, the volumetric velocity calculated using convective heat flow has to be converted to the true or darcian velocity if the same volume of water flows through a porous medium. By dividing 4.6 cm/year (volumetric velocity) by the effective porosity or specific yield of the rock between 130 m and 250 m, the vertical darcian velocity is calculated. Since core samples were not taken from this zone,

it is necessary to estimate the effective porosity from lithology logs of cuttings. Using .25 for the effective porosity, a vertical darcian velocity of 18.4 cm/year is calculated.

Assuming that the water table gradient is roughly the same as the elevation drop of the Gila River with linear map distance, a lateral velocity may be approximated by dividing the darcian vertical velocity (18.4 cm/year) by the water-table gradient (.27 percent). The approximate lateral darcian water velocity is 6815 cm/year. With this lateral darcian velocity the permeability of the sediment in Clifton 1 is calcualted to be 1.0396×10^3 darcys by applying Darcy's Law.

$$k = \frac{vdu}{\rho g \frac{\partial H}{\partial \ell}}$$

where

vd = darcian water velocity 6815 cm/year of 1.161×10^{-4} cm/sec

μ = viscosity of water, 0.1 gm/cm sec

ρ = density of water, 1.0 gm/cm^3

g = gravity, 780 cm/sec^2

$\frac{\partial H}{\partial \ell}$ = water table gradient, .0027 or 14 feet/mile

k = permeability, 1.026×10^{-5} cm^2 or 1.0396×10^3 darcys (1 darcy = 9.87×10^{-9} cm^2

The permeability estimated from the heat flow data indicates that a very good aquifer exists between 130 m and 250 m.

All of the measured heat-flow values in the Clifton area except HF1 and 80W6 are significantly influenced by local or regional water

flow. The low heat-flow values indicate lateral and downward water flow in permeable recharge areas. In order to conserve energy, the heat losses due to ground water recharge are balanced by heat gains in discharge areas. Discharge may occur by lateral-subsurface flow out of the area, or by springs discharging at the surface or into through-flowing rivers. Conservation of mass is required too. Water that is recharging aquifers or flowing into the subsurface must exit somewhere if the aquifer is saturated. The hot springs around Clifton are part of the conservation-of-mass-and-energy processes in the area.

The deeply circulating forced convective flows of water represented by the hot springs are heated by the high regional heat flux. The 2.3 HFU area heat flow is 0.3 to 0.4 HFU higher than the normal heat flow of the southern Basin and Range province. One or a combination of heat producing geologic phenomenon may account for the high heat flow. Heat from a cooling magma body is ruled out because there is no identified Holocene or Pleistocene silicic volcanism nor is the area's seismicity or heat flow of sufficient magnitude to indicate young plutonism. Therefore, the heat source is either high upper mantle temperatures or anomalous radiogenic heat production in the crust. Roy and others (1972) show that conductive surface heat flow is related to the amount of heat contributed by the mantle plus the heat contributed by radiogenic heat production in the crust. A linear relationship between surface heat flow and heat production in crystalline rock is delineated by Roy and others, 1972, when heat flow values from a single physiographic province are compared. The fol-

lowing equation, which is the same form as the mathematical statement describing a line, shows the heat flow relationships within each province:

$$Qs = Qm + A_o d$$

Equation 3

Qs = surface heat flow

Qm = mantle heat flow

A_o = heat production in the crust

d = depth to the base of heat producing layer

At Clifton, heat production of the Precambrian granite is tentatively determined as 6×10^{-13} cal/cm^3 sec (Bruce Taylor, pers. comm., 1980). Thus, heat production of the granite at Clifton appears normal. Roy and others (1972) determined the slope of equation (3), or the depth to the base of the heat producing crust, as 9.4 km for the Basin and Range province and the average mantle heat flow as 1.4 HFU for the Basin and Range province. Predicted surface heat at Clifton, using the tentative heat production value and the normal mantle heat flow and thickness of the heat producing layer of the crust in the Basin and Range province, is 1.96 HFU. Therefore, the mantle heat flow or the thickness of the heat producing layer at Clifton may be >1.6 HFU and/or >12 km, respectively, in order to account for the 0.3 HFU difference in the observed heat flow from the predicted heat flow. A thick heat producing layer is the preferred explanation of the high heat flow in the area because thick piles of mid-Tertiary volcanics add to the radiogenic heat producing layer. Diffusion of this heat into the Clifton-Morenci horst block where the conductive heat flow measurements are located facilitates measurement of the high heat flow.

Absence of Quaternary or late Pliocene basaltic volcanism argues against a mantle heat flow equal to or greater than 1.6 HFU.

CONCLUSIONS AND RECOMMENDATIONS

Geothermal potential of the lower San Francisco River region is outstanding for low- to moderate-temperature geothermal applications. Low- to moderate-temperature resources exist at shallow depths along fault zones transverse to regional water flow. These zones are characterized by hot springs that discharge geothermal waters in canyon bottoms of the Gila and San Francisco rivers and their tributaries. Additional hidden geothermal systems are likely to exist, which are not characterized by surface discharge of hot springs. Future exploration for additional low- to moderate-temperature resources should identify fault zones that cross transverse to the regional water table slope, preferably at discharge points of hydrologic basins.

Geothermometry of the hot springs suggests that resources greater than 130°C exist, with deep reservoir temperatures possibly as high as 180°C. Regional geology provides a special setting for possible forced convection to depths up to 4 km. The hot spring geothermometry data indicate that forced convection to great depth may occur. Lithostatic pressures at depths greater than 2 km tend to preclude fracture permeability by closing fractures to deep water flow. However, the regional stratigraphy includes units that are potentially very permeable due to inherent susceptibility to solution and persuasive brecciation, combined with primary porosity such as vesicularity or autobrecciation. The region lies on the intersection of major regional lineaments that are possibly crustal flaws. These lineaments may focus

present-day tectonic stress causing dilatory strain to open fractures. In addition, the area lies on the southwest boundary of the Datil-Mogollon volcanic field, which is inferred to overlie a mid-Tertiary batholith that has apparently had a profound influence on post Miocene strain in the crust as evidenced by a circling of graben structures. Present-day stress may also be modified by the rigid pluton to cause dilatory strain and opening deep fractures in the surrounding region.

The area lies on the north flank of a Mesozoic uplift. Mesozoic erosion has exposed potentially permeable Mississippian and Pennsylvanian carbonate rocks on uplift margins. Subsequent deposition of Cretaceous shales provided impermeable cap rocks.

Mid-Tertiary volcanism has piled up to 4 km of flows and tuffs in Tertiary basins that resulted from either collapse or sagging associated with volcanism or from faulting and/or low amplitude folding caused by Tertiary tectonic stress. These rocks buried Paleozoic strata to great depth. They consist of flows of potentially permeable vesicular andesite and basaltic andesite with intercalated impermeable tuffs and volcanoclastic sediments. In addition, autobrecciated felsic flows and plugs may provide vertical permeability.

Widespread faulting and great topographic relief with associated high precipitation in mountains provide a setting for deep forced convection. Impermeable cap rocks over potential reservoir rocks constrain the discharge of possible forced convective systems to limited flows in fault zones or brecciated felsic intrusions that have vertical permeability, thus conserving heat in deep reservoirs.

Regional heat flow in the Clifton area is 2.3 HFU. This heat flow

is about 0.3 HFU greater than the heat flow average for the Basin and Range province. The higher heat flow is either caused by greater heat production in the crust or by higher mantle (reduced) heat flow. Higher heat production is the most likely cause and is accomplished by either abnormally thick heat producing crustal layer or by anomalously high radiogenic heat production in the crystalline basement. Due to the great thickness of volcanic rocks, which are capable of high radiogenic heat production, an anomalously thick crustal heat-producing layer is the preferred explanation for the high heat flow because the Precambrian granite tentatively appears to have normal radiogenic heat production, and young basaltic volcanism and active faulting in other areas with high mantle heat flow are not observed.

Exploration for geothermal reservoirs with temperatures greater than 130°C and possibly up to 180°C seems warranted even though no young, <1 m.y. old, silicic volcanism is observed or inferred to occur in this area because these high temperature (>130°C) reservoirs are predicted by geothermometry. Reservoirs may occur along deep (2-4 km) segments of fault zones.

Since the surface discharge of known systems are sodium chloride waters with salinities up to 10,000 mg/l, and shallow ground water flow largely obscures conductive heat flow except in Precambrian granite, electrical geophysics, integrated with area geohydrology and geologic mapping, appear to be the best exploration approach for discovery of geothermal reservoirs with temperatures greater than 130°C in this area. Since subsurface resistivity is largely controlled by rock type, porosity and salinity, permeable faults or formations containing hot sodium

chloride water will have relatively (<20 ohm-meter) low subsurface resistivities. If water-saturated rock with temperatures greater than 180°C exists, very low resistivity will occur (<1 ohm-meter). Electromagnetic (EM) techniques appear to be the best geophysical tool because they are rapid, logistically simple, and may be easily interpreted to 3 to 4 km depths. Major fault zones and structures should be investigated first, especially faults transverse to regional ground water flow and faults associated with thermal springs. Because the potential moderate- to high-temperature geothermal systems are probably forced convective systems, areas with elevations exceeding 1525 m (5,000 ft) to 1830 m (6,000 ft) probably do not make good exploration targets.

Geochemical modeling of hot spring chemistry coupled with regional oxygen-deuterium isotope studies may provide additional information concerning recharge and reservoir rock type or flow paths within the geothermal systems characterized by hot springs.

Low- to moderate-temperature geothermal resources occur at Clifton and along the Gillard Hot Springs fault zone. Minimum exploration is necessary to site production holes for utilization of these resources. Exploration may include shallow, (less than 50 m) heat flow holes, shallow resistivity profiling, or "wildcat" production holes based on cross sections of detailed geologic mapping of faults known to control hot spring discharges. The Clifton Hot Spring system may be the most strategically located and economical low- to mdoerate-temperature geothermal resource in Arizona from the standpoint of a potential user and cost of exploring, drilling, and developing. Since the system naturally dis-

charges into the river, disposal of spent geothermal fluids may not be a problem. To conclude, further work is warranted to bring potential geothermal resources in the lower San Francisco River area into utilization.

TABLE 1A TERTIARY VOLCANIC STRATIGRAPHY IN THE CLIFTON AREA

NAME	LITHOLOGY	THICKNESS	AGE	CORRELATION/SYNONYMS	STRATIGRAPHIC POSITION	SOURCE	REFERENCES	RESERVOIR POTENTIAL
Rhyolite	Flow banded rhyolite, autobreccia, breccia, vitrophyre, & ash tuff	50-300	Early Miocene?	Enebro Mountain rhyolite, San Francisco rhyolite, Gray Peak rhyolite, Malpais rhyolite	Overlies, intrudes & intercalated with upper Prieto basaltic andesite	west-northwest oriented zone of dikes, plugs, rhyolite domes & a probable cauldron	Lindgren, 1905 Berry, 1976	May provide vertical fracture permeability for recharge or hot water flow.
Prieto basaltic andesite	Basaltic andesite flows 5-20 m thick & basaltic andesite breccia, amygdaloidal & weathered, microphenocryst of iddingsite	300-700+	Early Miocene-late Oligocene?	Bearwallow Mountain Formation, Sunset basalts	Unconformably overlies Clifton andesites. Contains a thin discontinuous "Turkey track" andesite at base	Possibly fissure eruptions or one or more large strato volcanoes	Lindgren, 1905 Berry, 1975	Unknown-numerous springs discharge in the San Francisco River Canyon from perched water in breccia zones & fractured flows, potential good shallow reservoir
Clifton andesite	Reddish brown andesite flows phenocrysts of plagioclase & iddingsite common	100	Oligocene?	Datil Group (restricted sense 40-28my), may correlate with red vesicular andesites in Blue Creek Basin	Unconformably overlies Clifton rhyolite ash flow tuff	unknown	Lindgren, 1905 Berry, 1976	Shallow hot water reservoir in fault zones near Clifton
Clifton rhyolite	Ash flow tuff, highly weathered, devitrified with eutaxitic texture phenocrysts of biotite & feldspar	50	32.9 my Damon & Assoc., 1966	Datil Group (restricted sense 40-28my)	Angular unconformity with Paleozoic rocks. In places unconformably overlies thin clastic sediments containing laramide intrusive & Paleozoic clasts. Gravel is possibly Eocene age?	Probable outflow sheet of presently unidentified volcano-tectonic feature (cauldron)	Lindgren, 1905 Berry, 1976 Damon & Assoc., 1966	Shallow hot water reservoir in fault zones near Clifton

TABLE 1B TERTIARY VOLCANIC STRATIGRAPHY IN THE GLENWOOD-MOGOLLON-LOWER FRISCO HOT SPRINGS AREA, NEW MEXICO

NAME	LITHOLOGY	THICKNESS	AGE	CORRELATION/SYNONYMS	STRATIGRAPHIC POSITION	SOURCE	REFERENCES	RESERVOIR POTENTIAL
Conglomerate	Locally derived conglomerate with interbedded basaltic flows in lower sections	100+	Post 20 my Pre-"Basin and Range"	Older "Gila Conglomerate" Gold Gulch Beds Juan Miller Conglomerate	Overlies Bearwallow Mountain Formation; faulted by "Basin & Range" faults. Lower part time equivalent to Bearwallow Mountain Formation	Locally derived deposition in low lying areas between volcanic centers	Heindl, 1967	Provides shallow aquifer for lower Frisco Hot Springs
Bear Mountain Formation	Dark basaltic andesites, basalt & minor latite flows & breccia	800	Early Miocene 20-22 my	Other early Miocene basaltic andesites	Overlies Deadwood Gulch Andesite & Last Chance Andesite	Numerous stratovolcano	Elston & others, 1973 Rhodes, 1976	Provides shallow aquifer for lower Frisco Hot Springs; numerous springs discharge in San Francisco River Canyon from perched water in breccia zones and fractured flows
Last Chance Andesite	Andesite flows and breccia	300	25.0 my Strangway & others, 1976	Lithologically identical to Mineral Creek Andesite. May represent same unit.	Interbedded & overlying Deadwood Gulch Rhyolite	Stratovolcano west of area	Elston and others, 1973 Rhodes, 1976 Strangway & others, 1976	Unknown
Deadwood Gulch Rhyolite	Rhyolite ash-flow & ash fall tuffs, tuffaceous sandstone, bedded rhyolite pumice	350	Oligocene Pre 25.0 my Post 27.3 my	Similar lithologies occur at the base of Fanney Rhyolite. May be correlative in time with Fanney Rhyolite, Jordan Canyon Rhyolite?	Underlies Last Chance Andesite	Moat filling rocks around resurgent dome of Bursum Cauldron	Rhodes, 1976 Elston and others, 1973	Unknown

TABLE 1B TERTIARY VOLCANIC STRATIGRAPHY IN THE GLENWOOD-MOGOLLON-LOWER FRISCO HOT SPRINGS AREA, NEW MEXICO Con't.

NAME	LITHOLOGY	THICKNESS	AGE	CORRELATIONS/SYNONYMS	STRATIGRAPHIC POSITION	SOURCE	REFERENCES	RESERVOIR POTENTIAL
Mineral Creek Andesite	Andesite flows and breccia, amygdaloidal texture	200	Between 27.3 & 27.5 my, Elston and others, 1973	Lithologically identical to Last Chance Andesite. May represent the same unit.	Intruded by Fanney Rhyolite	Flows from stratovolcano west of area	Rhodes, 1976 Elston and others, 1973	Unknown
Fanney Rhyolite	Rhyolite lava flows, breccias and tuffs, flow banded & spherulitic texture	700	Between 27.3 & 27.5 my, Elston and others, 1973	Intrudes and overlies Mineral Creek Andesite	Intrudes Mineral Creek Andesite	Ring fracture intrusives & domes of Bursum Cauldrons	Rhodes, 1976 Elston and others, 1973	May provide vertical permeability for recharge
Lower Volcanics	Rhyolite & quartz latite ash-flow tuff, breccia and andesitic lava flows	1100	Pre-28 my, post-Cretaceous	Datil Group (restricted sense, 40-28 my), Whitewater Creek Rhyolite, Cooney Quartz Latite	Underlies Mineral Creek Andesite	Unknown, possible cauldron tentatively called Mogollon Cauldron	Elston and others, 1976 Rhodes, 1976	Unknown. May have significant potential due to depth of burial if permeable units exist with hydrologic connections to surface.

TABLE 1C TERTIARY VOLCANIC STRATIGRAPHY IN THE BLUE RANGE PRIMITIVE AREA (NORTH)

NAME	LITHOLOGY	THICKNESS	AGE	CORRELATION/SYNONYMS	STRATIGRAPHIC POSITION	SOURCE	REFERENCES	RESERVOIR POTENTIAL
Ash flow tuff	Welded ash-flow tuff, individual cooling units separated by conglomerate & sandstones, gray to off-white	100-300	24.9 my Ratte and others, 1969	Cauldron outflow sheet?	Overlies Blue Range conglomerate	Possible outflow from unidentified cauldron	Ratte and others, 1969	Unknown
Blue Range conglomerate	Laharic & fluvial sediment derived from the pyroxene-hornblende andesite, local andesite flows, contains limestone, granite & schist clasts	700	Oligocene to late Eocene?	Datil Group (restricted sense, 40-28 my)	Lower section contains 2 ft. boulders of Pennsylvanian limestone & gneissic granite, upper part correlative with pyroxene-hornblende andesite, pre-Tertiary rocks not exposed	Pre-Tertiary basement and Tertiary Datil Group volcanics	Ratte and others, 1969	Unknown

TABLE 1D TERTIARY VOLCANIC STRATIGRAPHY IN THE BLUE RANGE PRIMITIVE AREA (SOUTH)

NAME	LITHOLOGY	THICKNESS	AGE	CORRELATIONS/SYNONYMS	STRATIGRAPHIC POSITION	SOURCE	REFERENCES	RESERVOIR POTENTIAL
Rose Peak Basaltic Andesite	Basaltic andesite flows & breccias, flows 2-3m thick & occasionally exhibit amygdaloidal texture	700	23.3 my, Ratte and others, 1969	Bearwallow Mountain Formation	Overlies & interbedded by Red Mountain, Horse-Maple Canyon rhyolite latite	Possible stratovolcano or fissure vents	Ratte and others, 1969; Berry, 1976	Unknown
Quartz-latite and rhyolite	Quartz-latite and rhyolite flows ash flow and air fall tuffs	250-1000	23.4 my, Ratte and others, 1969	Red Mountain cauldron, Squaw Creek cauldron, Horse Canyon-Maple Canyon cauldron, Pine Flat dome, Pipe Stem Mountain dome	Intrudes and interbedded in Rose Peak basaltic andesite	Small non-resurgent cauldrons or large dome complexes	Ratte and others, 1969; Berry, 1976	Provides vertically permeable rock for Hanna Creek Hot Springs geothermal system
Pyroxene-hornblende andesite	Flows & flow breccias of reddish-brown to gray pyroxene andesite & hornblende plagioclase andesite	700	37 my, Ratte and others, 1969	Datil Group (restricted sense, 40-28 my)	Underlies quartz-latite & rhyolite & Rose Peak basaltic andesite. Pre-Tertiary rocks not exposed.	Possible strato-volcano	Ratte and others, 1969; Berry, 1976	Unknown

TABLE 1E TERTIARY VOLCANIC STRATIGRAPHY IN THE JUAN MILLER BASIN

NAME	LITHOLOGY	THICKNESS	AGE	CORRELATIONS/SYNONYMS	STRATIGRAPHIC POSITION	SOURCE	REFERENCES	RESERVOIR POTENTIAL
Basaltic andesite	Gray, thin flows of basaltic andesite & andesite with olivine microphenocrysts, confined to Four Bar Mesa	50-70	Early Miocene?	Prieto basaltic andesite?	Overlies Juan Miller conglomerate	Fissure eruption	Berry, 1976	No geothermal potential
Juan Miller Conglomerate	Locally derived conglomerate of volcanic clasts that is interbedded with basaltic flows and rhyolitic ash flow tuffs, 7 units recognized along Juan Miller Road	300-500	Miocene - late Oligocene?	Gold Gulch Beds, Bonita Beds, older Gila Conglomerate. Unit is intercalated with 3 ash flow tuff units less than 50 meters thick	Overlies basaltic andesite. Lower 10 m intruded by basaltic andesite dikes, faulted with displacements less than 30 meters.	Locally derived clasts	Berry, 1976	Unknown. May be an aquiclude, interbedded basaltic flows possibly permeable
Basaltic andesite	Basaltic andesite	150-200	Miocene - late Oligocene?	Resembles Prieto basaltic andesite at Clifton	Only 10-20% exposed. Remainder of section in Humble Oil drill hole 33°17.5'N-109° 12.6'W, elevation is 4300'	Possible stratovolcano or fissure eruptions	Berry, 1976	Unknown
Pyroxene-hornblende andesite	Red-brown to gray flows & breccias of pyroxene andesite & hornblende-plagiclase andesite, generally weathered, minor intercalated flows of quartz latite	300-600+	37 my, Ratte and others, 1969	Datil Group (restricted sense, 40-28 my) - pyroxene-hornblende andesite of Blue Range Primitive area	Found only in Humble Oil drill hole, 33° 17.5'N-109°12.6'W, pre-Tertiary rocks not intersected by drill hole	Possible stratovolcano or fissure eruptions	Berry, 1976	Unknown. Potential aquifer in breccia zones or fractured flows

TABLE 1F TERTIARY VOLCANIC STRATIGRAPHY IN THE BONITA CREEK-EAGLE CREEK AREA

NAME	LITHOLOGY	THICKNESS	AGE	CORRELATION/SYNONYMS	STRATIGRAPHIC POSITION	SOURCE	REFERENCES	RESERVOIR POTENTIAL
Conglomerate	Well indurated conglomerate with flows of basaltic andesite & rhyolitic tuff in basal exposures. Contains no pre-Tertiary clasts. Comprised of mostly felsite clasts.	250-500	Miocene?	Older Gila Conglomerate of Gilbert, 1875; Bonita Beds, Heindl and McCullough, 1961; Gold Gulch Beds, Heindl,1967	Overlies basaltic andesite. Faulted into contact with pre-Tertiary rocks	Derived locally. Represents sediment deposition between volcanic centers	Heindl and McCullough, 1961; Berry, 1976	No geothermal potential
Upper basaltic andesite	Basaltic andesite flows & breccia with intercalated conglomerate lenses	200-400	Early Miocene?	Underlies conglomerate & overlies rhyolite	Overlies rhyolite, possibly correlative to upper basaltic andesite in Gila Mountains		Heindl and McCullough, 1961; Berry, 1976	Eagle Hot Springs discharges from basaltic andesite-conglomerate contact, hot wells in Eagle Creek in this unit
Rhyolite	Rhyolite flows & breccias, tuffs interbedded with basaltic andesite flows	300	Early Miocene, late Oligocene?	Intrudes and overlies basaltic andesite	Intrudes and overlies lower basaltic andesite. Possibly correlative to 25-26 my rhyolite-latite in Gila Mountains		Heindl and McCullough, 1961; Berry, 1976; Strangway & others,1976	Possible vertical permeability for recharge for geothermal systems
Lower basaltic andesite	Basaltic andesite flows & breccias, lenses of tuffaceous sandstone & conglomerate	350	Late Oligocene?	Overlies pre-Tertiary sedimentary, intrusive and volcanic rock	Intruded and overlain by rhyolite. Overlies pre-Tertiary rocks, possibly correlative to red basaltic andesite breccia in Gila Mountains.		Heindl and McCullough, 1961; Berry, 1976	Unknown

TABLE 1G TERTIARY VOLCANIC STRATIGRAPHY IN THE BLUE CREEK BASIN

NAME	LITHOLOGY	THICKNESS meters	AGE	CORRELATION/SYNONYMS	STRATIGRAPHIC POSITION	SOURCE	REFERENCES	RESERVOIR POTENTIAL
Mule Creek Rhyolite	Quartz latite - rhyolite flows, ash flow tuff & breccia intercalated with tuffaceous sediment, phenocrysts of quartz, plagioclase, sanadine, biotite & hornblende	600-700	18.6 my, Rhodes and Smith,1972	Deer Peak tuff ring, Harden Cienega vent, Mount Royal tuff ring	Overlies & intrudes Bearwallow Mountain Formation	Mule Creek non-resurgent cauldron & contemporary domes & diatremes	Rhodes and Smith, 1972; Seager and Clemons,1972; Wahl, 1980	Unknown. May provide vertical permeability for recharge
Bearwallow Mountain Formation	Dark gray vesicular basaltic andesite, olivine microphenocrysts	350	Early Miocene	Prieto basaltic andesite	Overlies "Turkey Track" andesite, Black Jack Canyon rhyolite and red vesicular andesite	Stratovolcanoes - Bear Mountain, Apple Gate Mtn, Brushy Mtn, Dry Section Mtn	Seager and Clemons,1972; Wahl, 1980; Elston, 1973	Unknown
"Turkey Track" Andesite	Reddish brown andesite with well-formed radiating phenocryst of plagioclase	270	Oligocene, early Miocene	Bearwallow Mountain Formation	Overlies Black Jack Canyon rhyolite	Stratovolcanoes	Seager and Clemons,1972; Wahl, 1980	Unknown
Upper rhyolite	Rhyolite flows, ash flow tuffs, breccias and air fall tuffs. Flows generally flow banded. Phenocrysts of quartz, sanadine & biotite	150-400	Oligocene, early Miocene?	Black Jack Canyon rhyolite, Twin Peaks rhyolite, Chalk Peak rhyolite	Overlies red vesicular andesite, in part contemporaneous with "Turkey Track" andesite and Bearwallow Mountain Formation	WNW and NE trending zones of rhyolite domes & dikes	Seager and Clemons,1972; Wahl, 1980	Unknown. May provide vertical permeability for recharge

TABLE 1G TERTIARY VOLCANIC STRATIGRAPHY IN THE BLUE CREEK BASIN
Con't.

NAME	LITHOLOGY	THICKNESS	AGE	CORRELATIONS/SYNONYMS	STRATIGRAPHIC POSITION	SOURCE	REFERENCES	RESERVOIR POTENTIAL
Red vesicular andesite	Red-purple brown amygdaloidal andesite & breccia. Intercalated with sills, plugs, flows & tuffs of rhyolite	300-1000	Late Oligocene	Amygdaloidal andesite, Wahl,1980; overlies Noah Mesa tuff that rests on Virden Dacite	Unconformably overlies Noah Mesa tuff (24.0 & 25.7 my fission track) Wahl, 1980	Small strato-volcanoes	Seager and Clemons,1972; Wahl, 1980	Unknown. Potentially significant aquifer in fractured zones
Virden Dacite	Red-purple brown nonvesicular dactite porphyry contains large phenocrysts of plagioclase. Commonly intercalated with tuffs & tuffaceous sediment.	600	31.3 my, Wahl,1980; 34.7 my, Elston & others, 1973	Overlain by Noah Mesa tuff, fission track dates 24.0 & 25.7 my,Wahl,1980; Datil Group (restricted sense, 40-28 my)	Unconformably overlies Steeple Rock flows and upper older andesite	Dacite domes & eruptive centers	Elston, 1973; Seager and Clemons,1972; Wahl, 1980	Unknown
Lower volcanics	Andesite flows and breccias, felsic tuffs and flows	2-3 xm	Pre-30 my, post-Eocene	Steeple Rock flow, older andesites, Mud Springs Tuff, School House Mountain Formation; Datil Group (restricted sense, 40-28 my)	Underlies Virden Dacite, base not exposed	Possible cauldron & fissure eruptions	Elston, 1960; Seager and Clemons,1972; Wahl, 1980	Unknown. May have significant potential due to depth of burial if permeable units exist with hydrologic connections to surface.

TABLE 2 Chemical analysis of groundwaters in the lower San Francisco River area

Results in milligrams per liter except as noted (see data sources)

Temperature in degrees celsius

Remarks:

S - spring	F(Flow in liter per second $x10^3$)
W - well	U - upstream from hot springs
D(depth in meters)	D - downstream from hot springs

Data sources:

1. Hem, 1950 (reported in parts per million)
2. Mariner and others, 1975
3. Swanberg and others, 1977
4. Ratte and others, 1969
5. Arizona Bureau of Geology and Mineral Technology, Geothermal Group
6. Files, U.S. Geological Survey, Tucson

Location: D-3-31-3 ADCC

quadrant township range section quarter

TABLE 2A ANALYSES OF CLIFTON HOT SPRINGS

Number	Sample	Location	Temperature C°	TDS	pH	Na	K	Na+K	Ca	Mg	Cl	SO_4	HCO_3+CO_3	SiO_2	Li	B	F	Remarks	Data Source
1	--	D-4-30-18CCA	71	13900	--	3300	220		880	22	7000	60	130	110	--	1.4	3.6		6
2	--	D-4-30-30CA	39	5526	7.0	1500	82		430	16	3150	72	163	55	2.6	0.64	2.3		2
3	A	D-4-30-18C	44	9696	6.6	2700	170		790	21	5700	62	146	94	4.1	1.4	2.7		2
4	B	D-4-30-18C	59	9352	7.1	2600	170		740	20	5500	68	146	95	4.0	1.2	2.8		2
5	213	D-4-30-30DB	48.8	8740	--	2540			767	37	5230	110	111	--	--	--	4.3		1
6	214	D-4-30-30DB	40	8880	--	2570			782	43	5280	138	136	--	--	--	4.1		1
7	215	D-4-30-30DB	37.8	8940	--	2620			754	41	5280	178	129	--	--	--	5.0		1
8	216	D-4-30-30DB	40.6	7490	--	2212			619	38	4470	68	152	--	--	--	3.6		1
9	217	D-4-30-30DB	43.3	9790	--	2608	142		860	41	5800	153	109	58	--	0.74	3.0		1
10	218	D-4-30-30DA	48.8	8330	--	2426			711	48	5000	75	126	--	--	--	4.0	W,D(6.7)	1
11	219	D-4-30-30DA	--	8830	--	2000			750	33	5260	120	128	--	--	--	--	W,D(6.7)	1
12	220	D-4-30-30DA	--	5320	--	1596	74		355	17	3030	99	168	57	--	2.5	4.1	W,D(24)	1
13	222	D-4-30-30BA	--	1930	--	583			145	13	1050	46	181	--	--	--	1.8	W,D(27.4)	1
14	235	D-4-30-30BA	--	2380	--	652	37		184	17	1300	44	208	42	--	1.5	1.0	W,D(27.4)	1
15	236	D-4-30-30BA	--	2160	--	561	35		168	16	1160	43	209	39	--	1.2	1.0	W,D(27.4)	1
16	AZ3	D-4-30-19CA	34.8	12576	7.7	3207	210		1064	52	6460	--	92	82	--	1.48	1.8		3
17	AZ5	D-4-30-18CD	48.0	14548	8.2	3586	243		926	23	7485	--	150	131	6.96	1.51	3.5		3
18	16	D-4-30-18C	61.0	7205	7.5	2015	175		601	13	4400	58	114	95	--	--	--		5
19	17	D-4-30-18C	45.0	10141	7.5	2502	239		959	23	6060	59	130	95	--	--	--		5
20	32W80	D-4-30-18CCDAC	70.0	11395	6.2	2700	195		800	21	6600	56	88	90	5.1	1.53	1.75		5
21	33W80	D-4-30-18CCDBB	70.0	10730	5.3	2650	176		748	21	6286	55	98	85	4.9	1.09	1.35		5
22	34W80	D-4-30-18CCBDD	67.0	10329	6.4	2650	180		728	21	6129	57	120	89	4.8	1.27	1.20		5
23	35W80	D-4-30-18CCBBD	67.0	9789	6.3	2450	159		707	20	5722	54	131	82	4.5	1.38	0.15		5
24	36W80	D-4-30-18CDCCC	50.0	14272	--	--	--		--	--	7213	--	--	88	5.4	1.64	0.40		5
25	37W80	D-4-30-19CADBC	32.0	--	6.9	--	--		--	--	2719	--	--	62	2.2	0.65	0.65		5
26	38W80	D-4-30-19CAAAA	33.0	10923	6.8	2350	138		735	41	7260	65	120	64	4.2	1.02	0.78		5
27	42W80	D-4-30-30DBCBA	38.0	10381	7.1	2280	103		757	33	5312	53	131	50	4.2	1.09	3.80		5
28	43W80	D-4-30-30DBDCC	31.0	2140	7.6	2140	113		701	45	5296	53	88	51	3.9	0.73	0.42		5

TABLE 2B ANALYSES OF SAN FRANCISCO RIVER NEAR CLIFTON HOT SPRINGS

Number	Sample	Location	Temperature C°	TDS	pH	Na	K	Na+K	Ca	Mg	Cl	SO_4	HCO_3+CO_3	SiO_2	Li	B Mg/l	F	Remarks	Data Source
29	168	D-4-30-18B	--	256	--	37			44	13	45	21	190	--	--	--	0.4	U,F(3.94)	1
30	182	D-4-30-30D	--	434	--	90			58	14	147	25	196	--	--	--	1.1	D,F(4.01)	1
31	AZ2	D-4-30-18CB	22.5	380	8.1	50	3.9		42	10.1	58	48	183	45	--	.02	0.65	U	3
32	AZ6	D-4-30-31DB	27.0	808	8.2	187	12		74	11.4	307	46	190	48	--	.08	0.83	D	3
33	40W80	D-4-29-12DDDA	19.0	208	8.7	65	4.4		10.8	11.7	68	24	86	38	0.1	0.36	0.92	U	5
34	41W80	D-4-30-31DBDA	22.0	--	7.8	184	13.3		30	12.3	358	29	131	43	0.3	<.01	1.55	D	5

TABLE 2C ANALYSES OF GILLARD HOT SPRINGS

Number	Sample	Location	Temperature C°	TDS	pH	Na	K	Ca	Mg	Cl	SO_4	HCO_3+CO_3	SiO_2	Li	B	F	Remarks	Data Source
35	AZ7	D-5-29-27AA	82	1244	8.0	411	13.2	20	0.7	464	175	220	98	1.01	0.4	10.6		3
36	--	D-5-29-27AA	82	1483	7.4	450	14	22	0.8	490	180	216	95	0.87	0.41	11		2
37	204	D-5-29-27AA	82.8	1224	--	437		27	3.5	470	174	228	--	--	0.8	--		1
38	205	D-5-29-27AA	76.7	1252	--	448		26	3.1	500	178	196	--	--	0.9	--		1
39	206	D-5-29-27AA	82.8	1242	--	450		22	2.2	480	182	215	--	--	0.7	--		1
40	207	D-5-29-27AA	--	1260	--	449		28	4.7	475	183	217	--	--	3.0	10		1
41	208	D-5-29-27AA	--	1357	--	494		24	3.9	520	193	224	--	--	0.8	12	W,D(7.9)	1
42	10W80	D-5-29-27AAC	81	1400	7.3	--	--	--	--	486	--	--	90	0.49	0.12	3.5		5
43	11W80	D-5-29-27AAC	82	1347	7.1	--	--	--	--	469	--	--	88	0.47	0.08	4.1		5
44	12W80	D-5-29-27AAC	84	1410	7.1	--	--	--	--	494	--	--	87	0.49	0.08	6.5		5
45	13W80	D-5-29-27AAC	66	1435	7.7	542	13	7.9	0.8	519	162	151	89	0.50	0.09	6.0		5

TABLE 2D ANALYSES OF GILA RIVER NEAR GILLARD HOT SPRINGS

Number	Sample	Location	Temperature C°	TDS	pH	Na	K	Ca	Mg	Cl	SO_4	HCO_3+CO_3	SiO_2	Li	B	F	Remarks	Data Source
46	AZ8	D-5-29-27AD	22	424	8.6	87	4.7	34	7.8	38	90	191	40	--	0.09	2.13	U	3
47	AZ9	D-5-29-27AB	24	432	8.5	97	5.1	32	7.3	50	90	199	50	--	0.08	2.32	D	3
48	14W80	D-5-29-27ABD	32	491	8.6	--	--	--	--	62	--	--	42	0.04	0.05	2.5	D	5
49	15W80	D-5-29-26BCB	30	438	8.6	--	--	--	--	52	--	--	37	0.02	0.02	2.0	U	5

TABLE 2E ANALYSES OF EAGLE CREEK HOT SPRINGS

Number	Sample	Location	Temperature C°	TDS	pH	Na	K	Ca	Mg	Cl	SO_4	HCO_3+CO_3	SiO_2	Li	B	F	Remarks	Data Source
50	16W80	D-4-28-35ABBA	42	626	7.0	159	7.7	25.0	1.3	121	49	209	21	.04	2.0	<.01		5
51	--	D-4-28-35AB	35	731	8.2	190	7.8	16.0	2.1	120	45	283	64	0.39	0.12	10.0		2
52	AZ4	D-4-28-35ABBA	42	676	8.1	198	9.0	14.4	2.2	120	77	288	67	6.96	0.15	10.2		3
53	45W80	D-4-28-35ABBA	42	658	8.3	179	9.5	3.4	2.4	126	51	197	60	0.4	<.01	8.0		5

TABLE 2F ANALYSES OF HANNA CREEK HOT SPRINGS

Number	Sample	Location	Temperature C°	TDS	pH	Na	K	Ca	Mg	Cl	SO_4	HCO_3+CO_3	SiO_2	Li	B	F	Remarks	Data Source
54	21	A-1-31-29AB	55.5	671	7.2	36	3.0	21	.1	343	15	32	39	--	--	--		5
55	--	A-1-31-29AB	49+	~600	~8.8	--	--	--	--	--	--	--	--	--	10	--		4

TABLE 2G ANALYSES OF LOWER FRISCO HOT SPRINGS

Number	Sample	Location New Mexico	Temperature C°	TDS	pH	Na	K	Ca	Mg	Cl	SO_4	HCO_3+CO_3	SiO_2	Li	B	F	Remarks	Data Source
56	135	C-12-20-23DB	45	1028	7.75	259	16.9	18	6	444	44	104	45	--	--	--		5
57	JW3	C-12-20-23BAC	43.3	992	7.9	207	15.6	50	6.8	445	58	129	75	0.48	0.3	1.4		3
58	JW4	C-12-20-23CB	40.0	768	7.9	216	11.3	39	7.4	295	44	137	65	0.34	0.2	1.5		3
59	JW5	C-12-20-23CAC	48.9	1280	7.8	406	18.8	54	6.9	574	90	108	91	0.65	0.4	1.8		3

TABLE 2H ANALYSES OF WARM SPRINGS (MARTINEZ RANCH AREA)

Number	Sample	Location	Temperature C°	TDS	pH	Na	K	Ca	Mg	Cl	SO_4	HCO_3+CO_3	SiO_2	Li	B	F	Remarks	Data Source
60	82	0-3-31-3ADCC	26.6	6594	7.7	1500	75	420	31	3391	56	750	48	2.46	4.0	1.5		5
61	83	33°12.6'N 109°7.6'W	25.5	479	8.7	48	0.6	11	33	16	85	225	76	0.16	4.1	1.2		5

TABLE 2I ANALYSES OF NON-THERMAL GROUNDWATER

Number	Sample	Location	Temperature C°	TDS	pH	Na	K	Na+K	Ca	Mg	Cl	SO_4	HCO_3+CO_3	SiO_2	Li	B	F	Remarks	Data Source
62	--	D-1-31-30ABA	15	253	--	26	2.7	44	12	5.7	6.3	240	41	--	.01	0.2	S	6
63	--	D-2-29-28CCA	10	227	--	7.6	1.4	30	25	2.8	7.1	210	58	--	<.01	0.1	S	6
64	--	D-2-30-4ACB	14	268	--	13	2.6	47	18	4.4	7.2	250	53	--	<.01	0.3	W	6
65	--	D-2-30-4ACC	15	282	--	14	2.7	51	19	4.8	7.1	268	67	--	.01	0.3	S	6
66	--	D-2-31-8CCA	16	278	--	14	2.8	50	22	5.2	11	270	57	--	.02	0.4	S	6
67	--	D-3-29-16CDA	12	386	--	11	0.9	96	29	5.7	15	240	35	--	.01	0.9	S	6
68	--	D-3-31-20DAB	21	308	7.2	11	8.4	46	13	6.8	130	63	42	--	.02	0.2	W	6
69	--	D-4-29-12DDA	20	342	--	48	3.3	49	14	69	27	190	38	--	.05	0.8	W	6
70	--	D-4-30-8ADA	17	482	--	30	3.3	86	29	16	50	380	90	--	.02	0.4	S	6

TABLE 2I ANALYSES OF NON-THERMAL GROUNDWATER, con't.

Number	Sample	Location	Temperature C°	TDS	pH	Na	K	Na+K	Ca	Mg	Cl	SO_4	HCO_3+CO_3	SiO_2	Li	B	F	Remarks	Data Source
71	--	D-4-32-18DAB	11	871	--	56	15		120	42	120	230	120	24	--	.02	0.1	W	6
72	--	D-4-32-20BAC	12	247	--	13	2.3		40	11	6.5	130	24	33	--	.01	0.1	W	6
73	15	D-4-30-18C	20.3	643	7.3	160	5.9		74	15	104	40	198	37	--	--	--	W,D(16.8)	5
74	39W80	D-4-30-19BACCD	23	514	7.4	188	11.8		6.2	3.5	148	42	208	44	0.3	<.01	0.9	S	5
75	44W80	D-4-28-24CCCDA	21	1137	8.5	64	6.1		42	46	25	400	121	40	0.1	0.44	0.6	S	5
76	46W80	D-5-30-17ABAAB	21	219	8.3	42	1.5		4.1	4.6	25	4	98	27	0.1	<.01	1.5	W	5
77	--	A-1-29-8DAB	10	198	--	5.6	0.7		30	19	1.5	1.9	190	53	--	<.01	0.1	S	6
78	--	A-1-32-17BDA	14	263	--	45	6.8		26	17	12	9.9	240	40	--	.04	0.5	W,D(183)	6
79	AZ1	D-4-28-27DC	16.8	420	8.2	23	3.1		50	27	8.8	27	305	86	--	.01	0.3	S	3
80	78	D-3-30-16DBB	23	939	7.7	120	4.0		63	41	254	52	225	69	0.2	4.3	1.5	S	5
81	84	33°13.6'N 109°6.5'W	16.1	316	7.8	45	3.3		18	14.1	33	24	194	48	0.05	4.1	1.3	S	5
82	85	33°13.8'N 109°5.9'W	24.0	322	7.9	53	3.5		20	9.3	36	18	281	46	0.05	3.4	1.5	S	5
83	86	33°14.2'N 109°2.7'W	17.2	487	7.7	62	5.5		33	19	68	21	182	55	0.05	3.7	1.3	S	5
84	87	33°13.7'N 109°1.8'W	17.0	314	8.0	43	3.9		22	7.4	29	18	125	41	0.05	3.8	1.3	S	5
85	88	33°12.6'N 109°0.6'W	16.1	238	7.7	31	2.9		16	5.7	23	18	121	39	0.04	2.7	1.2	S	5
86	243	D-4-29-3D	--	596	--	26			133	26	8	299	205	--	--	--	1.4	S	1
87	211	D-6-28-2AA	21.6	263	--	8.9			44	35	19	26	260	--	--	0.1	2.3	S	1
88	137	D-5-31-30BBB	21.5	413	7.1	26	2.2		36	16	9	57	199	19	--	--	--	W	5
89	138	D-5-30-13BAA	19.0	295	8.0	39	2.7		19	11	16	23	179	20	--	--	--	W	5
90	139	D-5-30-11CB	23.0	320	7.2	28	1.2		19	17	13	7	234	31	--	--	--	W,D(45.7)	5
91	140	D-5-30-11BD	25.0	288	7.3	28	1.2		23	14	9	3	222	22	--	--	--	W,D(152)	5

TABLE 3 GEOTHERMOMETRY OF CLIFTON HOT SPRINGS

Number	Sample	Temperature	pH	Cl	Na	K	Ca	SiO_2	Geothermometer Temperatures Na-K-Ca 4/3	Na-K-Ca 1/3	Quartz	Cation-anion balance
2	--	39	7.0	3150	1500	82	430	55	138	160	107	3.1
3	A	44	6.6	5700	2700	170	790	94	163	172	134	0.9
4	B	59	7.1	5500	2600	170	740	95	164	174	135	1.8
9	217	43.3	--	5800	2608	142	860	58	151	163	109	3.1
12	220	--	--	3030	1596	74	355	57	140	154	108	0.2
14	235	--	--	1300	652	37	184	42	117	155	94	2.9
15	236	--	--	1160	561	35	168	39	115	158	91	4.1
17	AZ5	48	7.9	7485	3586	243	926	131	181	179	153	0.4
18	16	61	7.5	4400	2015	175	601	95	168	186	135	3.2
19	17	45	7.5	6060	2502	239	959	95	172	191	135	5.5
26	38W80	33	8.0	7260	2350	138	735	64	153	167	114	4.5
1	--	71	--	7000	3300	220	880	110	176	178	143	3

Notes: For location of samples, data source, and additional analysis, see Table 2.
Temperatures in degrees Celsius
For Na-K-Ca 4/3 geothermometer temperatures greater than 100°C, use Na-K-Ca 1/3 temperatures.
Cation-anion balance is the per cent difference between milliequivalent totals of cations and anions.
Chemistry in milligrams per liter (mg/l)

Table 4. Heat Flow Data in the Lower San Francisco River Area

Heat Flow Hole	Bitter Creek (2)	E-2 (4)	80 W6 (5)
Latitude Degrees	32° 54'N	32° 50.6'N	33° 3.48'N 109° 14.36'W
Longitude Degrees	109° 02'W	108° 55.8'W	
Township section, township, range	sec. 20 T. 16S., R. 21W	sec. 8 T. 17S., R. 20W	SW¼, SW¼, NE¼, sec. 28 T. 4S., R. 30E.
Elevation Meters	1463	1761	1268
Mean Annual* Temperature °C	N/A	N/A	17.5
Thermal Gradient °C/km (Depth Interval)	45.7 ± 0.7 240'-390'	34.7 ± 0.30 (120-150) 38.75 ± 1.15 (150-170) 33.4 ± 0.79 (180-230)	25.45 (30-70) 22.46 (70-115) 25.64 (115-135)
Thermal Conductivity 10^{-3}cal/cm-sec-°C (Depth Interval)	6.72 240'-390'	5.98 ± 0.62 (120-150) 5.30 ± 0.37 (150-170) 5.62 ± 0.37 (180-230)	7.45 ± 0.8 (30-70) 10.39 ± 0.5 (70-115) 9.21 ± 1.5 (115-135)
Heat Flow 10^{-6}cal/cm^2-sec-°C (Depth Interval)	3.07(3) ± 0.09 240'-390'	2.08 (120-150) 2.04 (150-170) 1.88 (180-230)	1.89 (30-70) 2.33 (70-115) 2.36 (115-135)
Type Sample	Not Reported	Core	Cuttings
Lithology	Not Reported	Not Reported	Sandy dolomite, quartzite Granite or Arkose

(2) Data from Roy and others, 1968
(3) No Topographic correction
(4) Data from Shear, 1979
(5) Conductivity estimated from HF1 and HF2

Table 4 (con't.)

Heat Flow Data in the Lower San Francisco River Area

Heat Flow Hole	Morenci[1]	HF1	HF2	Clifton 1
Latitude Degrees	33° 05'	33° 5.9'	33° 2.7'	32° 56.7'
Longitude Degrees	109° 22'	109° 21.1'	109° 22.0'	109° 13.8'
Township section, township, range	sec. 16 T. 4S., R. 29E	NW¼, SE¼ sec. 10, T. 4S., R. 29E.	NE¼, NW¼, sec. 33, T. 4S., R. 29E.	NE¼, NE¼, sec. 1, T. 6S., R. 30E.
Elevation Meters	1296	1445	1341	1097
Mean Annual* Temperature °C	17.4	16.0	16.6	19.0
Thermal Gradient °C/km (Depth Interval)	22.7 ± 0.1 (340–580 m) 22.2 ± 0.6 (600–660 m)	25.8 (70–185 m) 23.0 (300–365 m)	9.4 (60–100 m) 16.1 (105–140 m)	12 (135–140 m) 20.0 (250–255 m)
Thermal Conductivity 10^{-3} cal/cm-sec-°C (Depth Interval)	6.1 ± 0.2 (340–580 m) 7.7 ± 0.9 (600–660 m)	8.73 ± .47 (70–185 m) 9.93 ± 1.7 (300–365 m)	10.4 (60–100 m) 6.5 (105–140 m)	4.3 (135–140 m) 4.5 (250–255 m)
Heat Flow 10^{-6} cal/cm²-sec (Depth Interval)	1.4 (340–580 m) 1.7 (600–660 m)	2.25 (70–185 m) 2.28 (300–365 m)	0.98 (60–100 m) 1.05 (105–140 m)	0.51 (135–140 m) 0.98 (250–255 m)
Type Sample	Core	Fragments	Fragments	Fragments
Lithology	granite ?	granite	orthoquartzite, dolomitic sandstone, granite	Coarse clastic sediment derived mostly from intermediate volcanics.

[1] Data from Reiter and Shearer, 1979.

*Obtained by interpolating mean annual temperatures from drill hole elevations using local weather station elevations and average temperatures.

BIBLIOGRAPHY

Armstrong, A. K. and Mamet, B. L., 1978, The Mississippian system of southwestern New Mexico and southeastern Arizona: in Land of Cochise, 29th Field Conference, New Mexico Geological Society Guidebook, p. 183-192.

Arnorsson, S., 1975, Application of the silica geothermometer in low temperature hydrothermal areas in Iceland: American Journal of Science, Vol. 275, p. 763-784.

Bennet, K. C., 1975, Geology and origin of the breccias in the Morenci-Metcalf District, Greenlee County, Arizona: unpub. M.S. Thesis, University of Arizona, 153 p.

Berry, R. C., 1976, Mid-Tertiary volcanic history and petrology of the White Mountains volcanic province, southeastern Arizona: unpub. Ph.D. Thesis, Princeton University, 317 p.

Billings, M. P., 1972, Structural Geology: Prentice-Hall, Inc., New Jersey, 606 p.

Boler, F., Klein, D., Christopherson, K., Hoover, D., 1980, Gravity observations: Clifton-Morenci area, Greenlee County, SE Arizona: U. S. Geological Survey Open-File Report, #80-96, 18 p.

Bredehoeft, J. D. and Papadopulos, I. S., 1965, Rates of vertical groundwater movement estimated from the earth's thermal profile: Water Resources Research, Vol. 1, No. 2, p. 325-328.

Bridwell, R. J., 1976, Lithosphere thinning and the Late Cenozoic thermal and tectonic regime of the northern Rio Grande Rift: in Vermejo Park, 27th Field Conference, New Mexico Geological Society Guidebook, p. 283-292.

Chapin, C. E. and Seager, W. R., 1975, Evolution of the Rio Grande Rift in the Socorro and Las Cruces Areas: in Las Cruces Country, 26th Field Conference, New Mexico Geological Society Guidebook, p. 297-322.

Chapin, C. E., Chamberlin, R. M., Osburn, G. R., Sanford, A. R., and White, D. W., 1978, Exploration framework of the Socorro Geothermal area, New Mexico: in Field guide to selected cauldrons and mining districts of the Datil-Mogollon volcanic field, New Mexico, New Mexico Geological Society Special Publication 7, p. 115-129.

Chapin, C. E., Sanford, A. R., White, D. W., Chamberlin, R. M., Osburn, G. R., 1979, Geological investigation of the Socorro Geothermal area: New Mexico Energy Institute Technical Report 26, New Mexico State University, 70 p.

Combs, J., 1974, Microearthquake investigation of the Mesa geothermal anomaly, Imperial Valley, California: Final Report to the U. S. Bureau of Reclamation: Riverside, University of California Institute of Geophysics and Planetary Physics, 37 p.

Coney, P. J., 1976, Structure, volcanic stratigraphy, and gravity across the Mogollon Plateau, New Mexico: in Cenozoic volcanism in southwestern New Mexico, New Mexico Geological Society Special Publication 5, p. 29-41.

Cooper, J. R., 1961, Turkey-track porphyry - A possible guide for correlation of Miocene rocks in southeastern Arizona: Arizona Geological Society Digest, Vol. IV, p. 17-33.

Cunningham, J. E., 1979, Geologic Map of the Clifton, Arizona area, 1:24,000: unpub., Arizona Bureau of Geology and Mineral Technology, Tucson.

Damon, P. E., and associates, 1966, Correlation and chronology of the ore deposits and volcanic rocks: Atomic Energy Commission Ann. Rept. No. 1966 COO-689-60, University of Arizona.

Davidson, E. S., 1973, Geohydrology and water resources of the Tucson basin, Arizona: U. S. Geological Survey Water Supply Paper 1939-E., 81 p.

Davis, G. H. and Coney, P. J., 1979, Geologic development of the Cordilleran metamorphic core complexes: Geology, Vol. 7, p. 120-124.

Davis, R. W., 1971, An analysis of gravity data from Tucson basin, Arizona: Arizona Geological Society Digest, Vol. IX, p. 103, 122.

Davis, S. N., 1964, Silica in streams and groundwater: American Journal of Science, Vol. 262, p. 870-891.

Decker, E. R. and Smithson, S. B., 1975, Heat flow and gravity interpretation in southern New Mexico and West Texas, Journal of Geophysical Research, Vol. 80, p. 2542-2552.

Domenico, P. A. and Palciauskas, V. V., 1973, Theoretical analysis of forced convective heat transfer in regional groundwater flow: Geological Society of America Bulletin, Vol. 84, p. 3803-3814.

Drewes, H., 1971 Geologic Map of the Mount Wrightson Quadrangle, Southeast of Tucson, Santa Cruz and Pima Counties, Arizona: U. S. Geological Survey Miscellaneous Investigation Map I-614.

Drewes, H., 1972, Structural geology of the Santa Rita Mountains, southwest of Tucson, Arizona: U. S. Geological Survey Professional Paper 748, 35 p.

Drewes, H. and Thorman, C. H., 1978, Major geologic structures between Lordsburg, New Mexico and Douglas and Tucson, Arizona: in Land of Cochise, 29th Field Conference, New Mexico Geological Society Guidebook, p. 291-295.

DuBois, S. M. and Smith, A. W., 1980, Earthquakes Causing Damage in Arizona: Fieldnotes, Arizona Bureau of Geology and Mineral Technology, Vol. 10, No. 3, p. 4-6.

Edmiston, R. C., 1979, Ore deposits as exploration models for geothermal reservoirs in carbonate rocks in the eastern Great Basin, Geothermal Resources Council transactions, Vol. 3, p. 181-184.

Elston, W. E., 1958, Burro uplift, northeastern unit of sedimentary basin of southwestern New Mexico and southeastern Arizona: American Association of Petroleum Geologists Bulletin, Vol. 42, p. 2513-2517.

Elston, W. E., 1968, Terminology and distribution of ash flows of the Mogollon-Silver City-Lordsburg Region, New Mexico: Arizona Geological Society Guidebook III, Southern Arizona, p. 231-240.

Elston, W. E., 1960, Reconnaissance geologic map of Virden thirty-minute quadrangle: New Mexico Bureau of Mines and Mineral Resources Geologic Map 15.

Elston, W. E., Damon, P. E., Coney, P. J., Rhodes, R. C., Smith, E. I., and Bikerman, M. E., 1973, Tertiary volcanic rocks, Mogollon-Datil Province, New Mexico, and surrounding region: K-AR dates patterns of eruption, and periods of mineralization, Geological Society of America Bulletin, Vol. 84, p. 2259-2274.

Elston, W. E., Rhodes, R. C., Coney, P. J., and Deal, E. G., 1976, Progress report on the Mogollon Plateau volcanic field, southwestern New Mexico, No. 3-surface expression of a pluton, in Cenozoic volcanism in southwestern New Mexico: New Mexico Geological Society Special Publication 5, p. 3-28.

Elston, W. E., Erb, E. E., Deal, E. G., 1979, Tertiary geology of Hidalgo County, New Mexico, New Mexico Bureau of Mines and Mineral Resources, New Mexico Geology, Vol. 1, No. 1, p. 1-6.

Evans, D. M., 1966, Man-made earthquakes in Denver: Geotimes, Vol. 10, p. 11-18.

Feth, J. H. and Hem, J. D., 1963, Reconnaissance of headwater springs in the Gila River drainage basin, Arizona: U. S. Geological Survey Water-Supply Paper 1619H, 54 p.

Foster, R. W., 1964, Stratigraphy and petroleum possibilities of Catron County, New Mexico: New Mexico Bureau of Mines and Mineral Resources Bulletin 85, 55 p.

Fournier, R. O., 1977, Chemical geothermometers and mixing models for geothermal systems: Pergamon Press, Geothermics, Vol. 5, p. 441-50.

Fournier, R. O., 1979, Geochemical and hydrologic considerations and the use of enthalpy-chloride diagrams in the prediction of underground conditions in hot springs systems: Journal of Volcanology and Geothermal Research, Vol. 5, p. 1-16.

Fournier, R. O. and Potter, R. W., 1978, A magnesium correction for the Na-K-Ca chemical geothermometer: U. S. Geological Survey Open-File Report 78-986, 23 p.

Fournier, R. O., and Rowe, J. J., 1966, Estimation of underground temperatures from silica content of water from hot springs and wet steam wells: American Journal of Science, Vol. 264, p. 685-697.

Fournier, R. O. and Truesdell, A. H., 1973, An empirical Na-K-Ca geothermometer for neutral waters: Geochem et Cosmochim Acta, Vol. 37, p. 1255-1275.

Fournier, R. O. and Truesdell, A. H., 1974, Geochemical indicators of subsurface temperature-part 2, estimation of temperature and fraction of hot water mixed with cold water: U. S. Geological Survey Journal of Research, Vol. 2, No. 3, p. 263-270.

Fournier, R. O., White, D. E., and Truesdell, A. H., 1974, Geochemical indicators of subsurface temperature-part 1, basic assumptions: U. S. Geological Survey Journal of Research, Vol. 2, No. 3, p. 259-262.

Garrels, R. M. and Mackenzie, F. T., 1967, Origin of the chemical compositions of some springs and lakes: in equilibrium concepts in natural water systems: American Chemical Society, Washington, D.C., p. 222-242.

Gilbert, G. K., 1887, Report on the Geology of Portions of New Mexico and Arizona: U. S. Geog. and Geol. Surveys W. 100th Meridian Report.

Gish, D. M., 1980, A refraction study of deep crustal structure of the Basin and Range-Colorado Plateau in eastern Arizona: unpub. M.S. Thesis, University of Arizona, 32 p.

Harbour, J., 1967, Stratigraphy and sedimentogy of the upper Safford basin sediments: unpub. Ph.D. Thesis, University of Arizona, 242 p.

Harder, V., Morgan, P. and Swanberg, C. A., 1980, Geothermal resources in the Rio Grande Rift: Origins and Potential: Geothermal Resources Council transactions Vol. 4, p. 61-64.

Hayes, P. T., 1978, Cambrian and Ordovician rocks of southeastern Arizona and southwestern New Mexico: in Land of Cochise, 29th Field Conference, New Mexico Geological Society Guidebook, p. 165-173.

Heindl, L. A., 1958, Cenozoic alluvial deposits of the upper Gila River area, New Mexico and Arizona: unpub. Ph.D. Thesis, University of Arizona, 249 p.

Heindl, L. A., 1962, Should the term "Gila Conglomerate" be abandoned?: Arizona Geological Society Digest, Vol. V, p. 73-88.

Heindl, L. A., 1967, Groundwater in fractured volcanic rocks in southern Arizona: in Hydrology of fractured rocks-Dubrovnik symposium, 1965 proc. Vol. 2, International Association of Sci. Hydrol. Pub. 74, p. 503-513.

Heindl, L. A., and McCullough, R. A., 1961, Geology and Availability of Water in the Lower Bonita Creek Area, Graham County, Arizona: U. S. Geological Survey Water Supply Paper 1589, 56 p.

Hem, J. D., 1950, Quality of water of the Gila River above Coolidge Dam, Arizona: U. S. Geological Survey Water-Supply Paper 1104, 230 p.

Hewitt, C. H., 1959, Geology and mineral deposits of the northern Big Burro Mountains-Redrock area, Grant County, New Mexico: New Mexico Bureau of Mines and Mineral Resources Bulletin 60, 151 p.

Hoover, D. B. and Long, C. L., 1975, Audio-magnetotelluric methods in reconnaissance geothermal exploration: in Proceedings, Second United Nations Symposium on the development and use of geothermal resources, Vol. 2, p. 1059-1064.

Kilty, K. S., Chapman, D. S., and Mase, C. W., 1979, Forced convective heat transfer in the Monroe Hot Springs geothermal system: Journal of Volcanology and Geothermal Research, Vol. 6, p. 257-277.

Klein, D., Long, C., Christopherson, K. and Boler, F., 1980, Reconnaissance geophysics in the Clifton and Gillard geothermal areas, southeastern Arizona: U. S. Geological Survey Open-File Report 80-325, 19 p.

Kottlowski, F. E., 1963, Paleozoic and Mesozoic strata of southwestern and southcentral New Mexico: New Mexico Bureau of Mines and Mineral Resources Bulletin 79, 100 p.

Lachenbruch, A. H. and Sass, J. H., 1977, Heat flow in the United States and the thermal regime of the crust: American Geophysical Union Monograph 21, p. 248-257.

Landis, E. R., Ratte, J. C. and Myers, D. A., 1971, Carbonate clasts in epiclastic volcanic rocks and their paleotectonic implications, Blue Range Primitive area, Arizona and New Mexico: U. S. Geological Survey Professional Paper 750-C, p. C58-C64.

Langton, J. M., 1973, Ore genesis in the Morenci-Metcalf District: AIME transaction, Vol. 254, p. 248-257.

Lindgren, W., 1905, Description of the Clifton quadrangle: U. S. Geological Survey Geologic Atlas, Folio 129.

Lindgren, W., 1905, The copper deposits of the Clifton-Morenci District, Arizona: U. S. Geological Survey Professional Paper 43, 375 p.

Luedke, R. G. and Smith, R. L., 1978, Map showing distribution, composition and age of late Cenozoic volcanic centers in Arizona and New Mexico, 1:1,000,000: U. S. Geological Survey Miscellaneous Investigation Series Map I-1091-A.

Lutton, R. J., 1958, Some structural features in southern Arizona: Unpub. M.S. Thesis, University of Arizona, 138 p.

Lysonski, J. C., Sumner, J. S., Aiken, C. and Schmidt, J. S., 1980, The complete residual Bouguer gravity anomaly map of Arizona (IGSN71), 1:500,000: Arizona Bureau of Geology and Mineral Technology.

Mann, L. J., 1980, Maps showing hydrologic conditions in the San Francisco River area, Greenlee County, Arizona, 1978-a Reconnaissance Study, U. S. Geological Survey Water-Resources Investigations Open-File Report 80-441.

Mansure, J. and Reiter, M., 1979, A vertical groundwater movement correction for heat flow: Journal Geophysical Research, Vol. 84, No. B7, p. 3490-3496.

Mariner, R. H., Presser, D. D. and Evans, W. C., 1977, Chemical, isotopic, and gas compositions of selected thermal springs in Arizona, New Mexico, and Utah: U. S. Geological Survey Open-File Report 77-654, 42 p.

Merrill, R. K., and Pewe, T. L., 1977, Late Cenozoic geology of the White Mountains, Arizona: Arizona Bureau of Geology and Mineral Technology Special Paper No. 1, 65 p.

McKee, E. D., 1951, Sedimentary basins of Arizona and adjoining area: Geological Society of America Bulletin, Vol. 62, p. 481-506.

Moolick, R. T. and Durek, J. J., 1966, The Morenci District, in Geology of the porphyry copper deposits, southwestern North America, edited by S. R. Titley and C. R. Hicks: University of Arizona Press, p. 221-233.

Morrison, R. B., 1965, Geologic map of the Duncan and Canador Peak quadrangles, Arizona and New Mexico: U. S. Geological Survey Miscellaneous Geological Investigations Map I-42, 1:48,000, text 7 p.

Morgan, P., Swanberg, C. A., and Lohse, R. L., 1979, Borehole temperature studies of the Las Alturas geothermal anomaly, New Mexico: Geothermal Resources Council, transactions, Vol. 3, p. 469-472.

Nehring, N. L. and Mariner, R. H., 1979, Sulfate-water isotopic equilibrium temperatures for thermal springs and wells of the Great Basin: Geothermal Resources Council, transactions, Vol. 3, p. 485-488.

Parasnis, D. S., 1971, Temperature extrapolation in infinite time in geothermal measurements: Geophysical Prospecting, Vol. 19, p. 612-614.

Parasnis, D. S., 1979, Principles of applied geophysics, 3rd Ed., Halsted Press, New York, 275 p.

Percious, J. K., 1968, Geology and geochronology of the Del Bac Hills, Pima County, Arizona: Arizona Geological Society Guidebook III, p. 199-207.

Peirce, H. W., 1976, Elements of Paleozoic tectonics in Arizona: Arizona Geological Society Tectonic Digest, Vol. X, p. 37-57.

Press, F., 1975, Earthquake prediction: Scientific American, Vol. 232, No. 5, p. 14-23.

Rantz, S. E. and Eakin, T. E., 1971, A summary of methods for collection and analysis of basic hydrologic data for arid regions: U. S. Geological Survey Open-File Report, 125 p.

Ransome, F. L., 1903, Geology of the Globe Copper District, Arizona: U. S. Geological Survey Professional Paper 12, 168 p.

Ratte, J. C., Landis, E. R., Gaskill, D. L., and Rabbe, R. G., 1969, Mineral Resources of the Blue Range Primitive area, Greenlee County, Arizona, and Catron County, New Mexico: U. S. Geological Survey Bulletin 1261-E, 91 p.

Reber, L. E., Jr., 1916, The mineralization at Clifton-Morenci: Economic Geology, Vol. 11, p. 528-573.

Rehrig, W. A. and Heidrick, T. L., 1976, Regional tectonic stress during the Laramide and late Tertiary intrusive periods, Basin and Range Province, Arizona: in Tectonic Digest, Arizona Geological Society Digest, Vol. X, p. 205-228.

Reiter, M., Edwards, C. L., Hartman, H., and Weidman, C., 1976, Terrestrial Heat Flow along the Rio Grande Rift, New Mexico and Southern Colorado, Geological Society of America Bulletin, Vol. 86, p. 811.

Reiter, M. and Shearer, C., 1979, Terrestrial heat flow in eastern Arizona, A First Report: Journal of Geophysical Research, Vol. 84, No. B11, p. 6115-6120.

Rhodes, R. C., 1976A, Volcanic geology of the Mogollon Range and adjacent areas, Catron and Grant Counties, New Mexico: in Cenozoic volcanism in southwestern New Mexico, New Mexico Geological Society Special Publication 5, p. 42-9.

Rhodes, R. C., 1976B, Petrologic framework of the Mogollon Plateau volcanic ring complex, New Mexico-surface expression of a major batholith: in Cenozoic volcanism in southwestern New Mexico, New Mexico Geological Society Special Publication 5, p. 103-112.

Rhodes, R. C. and Smith, E. I., 1972, Geology and tectonic setting of the Mule Creek Caldera, New Mexico, U.S.A.: Bulletin of Volcanology, Vol. 36, p. 401-411.

Ross, C. A., 1973, Pennsylvanian and early Permian depositional history, southeastern Arizona: American Association of Petroleum Geologists Bulletin, Vol. 57, p. 887-912.

Roy, R. F., Decker, E. R., Blackwell, D. D. and Birch, F., 1968, Heat flow in the United States: Journal of Geophysical Research, Vol. 73, No. 16, p. 5207-5221.

Roy, R.F., Blackwell, D.D. and Decker, E. R., 1972, Continental heat flow in The Nature of the Solid Earth, Robertson, E.C., ed.,: McGraw-Hill, Inc., p. 506-543.

Sass, J. H., Lachenbruch, A. H., and Munroe, R. J., 1971, Thermal conductivity of rocks from measurements of fragments and its application to heat flow determination: Journal of Geophysical Research, Vol. 76, p. 3391-3401.

Sauck, W. A., Sumner, J. S. and Christensen, J. P., 1971, Aeromagnetic map of the northern part of the Tucson basin, Pima County, Arizona: Arizona Geological Society Digest, Vol. 9, p. 123-135.

Sbar, M. L., 1979, Analysis of short term microearthquake activity related to potential geothermal areas in Arizona: in Arizona geothermal energy appraisal studies, final report June 1978-March 1980, Arizona Bureau of Geology and Mineral Technology, p. 1-11.

Scarborough, R. B. and Peirce, H. W., 1978, Late Cenozoic basins of Arizona: in Land of Cochise, 29th Field Conference, New Mexico Geological Society Guidebook p. 253-259.

Schmitt, H. A., 1966, The porphyry copper deposits in their regional setting: in Titley, R. S. and Hicks, C. L., Eds., Geology of the porphyry copper deposits, southwestern North America: Tucson, University of Arizona Press, p. 17-23.

Seager, W. R. and Clemons, R. E., 1972, Volcanic chronology and structure of the Blue Creek basin region between Clifton, Arizona and Cliff, New Mexico, unpub. manuscript, 18 p.

Seager, W. R. and Morgan, P., 1979, Rio Grande Rift in southern new Mexico, West Texas, and northern Chihuahua: in Riecker, R. E., Ed., Rio Grande Rift: Tectonics and Magmatism: American Geophysical Union, p. 87-106.

Sellers, W. D. and Hill, R. H., Eds., 1974, Arizona climate 1931-1972, revised 2nd ed.: University of Arizona Press, Tucson, Arizona, 616 p.

Schumacher, D., 1978, Devonian stratigraphy and correlations in southeastern Arizona: in Land of Cochise, 29th Field Conference, New Mexico Geological Society Guidebook, p. 175-181.

Shearer, C. R., 1979, A regional terrestrial heat-flow study in Arizona: unpub. Ph.D. dissertation, New Mexico Institute of Mining and Technology, Socorro, New Mexico, 184 p.

Silver, L. T., 1978, Precambrian formations and precambrian history in Cochise County, Southeastern Arizona: in Land of Cochise, 29th Field Conference, New Mexico Geological Society Guidebook, p. 157-163.

Smith, P. J., 1973, Topics in geophysics: MIT Press, Cambridge, MA, 246 p.

Stone, C., 1979, An overview of the geothermal potential of the Springerville area, Arizona: in geothermal reservoir site evaluation in Arizona, semi-annual progress report for the period July 15, 1978-January 15, 1979, Arizona Bureau of Geology and Mineral Technology, p. 1-25.

Strangway, D. W., Simpson, J. and York, D., 1976, Paleomagnetic studies of volcanic rocks from the Mogollon Plateau area of Arizona and New Mexico: in Cenozoic volcanism in southwestern New Mexico, New Mexico Geological Society Special Publication 5, p. 119-124.

Summers, W. K., 1976, Catalog of Thermal Waters in New Mexico, New Mexico Bureau of Mines and Mineral Resources Hydrologic Report 4, 80 p.

Sumner, J. S., 1976, Earthquakes in Arizona: Fieldnotes, Arizona Bureau of Mines, Vol. 6., No. 1, p. 1-5.

Swan, M. M., 1976, The Stockton Pass Fault: An Element of the Texas Lineament: Unpub. M.S. Thesis, University of Arizona, 119 p.

Swanberg, C. A., Morgan, P., Stoyer, C. H., and Witcher, J. C., 1977, An appraisal study of the geothermal resources of Arizona and adjacent areas in New Mexico and Utah and their value for desalination and other uses: New Mexico Energy Institute Report 6, New Mexico State University, 76 p.

Titley, S. R., 1976, Evidence for a Mesozoic linear tectonic pattern in southeastern Arizona: in Tectonic Digest, Arizona Geological Society Digest, Vol. X, p. 71-101.

USGS, 1977, U. S. Geological Survey Water Resources Data Report for Arizona, AZ-77-1.

USGS, 1978, U. S. Geological Survey Water Resources Data Report for Arizona, AZ-78-1.

Turner, G. L., 1962, The Deming axis, southeastern Arizona, New Mexico and Trans-Pecos, Texas: New Mexico Geological Society Guidebook-Mogollon Rim, 13th Field Conference, 1962, p. 59-71.

Vroman, J. P., 1976, The Black Mountain Fault: in Tectonic Digest, Arizona Geological Society Digest, Vol. X, p. 341-345.

Wahl, D.E., Jr., 1980, Mid-Tertiary volcanic geology in parts of Greenlee County, Arizona, Grant and Hidalgo Counties, New Mexico: unpub. Ph.D. Dissertation, Arizona State University, 147 p.

Ward, P. L., 1972, Microearthquakes: prospecting tool and possible hazard in the development of geothermal resources: Geothermics, Vol. 1, p. 3-12.

Weber, R. H. and Willard, M. E., 1959, Reconnaissance geologic map of Mogollon thirty-minute qudrangle: New Mexico Bureau of Mines and Mineral Resources Geologic Map 10.

Whiteford, P. C., 1975, Assessment of the audio-magnetotelluric method for geothermal resistivity surveying: in Proceedings, Second United Nations Symposium on the development and use of geothermal resources, Vol. 2, p. 1255-1261.

Wilson, E. D. and Moore, R. T., 1958, Geologic map of Graham and Greenlee Counties, Arizona: Tucson, Arizona Bureau of Mines.

Witcher, J. C., 1979, A progress report of geothermal investigations in the Clifton area: in geothermal reservoir site evaluation in Arizona, semiannual progress report for the period July 15, 1978-January 15, 1979, Department of Energy contract EG-77-S-02-4362: Arizona Bureau of Geology and Mineral Technology, Geological Survey Branch, Geothermal Group, University of Arizona, p. 26-41.

Witcher, J. C., 1979, A geothermal reconnaissance study of the San Francisco River Between Clifton Arizona, and Pleasanton, New Mexico: in geothermal reservoir site evaluation in Arizona, progress report, January 16-November 1, 1979, Arizona Bureau of Geology and Mineral Technology, p. 156-173.

Witcher, J. C. and Stone, C., 1980, Heat flow and the thermal regime in the Clifton, Arizona area: in Arizona geothermal energy appraisal studies-final report June 1978-March 1980, Arizona Bureau of Geology and Mineral Technology, for WPRS and DOE under contract EG-77-S-02-4362, p. 117-146.

Woodward, L. A., Callender, J. F., Gries, J., Seager, W. R., Chapin, C. E., Shaffer, W. L. and Zilinski, R. E., 1975, Tectonic Map of the Rio Grande Region, Colorado-New Mexico Border to Presidio, Texas, 1:1,000,000, New Mexico Geological Society.